Chiral and non-linear optical responses in topological metals

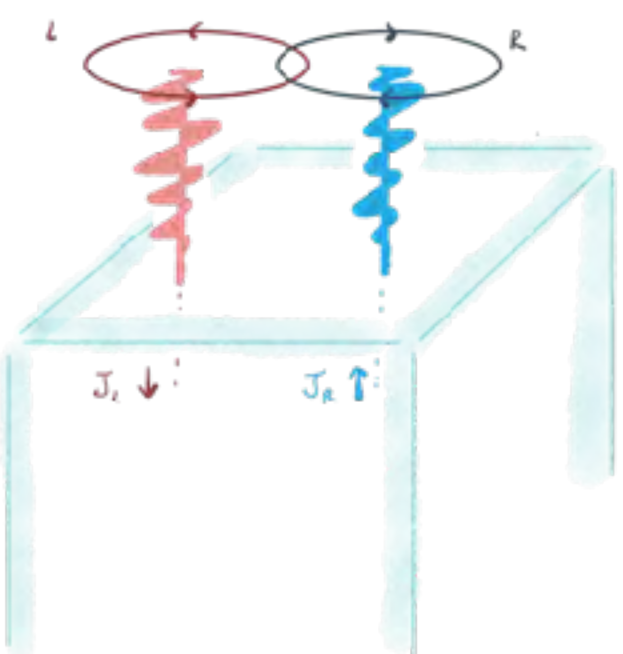

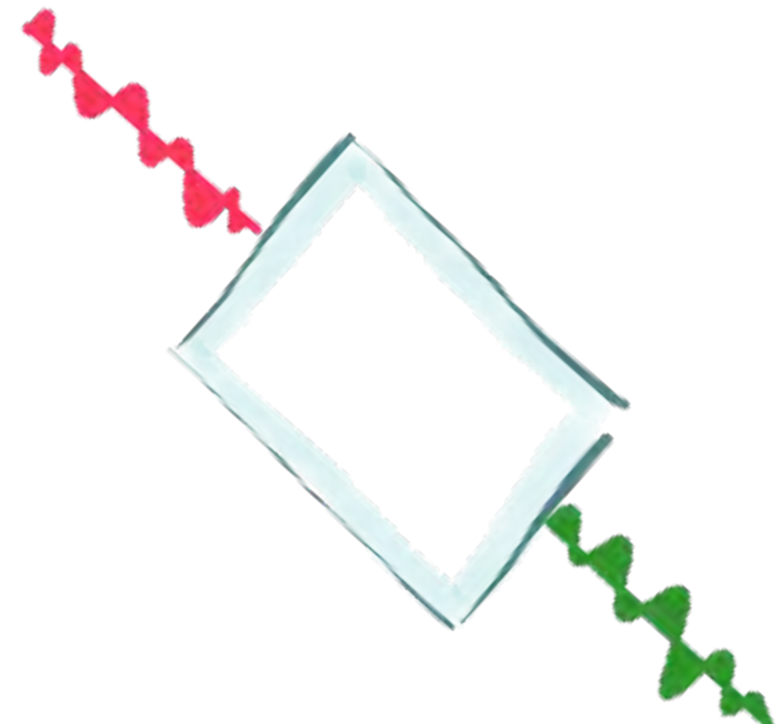

F. de Juan, AGG, T. Morimoto, J. E. Moore
Nat. Comm. 8, 15995 (2017)

F. Flicker, F. de Juan, T. Morimoto, B. Bradlyn, M. Vergniory, AGG 1806.09642

S. Pakantar et al.
1804.06973

Quantization

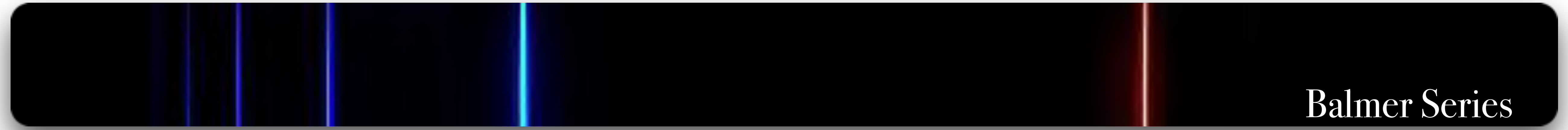

In solids, quantization occurs typically as a **linear response** of **insulators**

Quantum Hall effect

von Klitzing, Tsui, Stormer (80's)

Kerr/Faraday rotation in topological insulators

L. Wu, et al. Science (2016)

Large magnitude

Solar cells

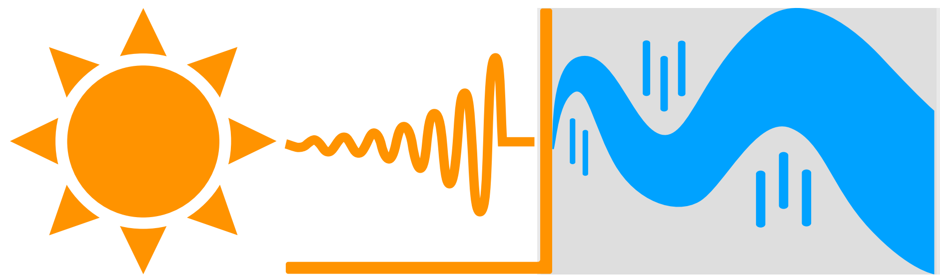

$$j(0) \sim \sigma^{(2)} I(\omega)$$

2nd harmonic generation

$$j(2\omega) \sim \sigma^{(2)} I(\omega)$$

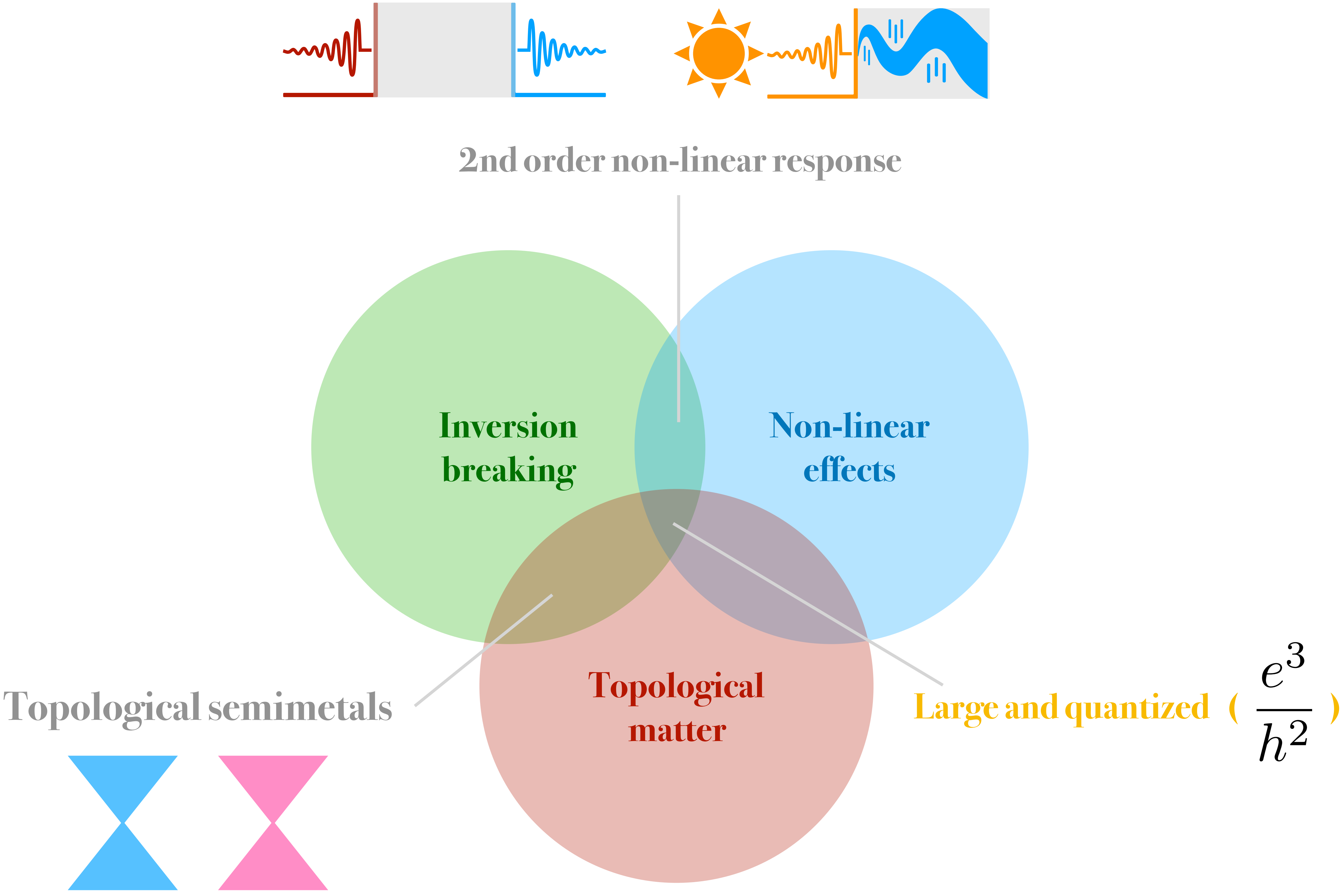
2nd order non-linear response
Inversion breaking
Non-linear effects
Topological matter
Topological semimetals
Large and quantized $\left(\frac{e^3}{h^2}\right)$

Chiral topological metals have large and quantized non linear responses

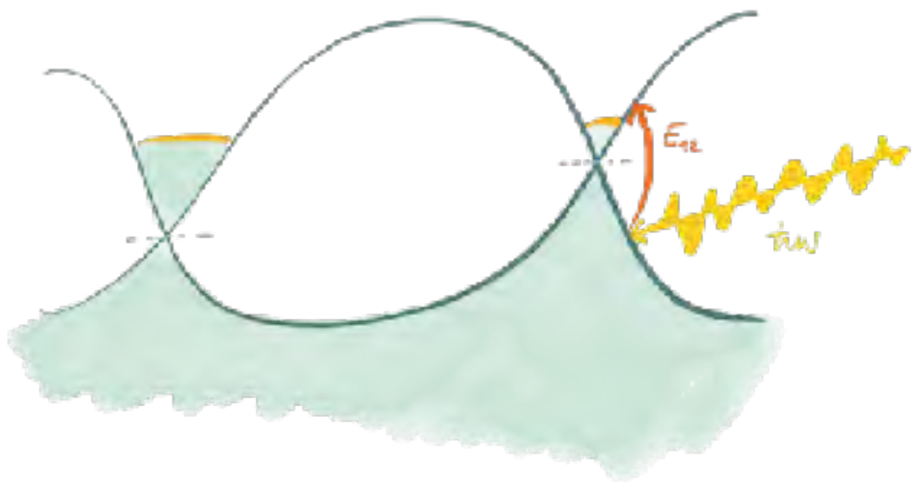

Non-linear responses

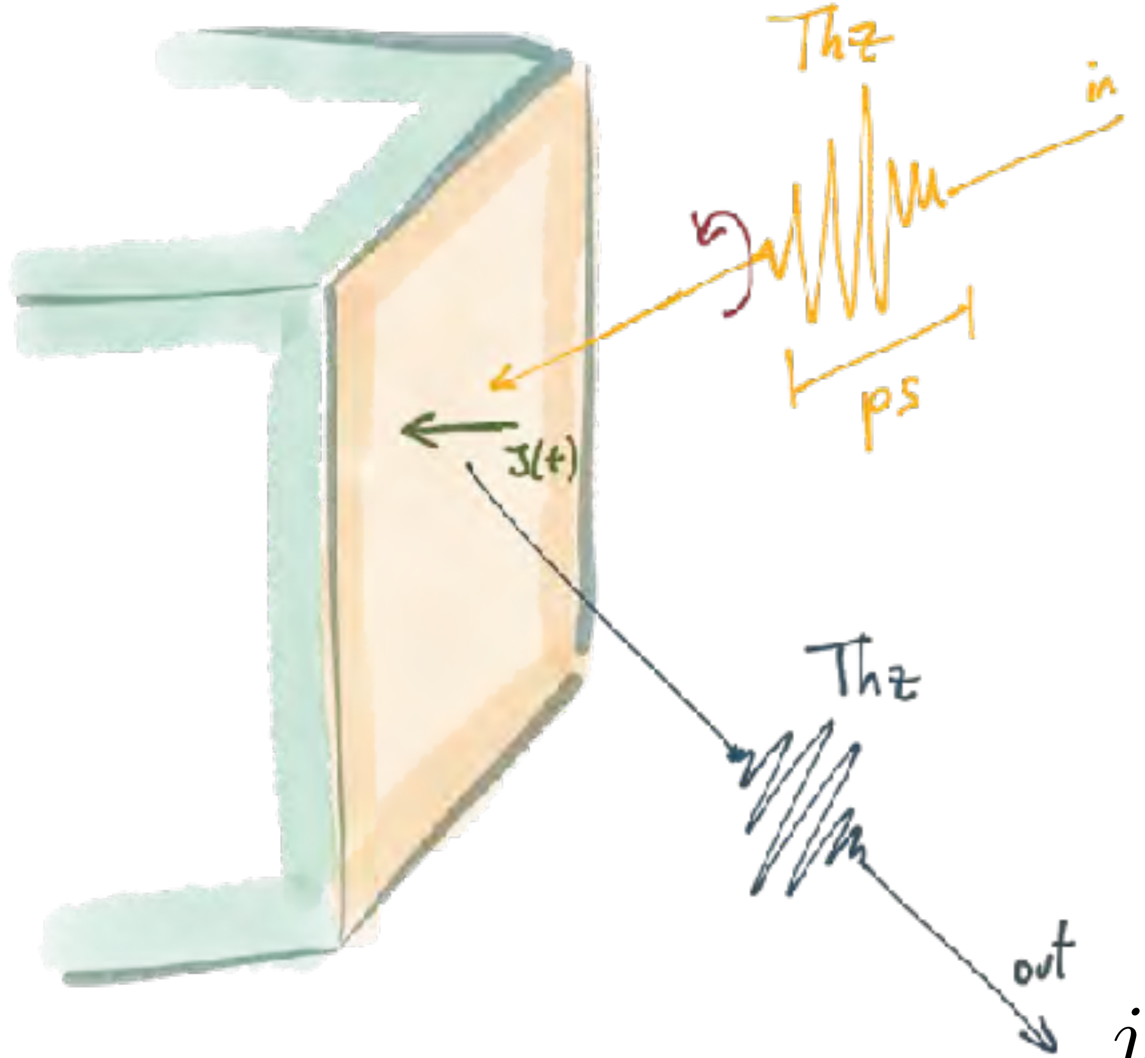

needs inversion breaking

$$j_i = \sigma_{ij} E_j + \sigma_{ijl} E_j E_l + \cdots$$

Traditional: GaAs, $BaTiO_3$

Bergfeld and Daum PRL '99

Young and Rappe PRL '15

Topological: TaAs, Bi_2Se_3

Ma et. al. Nat. Phys '17 (MIT)

Wu et al Nat. Phys '17 (Berkeley)

Bas et al Opt. Exp.'16 (Toronto/Virginia)

Osterhoudt et al. arXiv '17

Second order zoo

$$j_i \propto \sigma_{ijl} E_j E_l$$

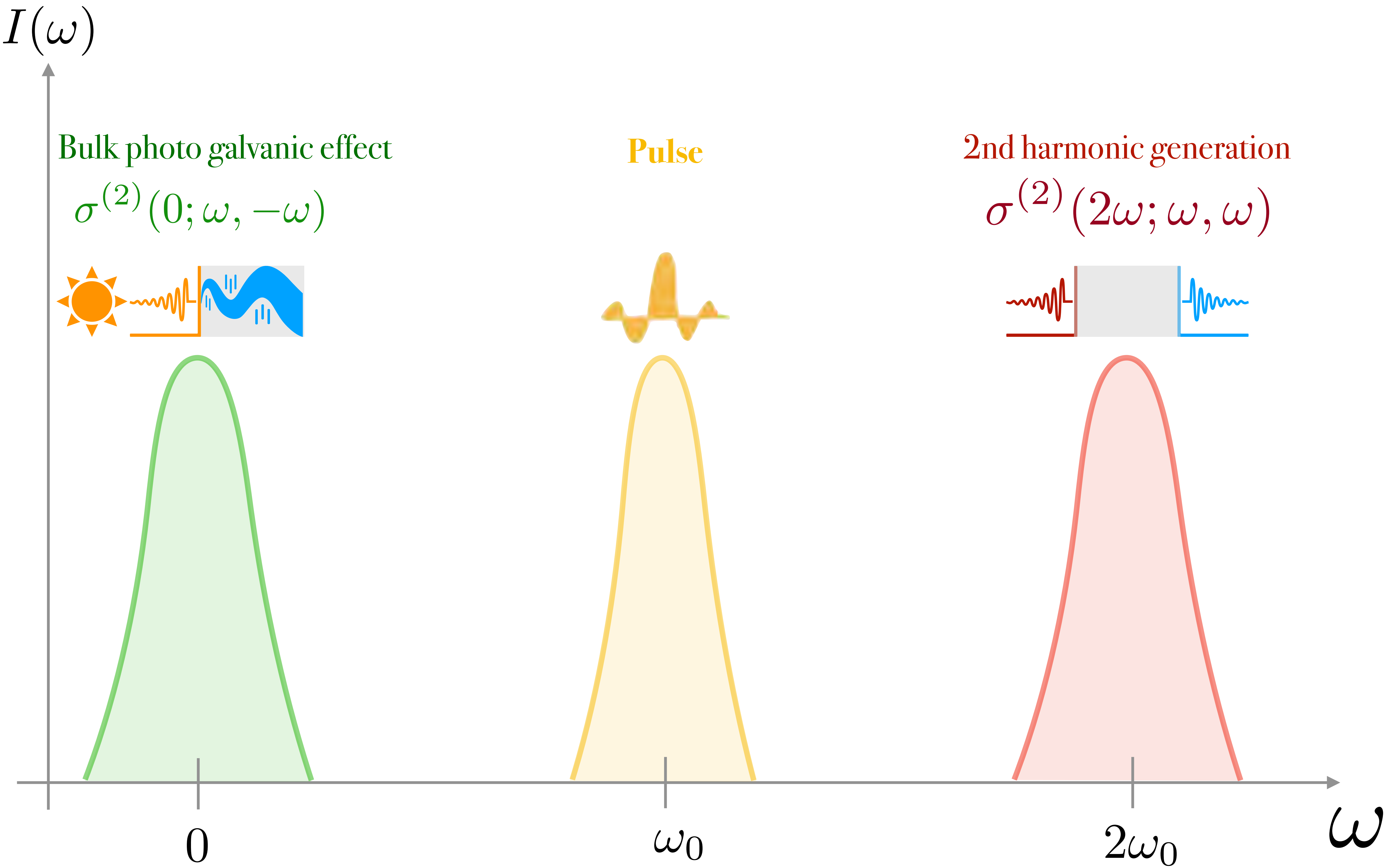

Second order zoo

$$j_i \propto \sigma_{ijl} E_j E_l$$

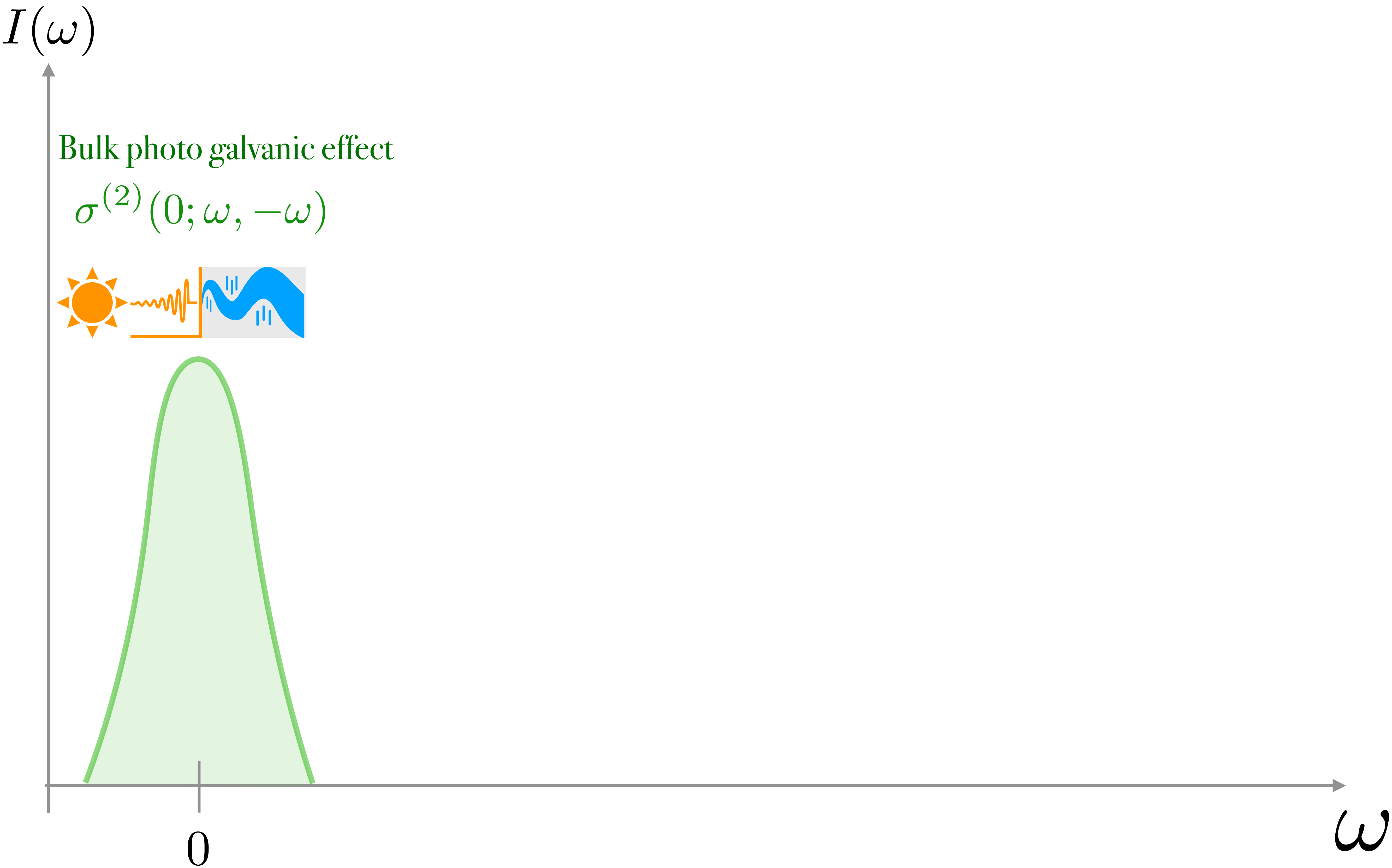

Second order zoo

$$j_i \propto \sigma_{ijl} E_j E_l$$

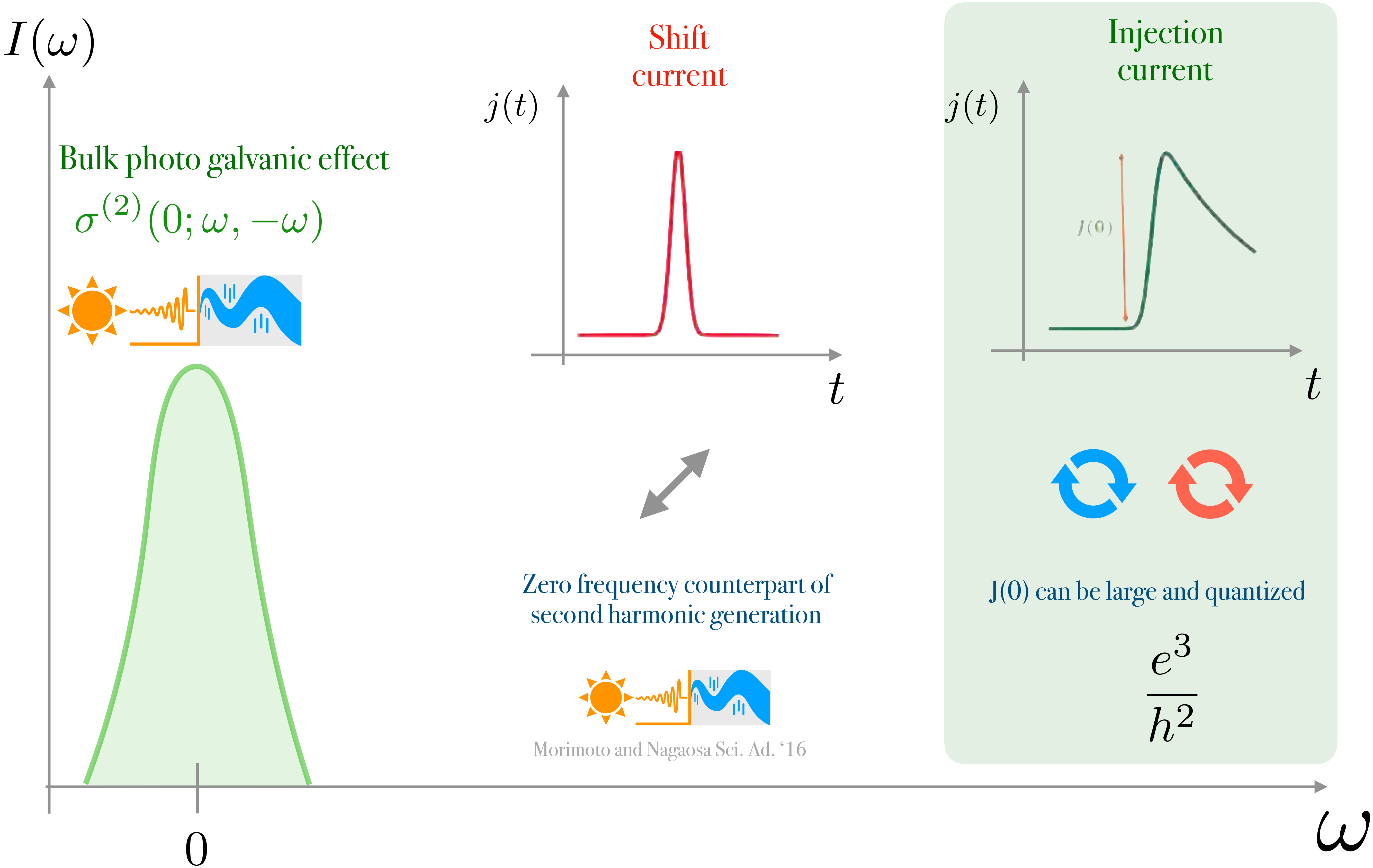

Second order zoo

$$j_i \propto \sigma_{ijl} E_j E_l$$

Injection current

$\propto (i\omega)^{-1}$

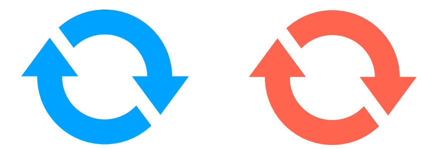

$$(\mathbf{E} \times \mathbf{E}^*)_j$$

Sipe, Shkrebtii, PRB (2000)

Chan, et al PRB(R) (2016)

Second order zoo

$$j_i \propto \sigma_{ijl} E_j E_l$$

Injection current

$\propto (i\omega)^{-1}$

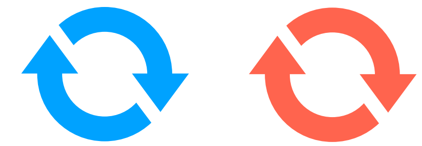

$$\frac{dj_i}{dt}$$

$$(\mathbf{E} \times \mathbf{E}^*)_j$$

Sipe, Shkrebtii, PRB (2000)

Chan, et al PRB(R) (2016)

Second order zoo

$$j_i \propto \sigma_{ijl} E_j E_l$$

Injection current

$\propto (i\omega)^{-1}$

$$\frac{dj_i}{dt} = \beta_{ij}(\omega)(\mathbf{E} \times \mathbf{E}^*)_j$$

electron linear momentum rate ← photon angular momentum density

Sipe, Shkrebtii, PRB (2000)

Chan, et al PRB(R) (2016)

Second order zoo

$$j_i \propto \sigma_{ijl} E_j E_l$$

Injection current

$\propto (i\omega)^{-1}$

Linear momentum // i

$$\frac{dj_i}{dt} = \beta_{ij}(\omega)(\mathbf{E} \times \mathbf{E}^*)_j$$

Angular momentum // j

$\mathrm{Tr}[\beta]$

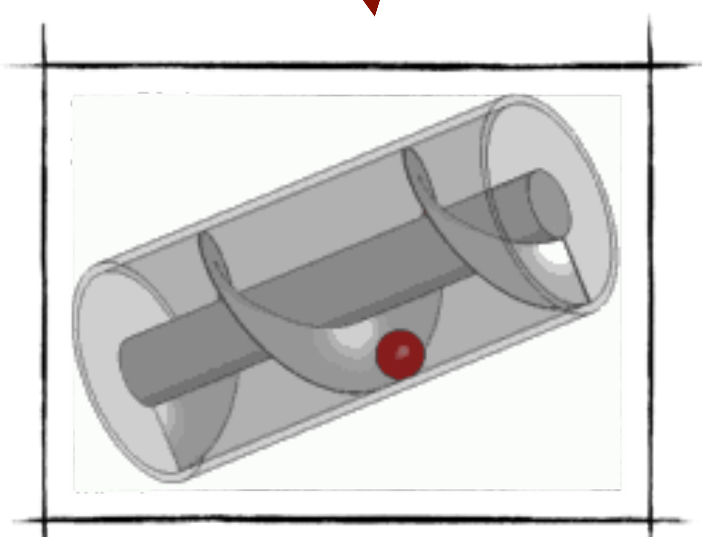

classical screw!

Lesson*

$\mathrm{Tr}[\beta] \neq 0$ ⟷ Mirror-free (chiral) point groups

*__Brute force way:__ transform tensor under point group symmetries and check for non-vanishing components

Topological metals have large and quantized injection currents

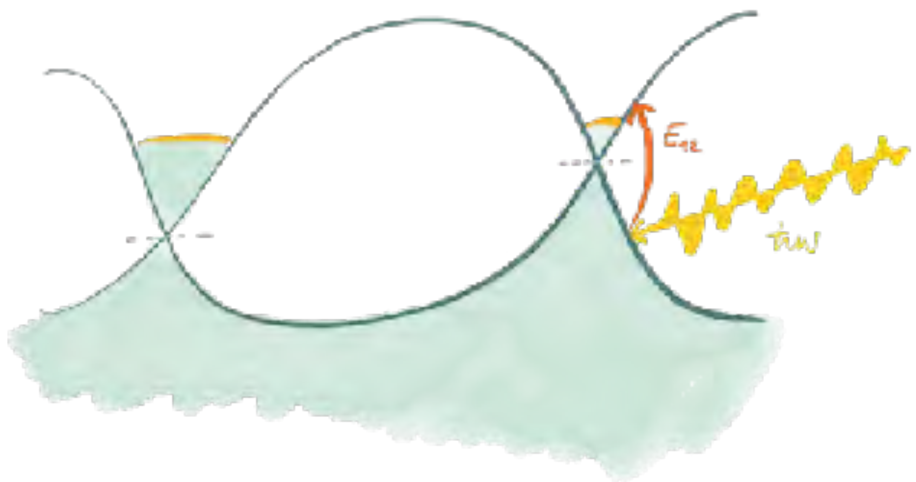

F. de Juan, AGG, T. Morimoto, J. E. Moore Nat. Comm. '17

Injection current

$$\frac{dj_i}{dt} = \beta_{ij}(\omega)(\mathbf{E} \times \mathbf{E}^*)_j$$

$\mathrm{Tr}[\beta]$

Two band model

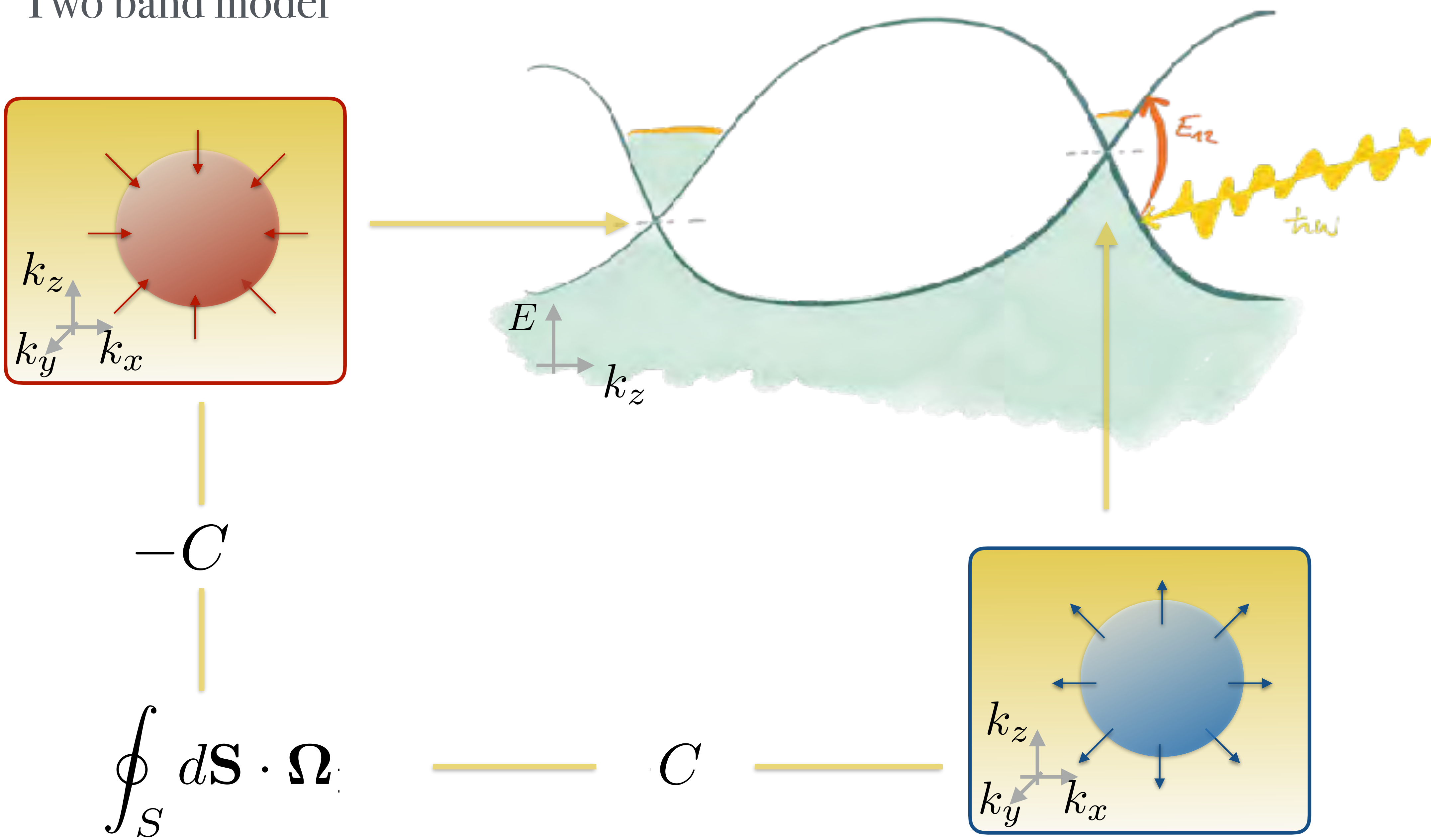

Injection current

$$\frac{dj_i}{dt} = \beta_{ij}(\omega)(\mathbf{E} \times \mathbf{E}^*)_j$$

$\mathrm{Tr}[\beta]$

Two band model

$$\frac{d\Delta j_i}{dt} = \frac{1}{2}\Bigg($$

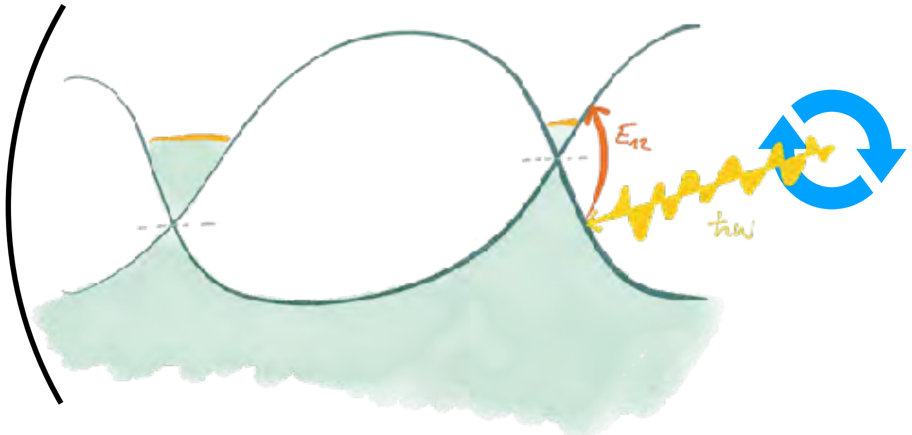

$$-$$

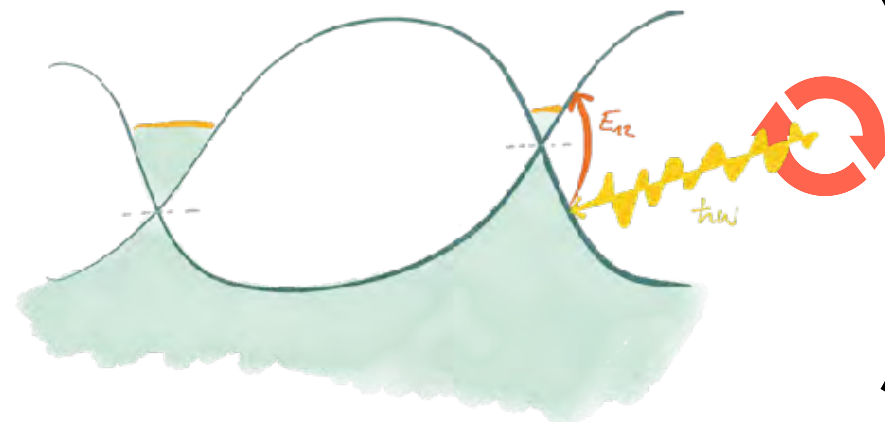

$$\Bigg)$$

= group velocity x excitation rate

$$\Delta\Gamma_{\mathbf{k}}(\omega) \rightarrow \pi\frac{e^2}{2h}|E|^2\Omega^i_{\mathbf{k}}\delta(\varepsilon_1 - \varepsilon_0 - \hbar\omega)$$

Fermi's golden rule

$$\Gamma \propto |v_x \pm iv_y|^2 \mathrm{JDOS}$$

Vanderbilt, Souza '13

D. T. Tran, A. Dauphin, AGG et al Sci. Adv '17

Injection current

$$\frac{dj_i}{dt} = \beta_{ij}(\omega)(\mathbf{E} \times \mathbf{E}^*)_j$$

$$\mathrm{Tr}[\beta]$$

Two band model

$$\frac{d\Delta j_i}{dt} = \frac{1}{2}\Bigg($$

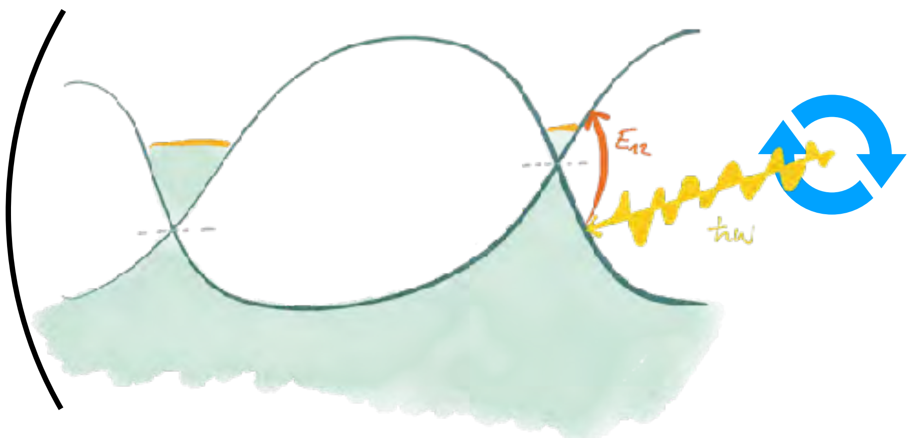

$$-$$

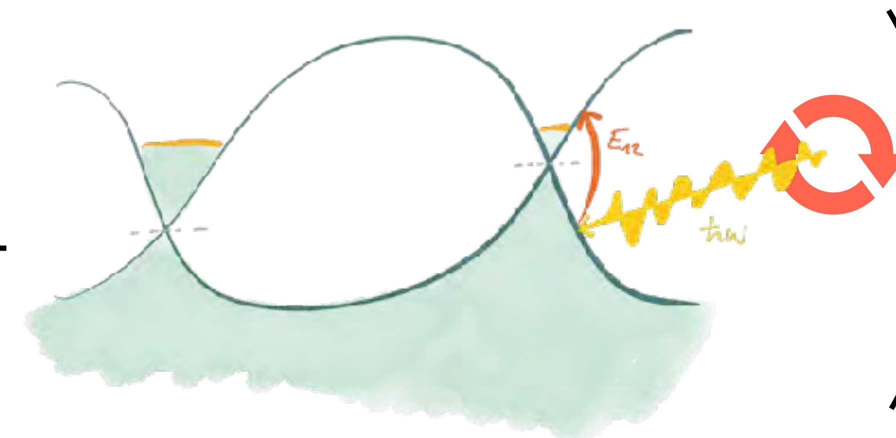

$$\Bigg)$$

= group velocity x excitation rate

$$\frac{d\Delta j_i}{dt} = e \int \frac{d^3k}{(2\pi)^3} (v_1^i - v_0^i) \Delta\Gamma_{\mathbf{k}}(\omega) \longrightarrow \pi \frac{e^2}{2h} |E|^2 \Omega_{\mathbf{k}}^i \delta(\varepsilon_1 - \varepsilon_0 - \hbar\omega)$$

Fermi's golden rule

$$\Gamma \propto |v_x \pm i v_y|^2 \mathrm{JDOS}$$

Vanderbilt, Souza '13

D. T. Tran, A. Dauphin, AGG et al Sci. Adv '17

Injection current

$$\frac{dj_i}{dt} = \beta_{ij}(\omega)(\mathbf{E} \times \mathbf{E}^*)_j$$

$\mathrm{Tr}[\beta]$

Two band model

$$\frac{d\Delta j_i}{dt} = \frac{1}{2}\Bigg($$

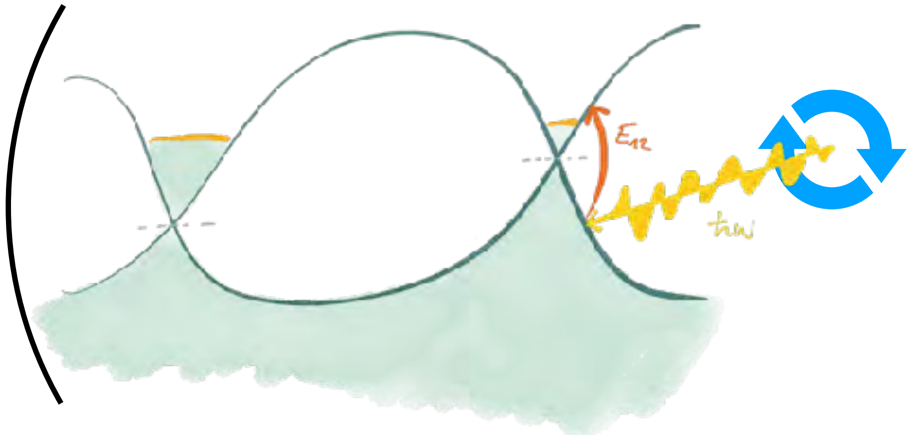

$-$

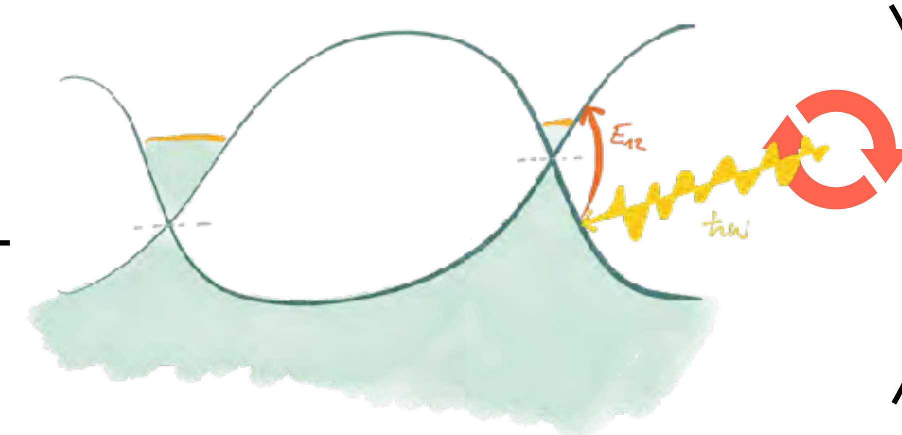

$$\Bigg)$$

= group velocity x excitation rate

$$\frac{d\Delta j_i}{dt} = e \int \frac{d^3k}{(2\pi)^3}(v_1^i - v_0^i)\Delta\Gamma_{\mathbf{k}}(\omega) \longrightarrow \pi\frac{e^2}{2h}|E|^2\Omega^i_{\mathbf{k}}\delta(\varepsilon_1 - \varepsilon_0 - \hbar\omega)$$

$$\mathrm{Tr}[\beta] = i\frac{e^3}{2h^2}\oint_S d\mathbf{S} \cdot \mathbf{\Omega_1}$$

Injection current

$$\frac{dj_i}{dt} = \beta_{ij}(\omega)(\mathbf{E} \times \mathbf{E}^*)_j$$

$\mathrm{Tr}[\beta]$

Two band model

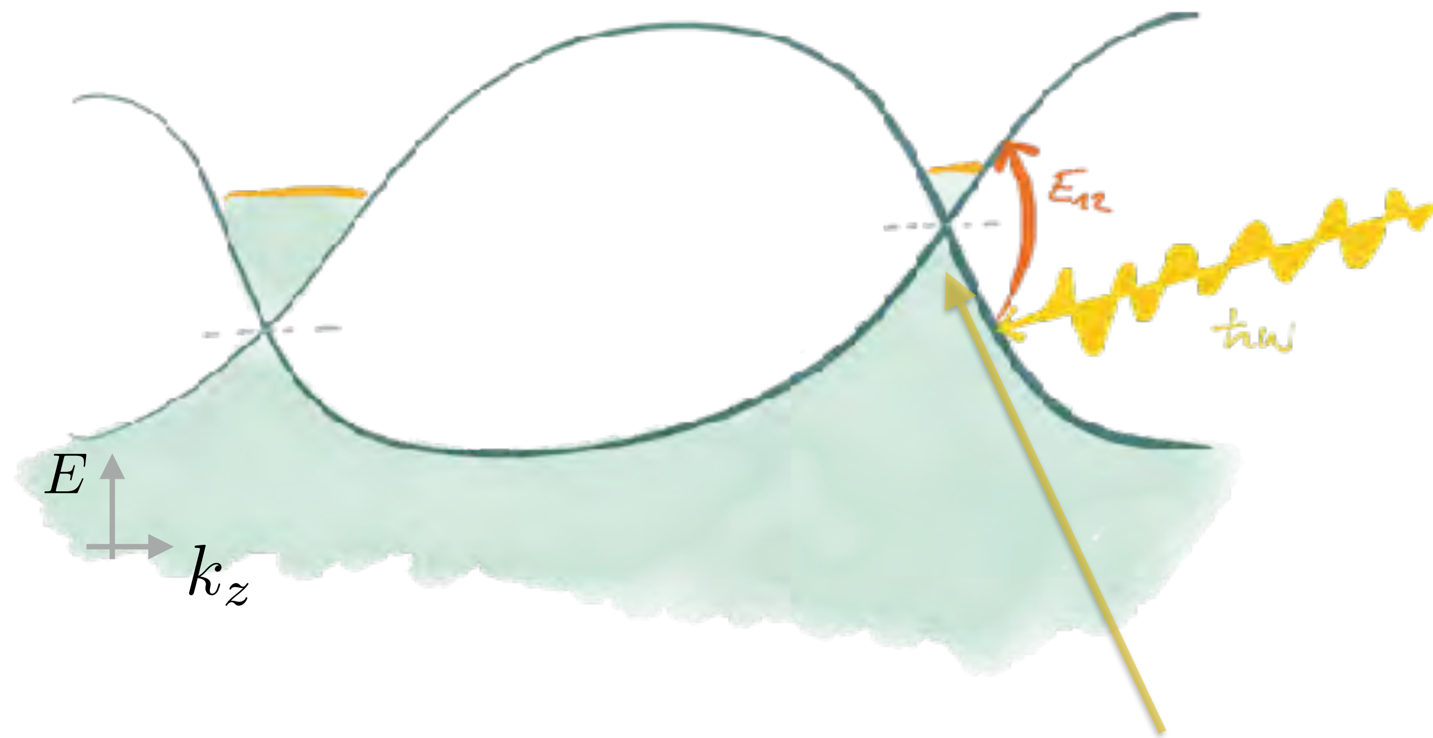

$$\mathrm{Tr}[\beta] = i\frac{e^3}{2h^2}\oint_S d\mathbf{S}\cdot\mathbf{\Omega_1} = i\pi\frac{e^3}{h^2}C$$

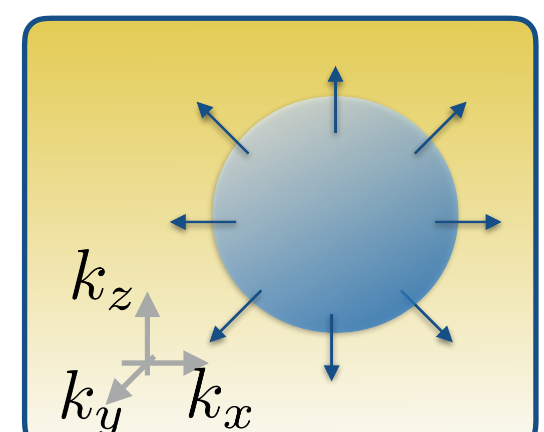

Candidates

SrSi$_2$

Huang, et al. PNAS **113** 1180 (2015)

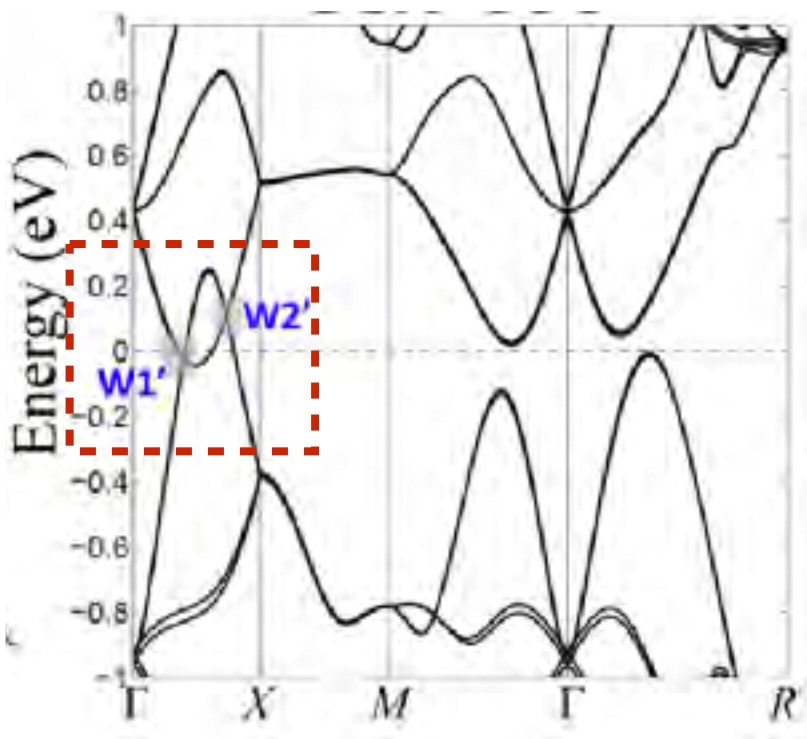

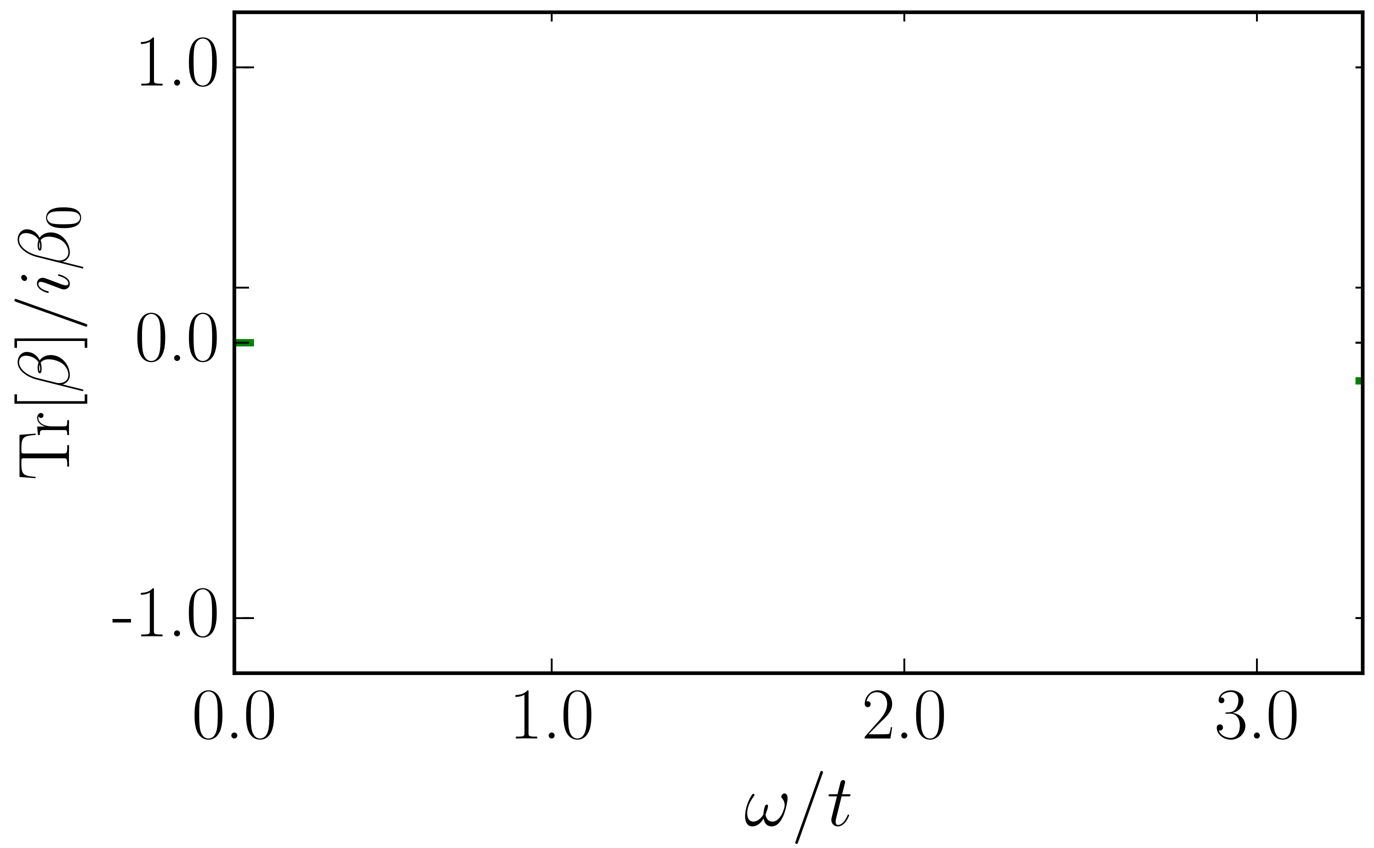

Chiral Weyls

F. de Juan, AGG, T. Morimoto, J. E. Moore Nat. Comm. '17

Candidates

non-universal

universal

$SrSi_2$

Huang, et al. PNAS **113** 1180 (2015)

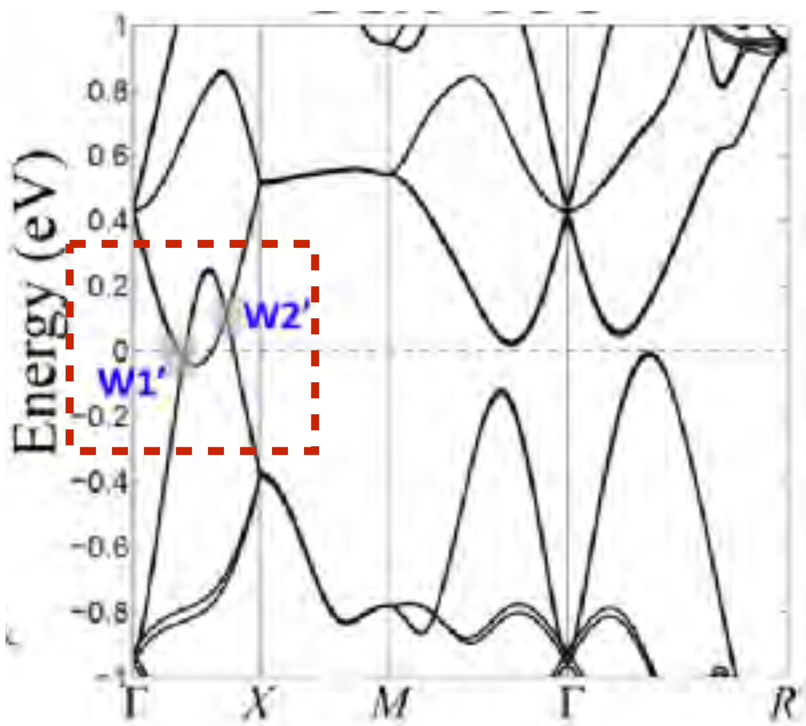

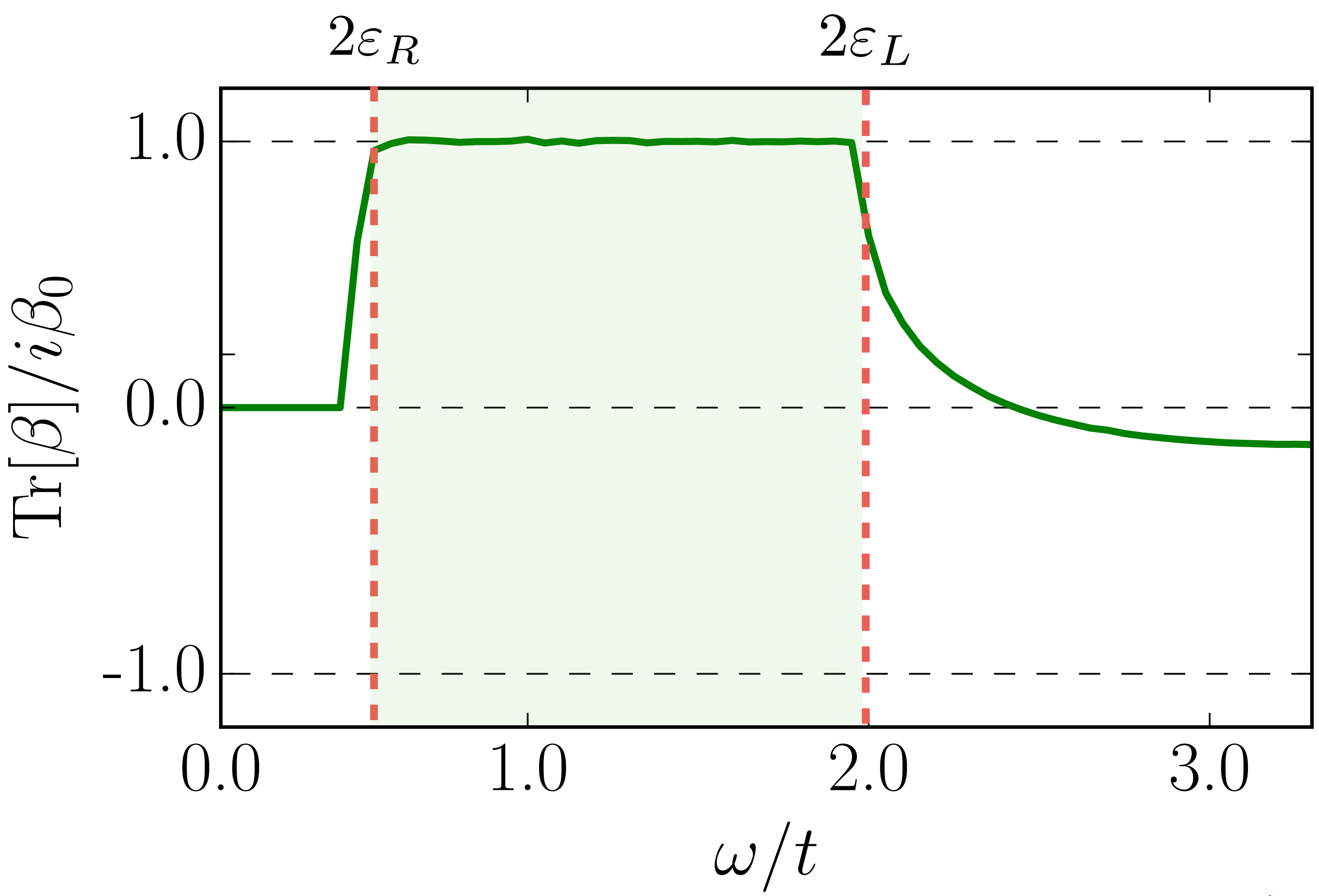

$$\pi \frac{e^3}{h^2} C + \mathcal{O}\left(\frac{\omega^2}{\Delta E^2}\right)$$

Chiral Weyls

multi-band correction

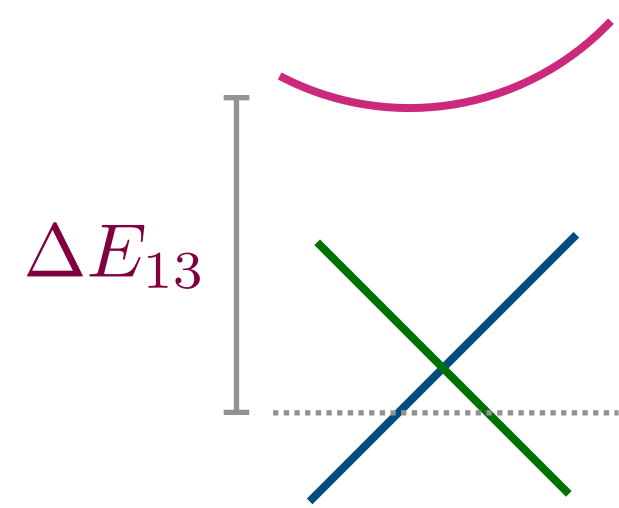

F. de Juan, AGG, T. Morimoto, J. E. Moore Nat. Comm. '17

Candidates

Chiral Weyls

$SrSi_2$

Huang, et al. PNAS **113** 1180 (2015)

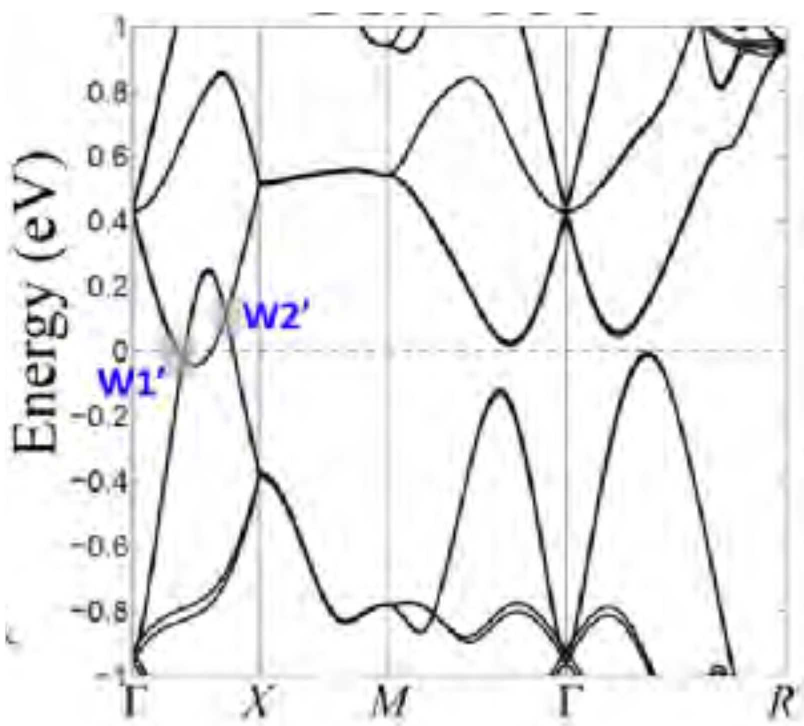

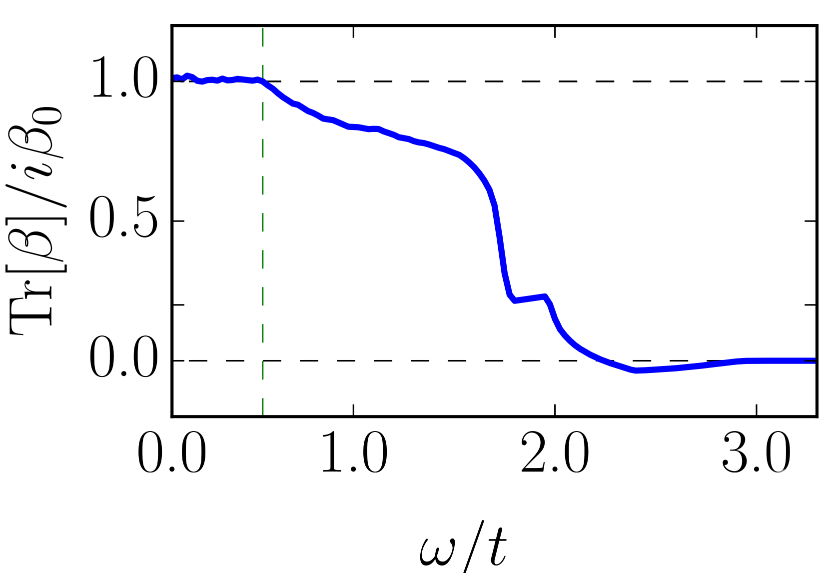

F. de Juan, AGG, T. Morimoto, J. E. Moore Nat. Comm. '17

Candidates

Chiral Weyls

$SrSi_2$

Huang, et al. PNAS **113** 1180 (2015)

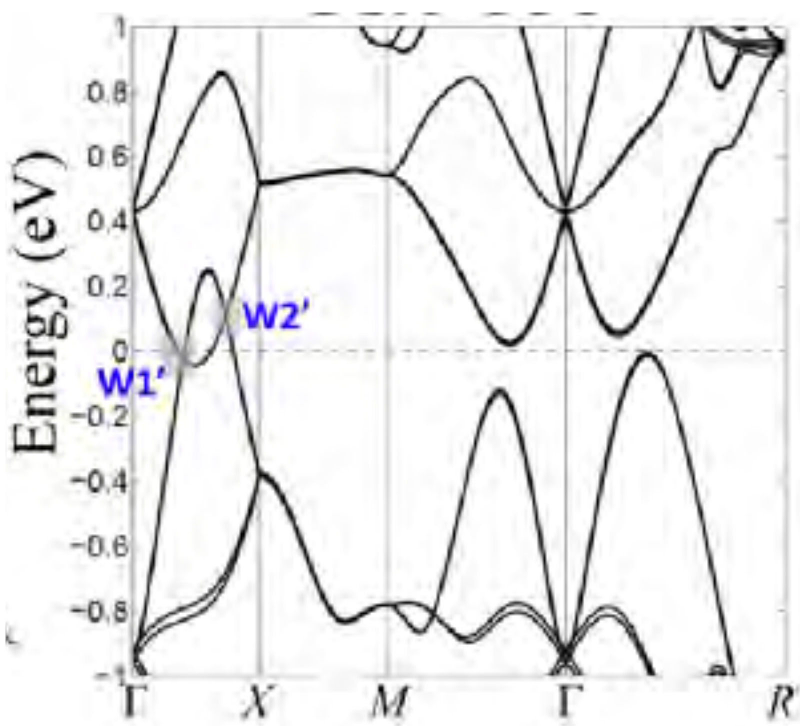

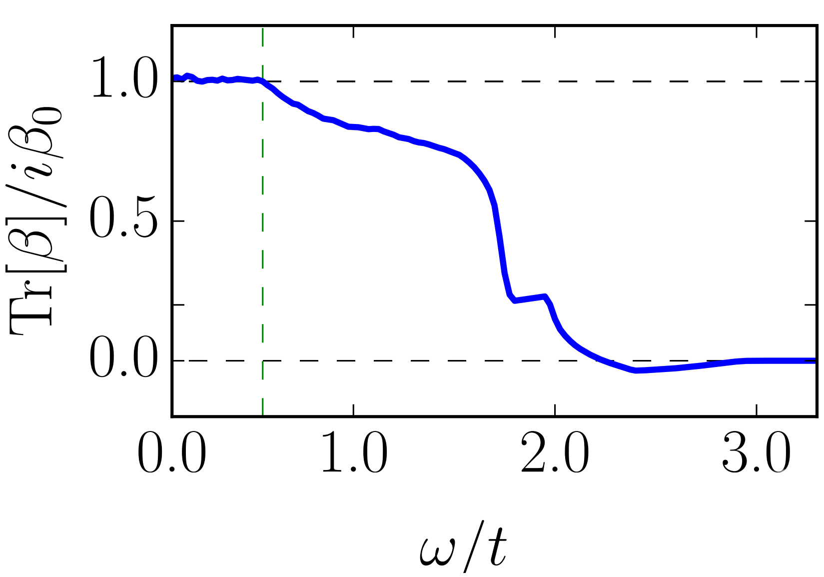

Kramers Weyls

Tellurium

Hirayama, PRL **114**, 206401 (2015)

Chang et. al arXiv: 1611.07925

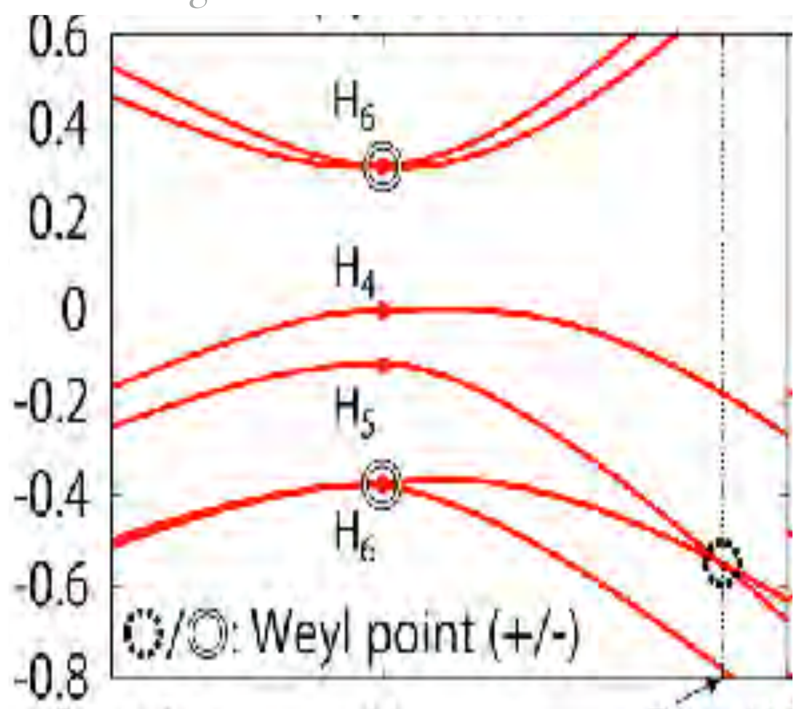

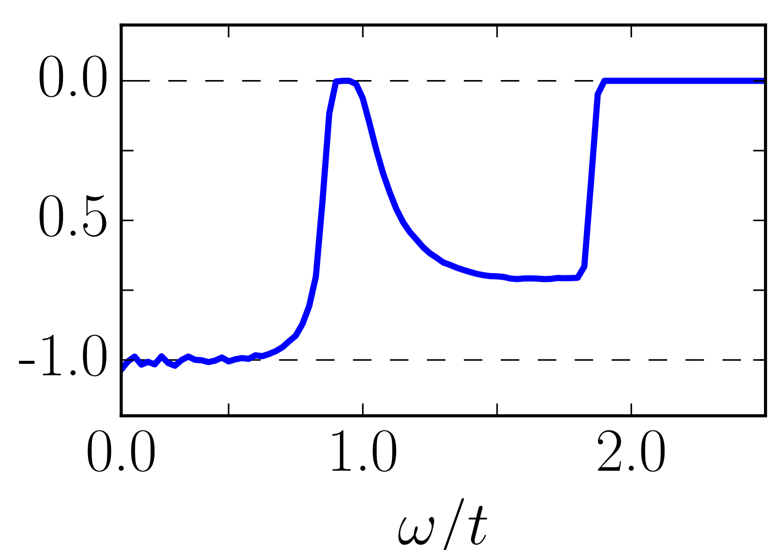

F. de Juan, AGG, T. Morimoto, J. E. Moore Nat. Comm. '17

Candidates

Chiral Weyls

$SrSi_2$

Huang, et al. PNAS **113** 1180 (2015)

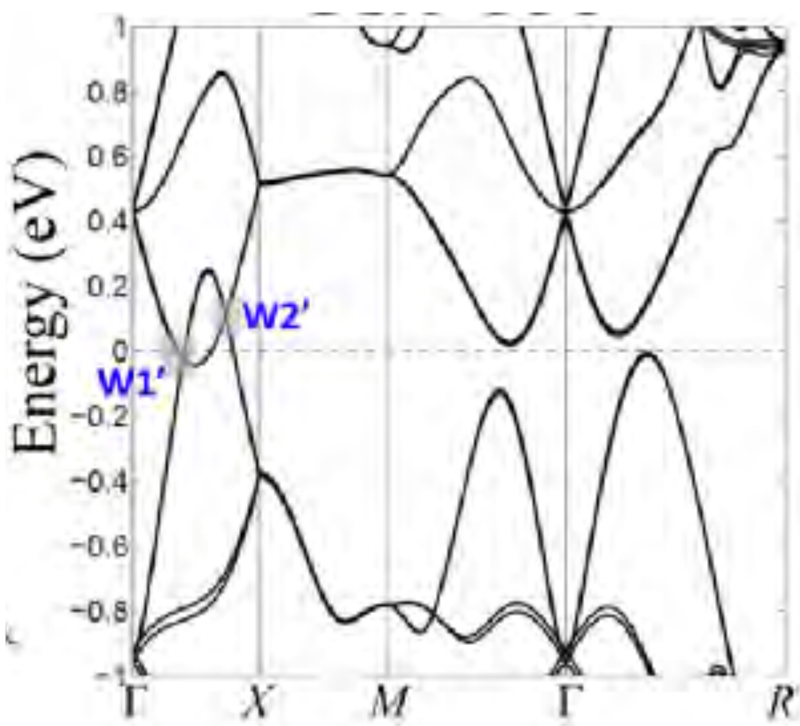

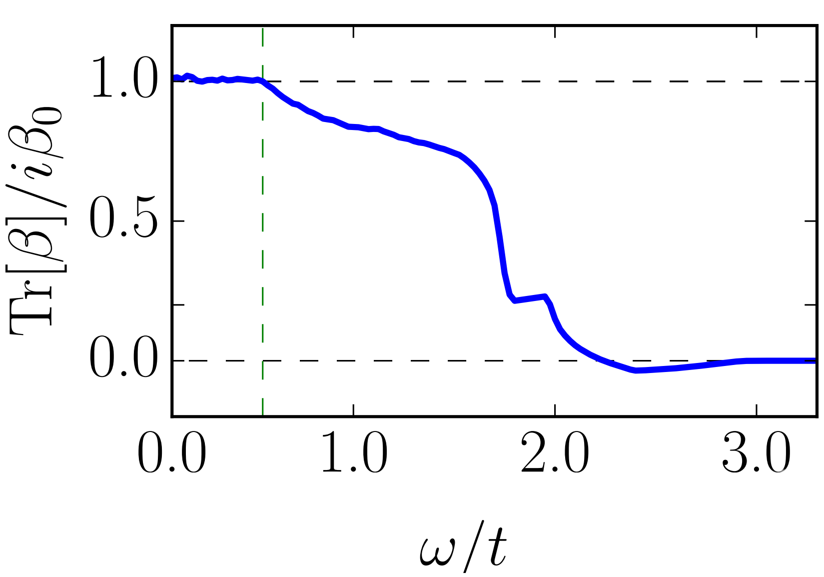

Kramers Weyls

Tellurium

Hirayama, PRL **114**, 206401 (2015)

Chang et. al arXiv: 1611.07925

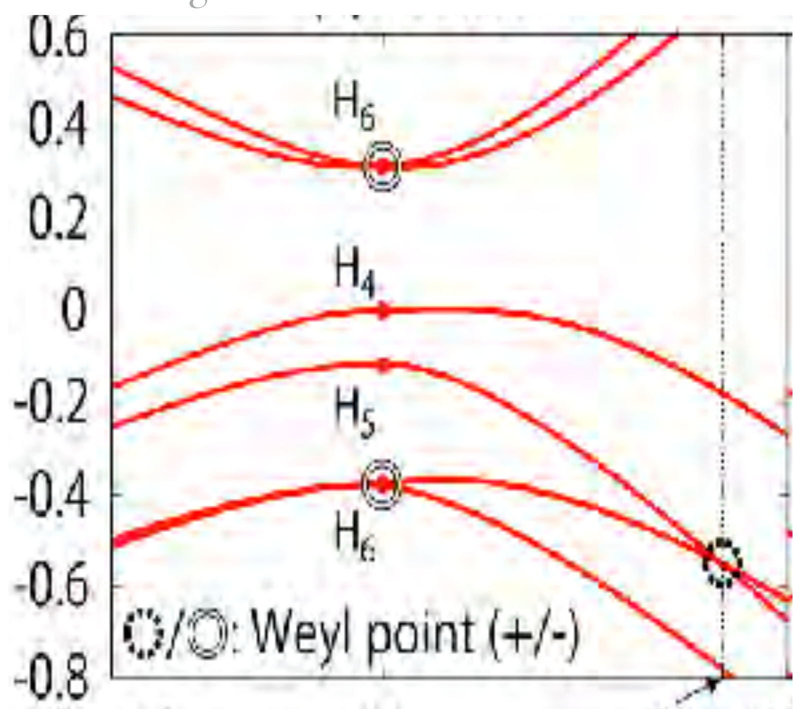

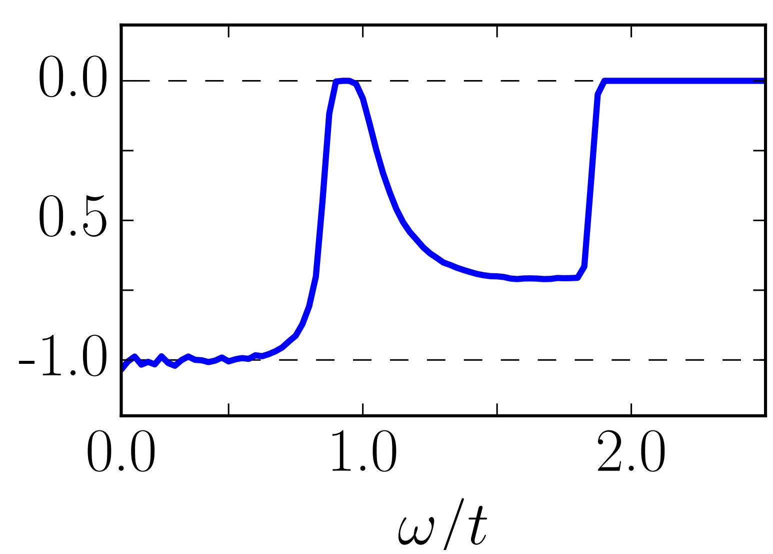

RhSi

Chang et. al PRL '17

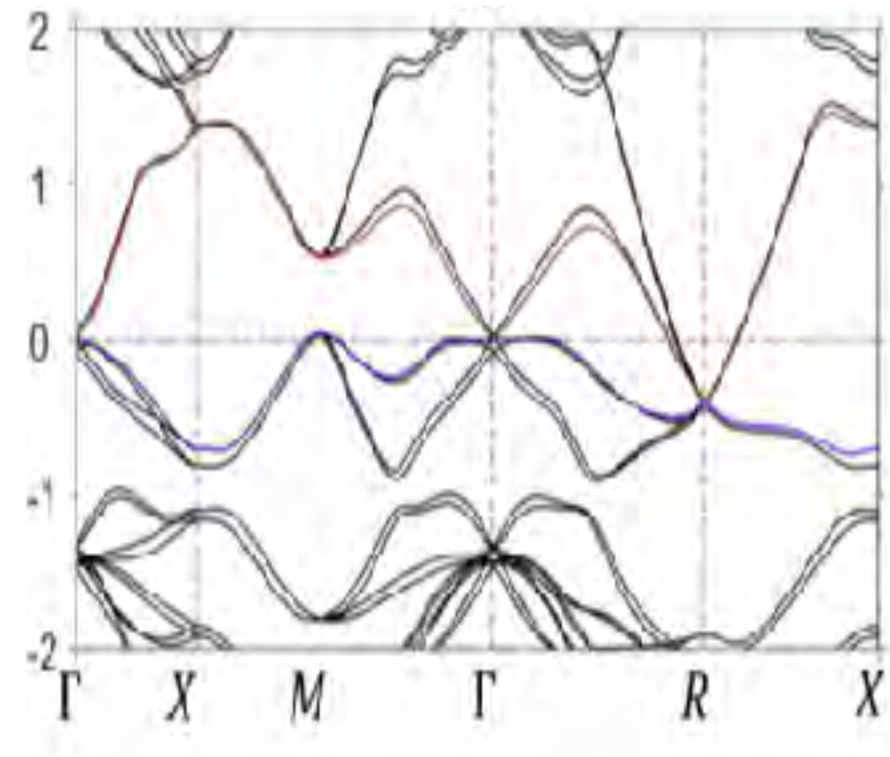

F. de Juan, AGG, T. Morimoto, J. E. Moore Nat. Comm. '17

Candidates

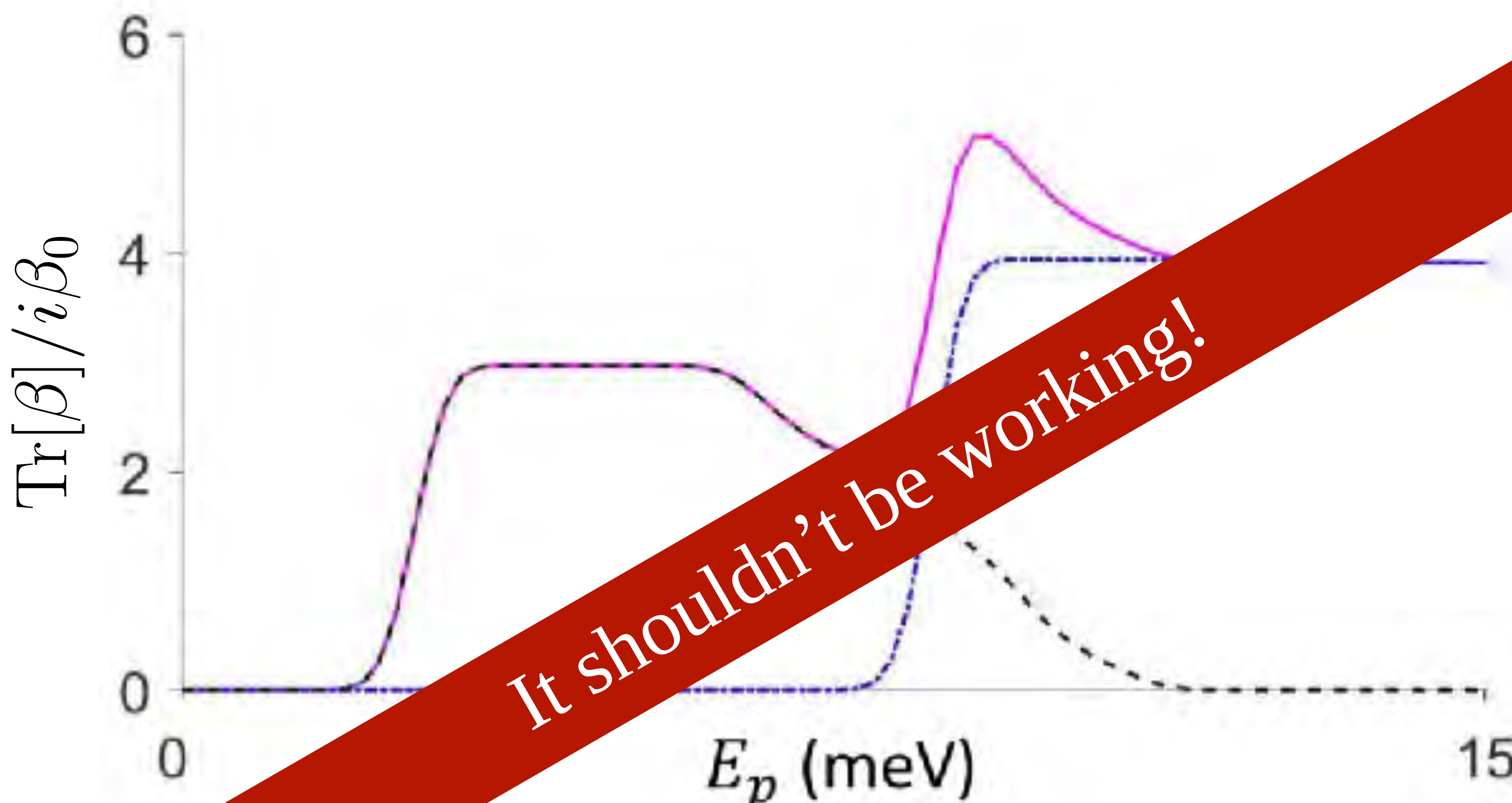

It shouldn't be working!

RhSi

Chang et. al PRL '17

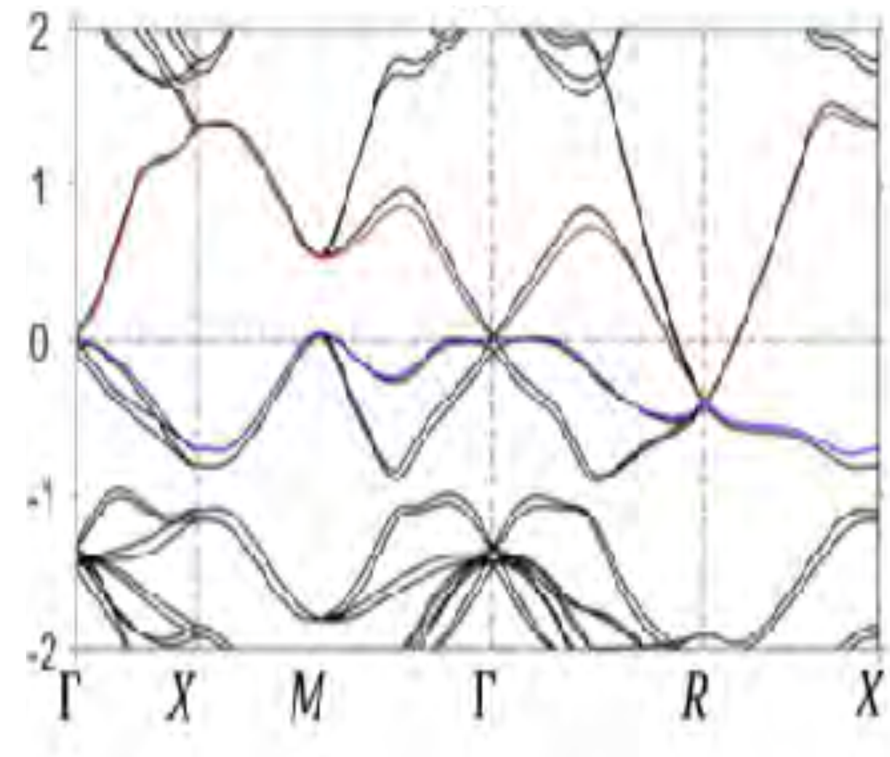

multi-band correction

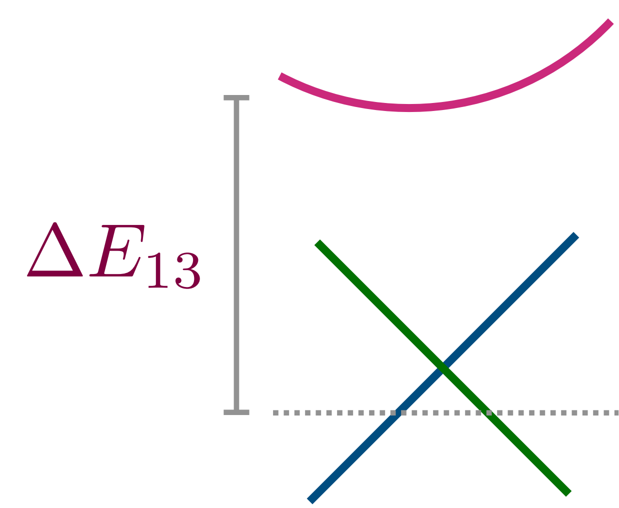

$$+\mathcal{O}\left(\frac{\omega^2}{\Delta E^2}\right)$$

Quantized injection with multifold fermions

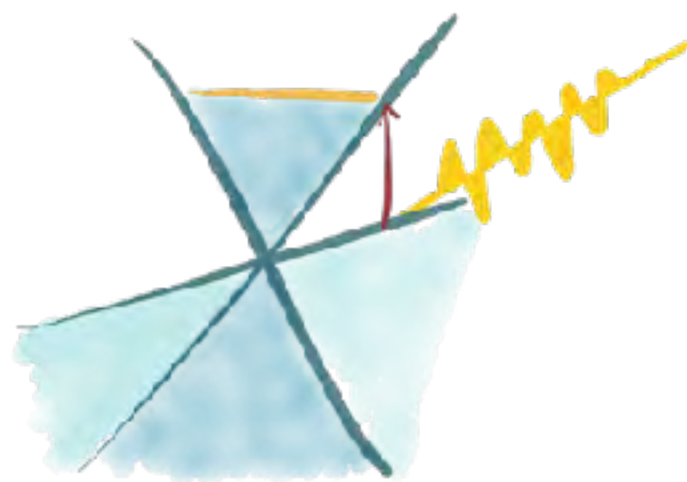

Felix Flicker, Fernando de Juan, Takahiro Morimoto

Maia Vergniory, Barry Bradlyn

Types of multifold fermions

2-fold = Weyl

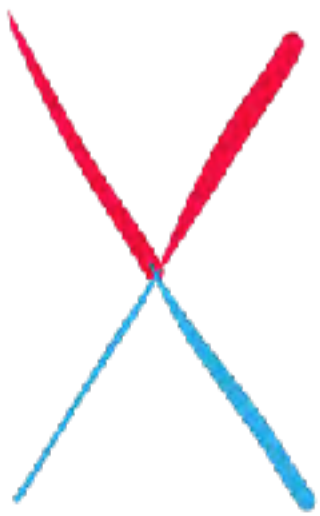

C_n

1

0

-1

Types of multifold fermions

2-fold = Weyl

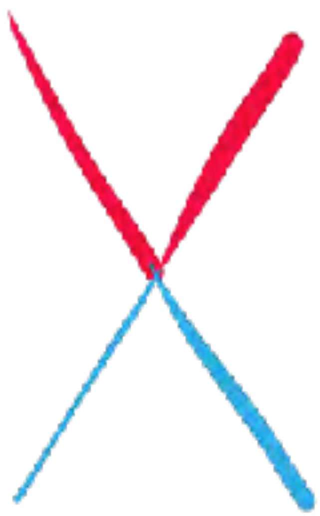

4-fold

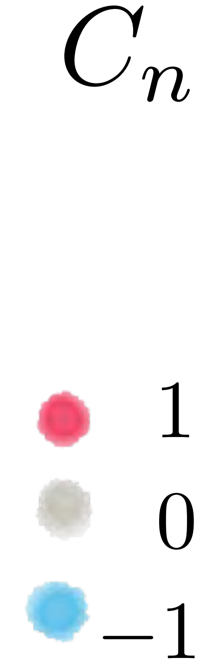

Bradlyn, Cano, Wang, Vergniory et al Science (2016)
Wieder, Kim et. al. PRL (2016)   Tao, Zhou, Zhang 1706.03817

Types of multifold fermions

2-fold = Weyl

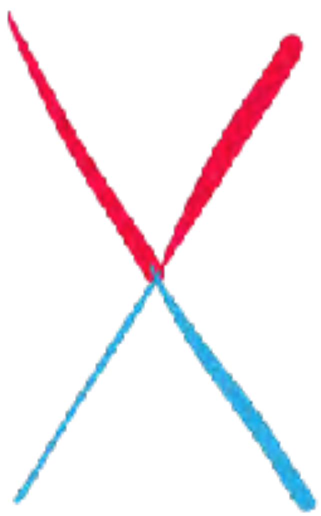

4-fold

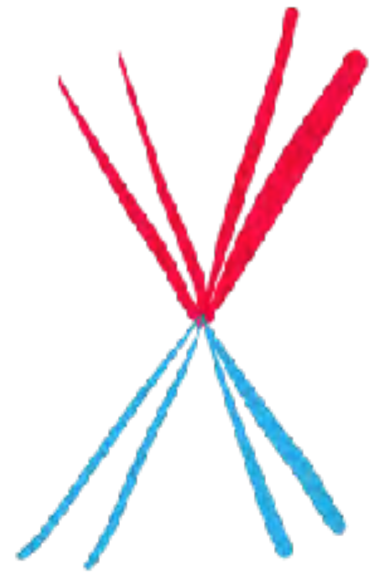

3-fold

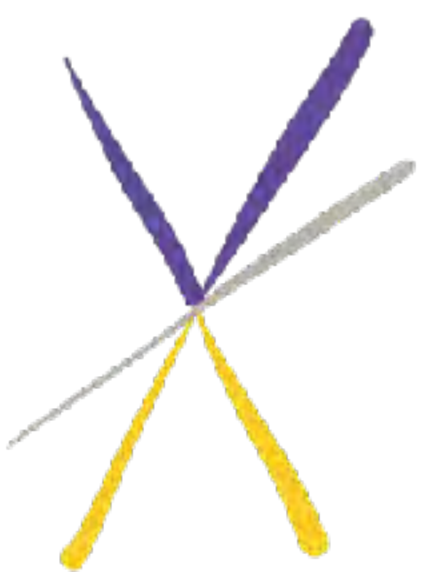

Bradlyn, Cano, Wang, Vergniory et al Science (2016)

Wieder, Kim et. al. PRL (2016)   Tao, Zhou, Zhang 1706.03817

Types of multifold fermions

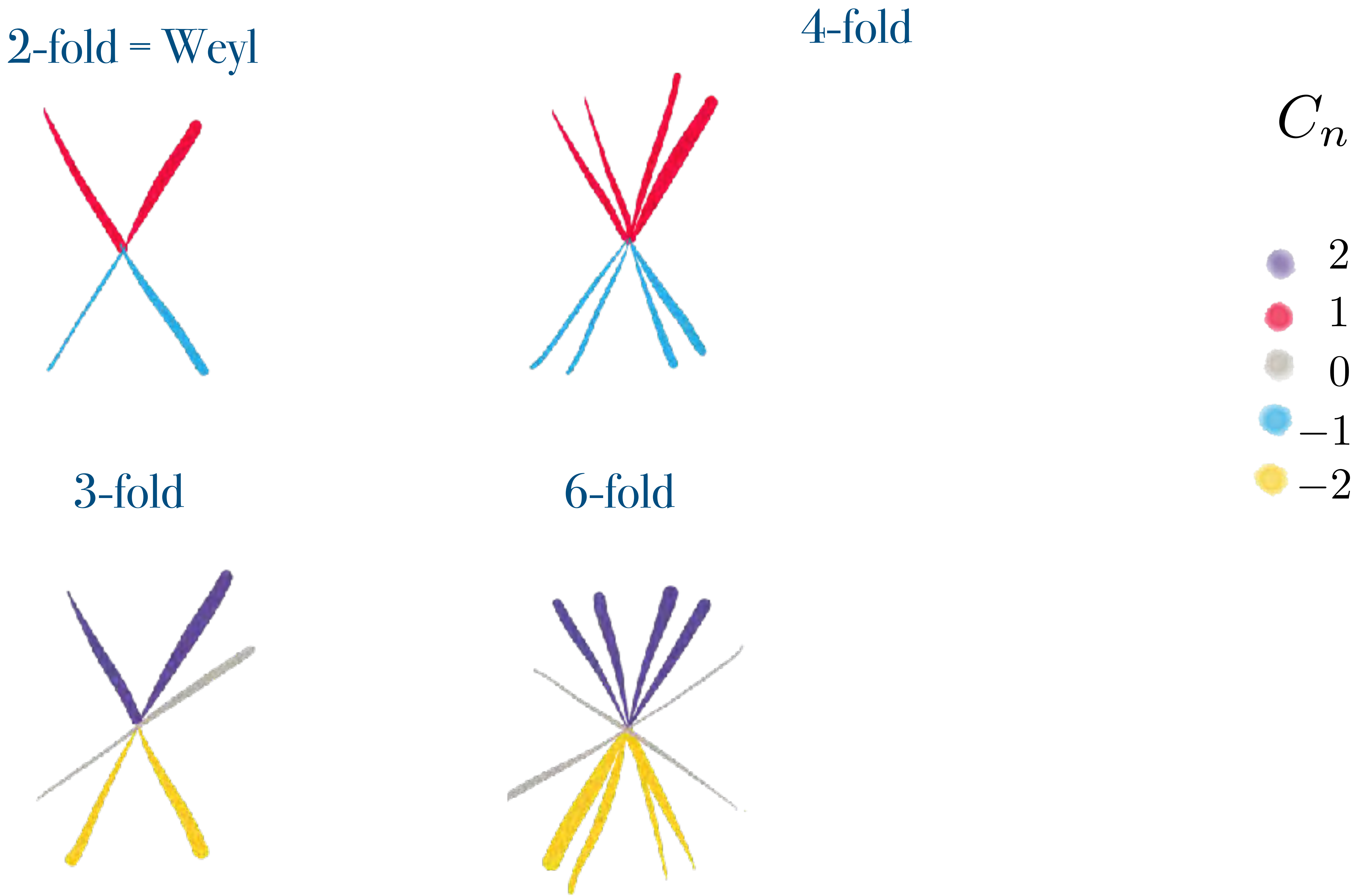

Bradlyn, Cano, Wang, Vergniory et al Science (2016)

Wieder, Kim et. al. PRL (2016) Tao, Zhou, Zhang 1706.03817

Types of multifold fermions

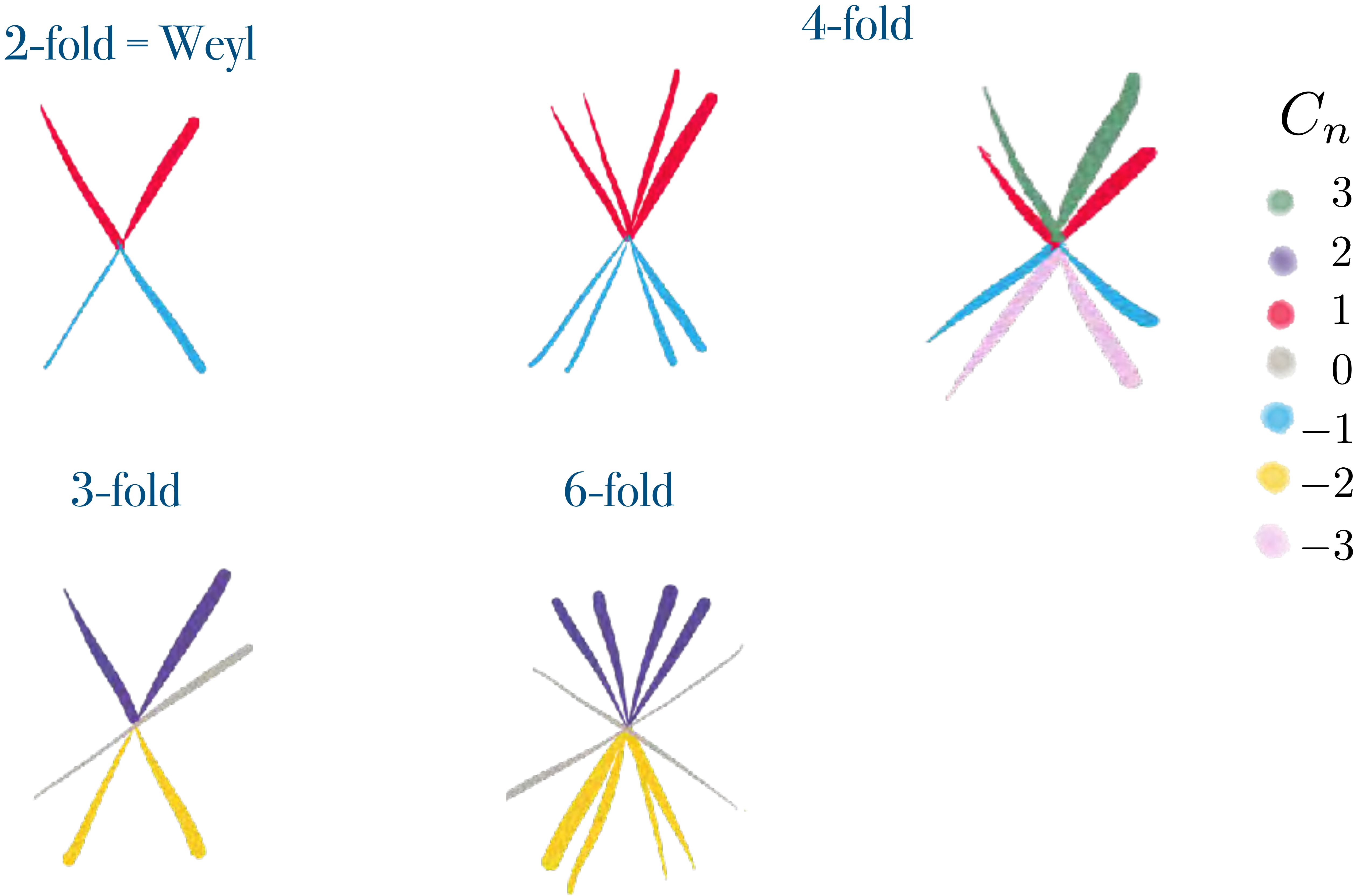

Bradlyn, Cano, Wang, Vergniory et al Science (2016)

Wieder, Kim et. al. PRL (2016)   Tao, Zhou, Zhang 1706.03817

Types of multifold fermions

2-fold = Weyl

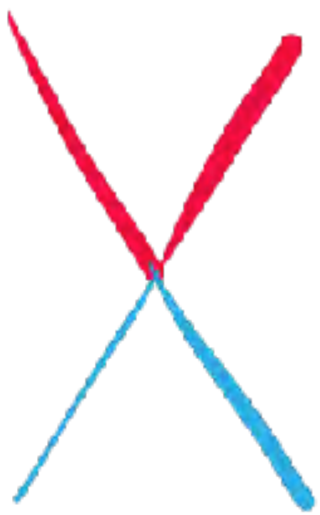

4-fold

3-fold

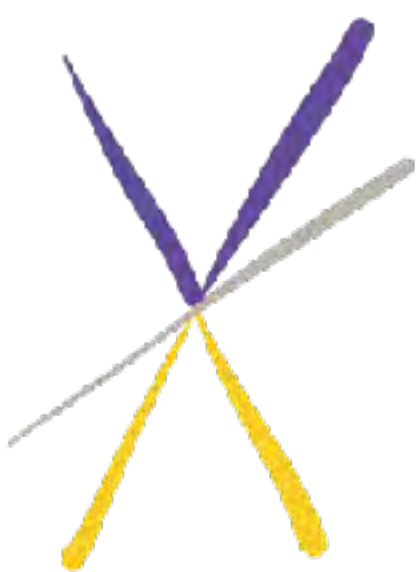

6-fold

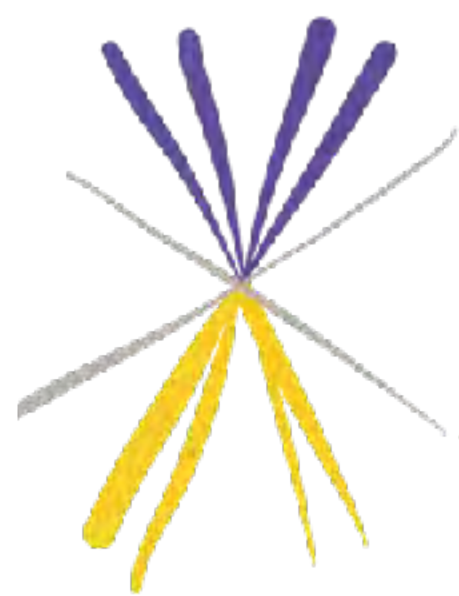

8-fold

Bradlyn, Cano, Wang, Vergniory et al Science (2016)
Wieder, Kim et. al. PRL (2016) Tao, Zhou, Zhang 1706.03817

Types of **chiral** multifold fermions

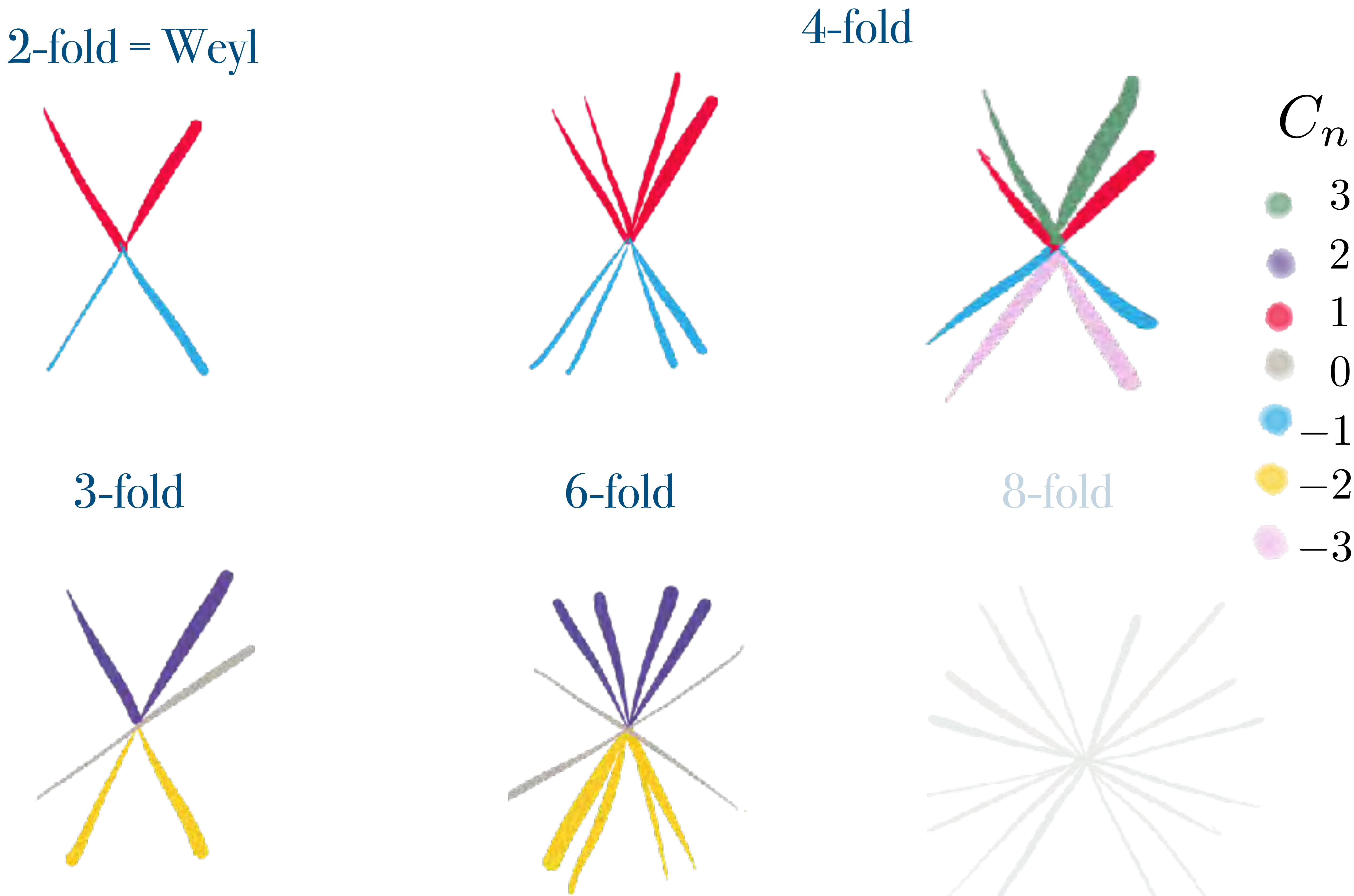

Bradlyn, Cano, Wang, Vergniory et al Science (2016)
Wieder, Kim et. al. PRL (2016) Tao, Zhou, Zhang 1706.03817

Space groups that host chiral multifold fermions

node	C_n	No SO	SO
Threefold (spin-1)	$-2, 0, 2$	$195-199,\ 207-214$	$199, 214$
Sixfold (doubled spin-1)	$(-2, 0, 2) \times 2$	–	$198, 212, 213$
Fourfold (spin-3/2)	$-3, -1, 1, 3$	–	$195-199\ ,\ 207-214$
Fourfold (doubled spin-1/2)	$(-1, 1) \times 2$	$19, 92, 96, 198, 212, 213$	$18, 19, 90, 92, 94, 96, 198, 212, 213$

Space groups that host chiral multifold fermions

node	C_n	No SO	SO
Threefold (spin-1)	$-2, 0, 2$	$195-199,\ 207-214$	$199, 214$
Sixfold (doubled spin-1)	$(-2, 0, 2) \times 2$	–	$198, 212, 213$
Fourfold (spin-3/2)	$-3, -1, 1, 3$	–	$195-199\ ,\ 207-214$
Fourfold (doubled spin-1/2)	$(-1, 1) \times 2$	$19, 92, 96, 198, 212, 213$	$18, 19, 90, 92, 94, 96, 198, 212, 213$

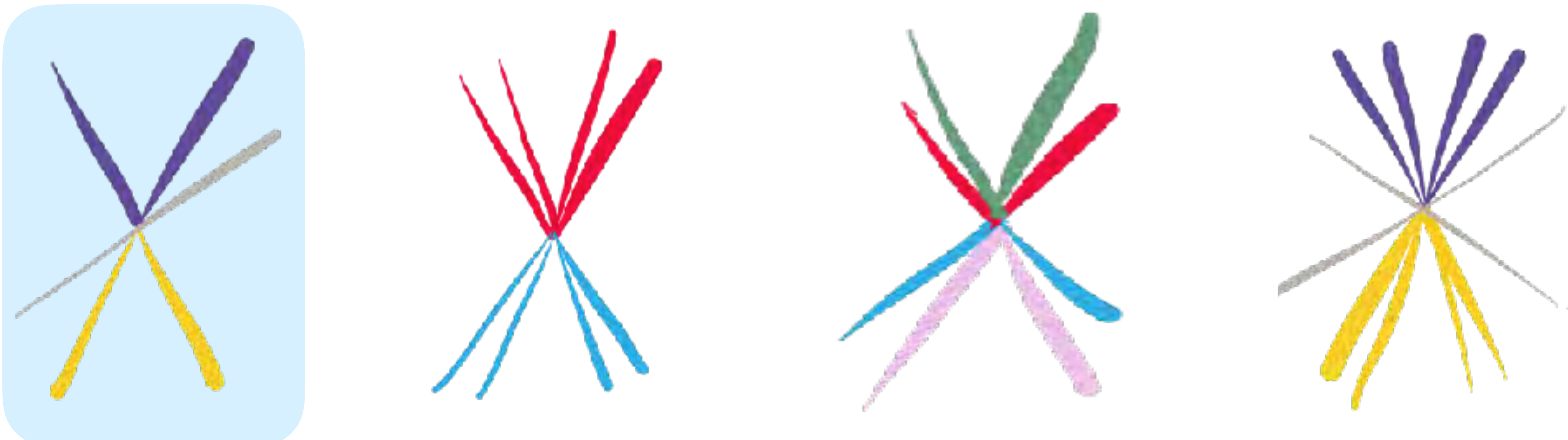

Space groups that host chiral multifold fermions

node	C_n	No SO	SO
Threefold (spin-1)	$-2, 0, 2$	$195-199,\ 207-214$	$199, 214$
Sixfold (doubled spin-1)	$(-2, 0, 2) \times 2$	–	$198, 212, 213$
Fourfold (spin-3/2)	$-3, -1, 1, 3$	–	$195-199\ ,\ 207-214$
Fourfold (doubled spin-1/2)	$(-1, 1) \times 2$	$19, 92, 96, 198, 212, 213$	$18, 19, 90, 92, 94, 96, 198, 212, 213$

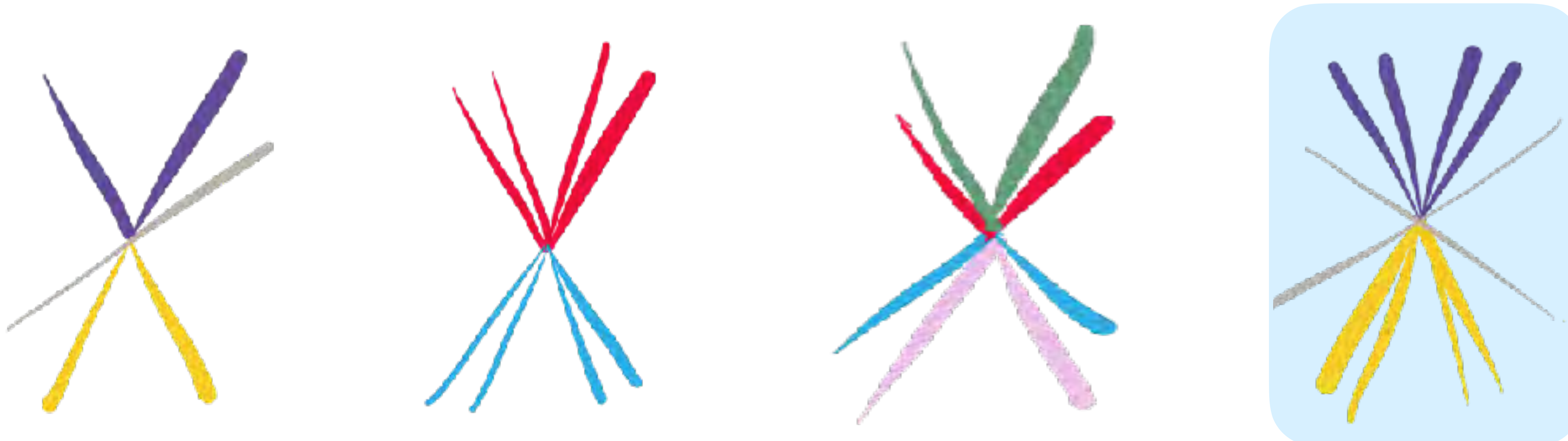

Space groups that host chiral multifold fermions

node	C_n	No SO	SO
Threefold (spin-1)	$-2, 0, 2$	$195-199,\ 207-214$	$199, 214$
Sixfold (doubled spin-1)	$(-2, 0, 2) \times 2$	–	$198, 212, 213$
Fourfold (spin-3/2)	$-3, -1, 1, 3$	–	$195-199\ ,\ 207-214$
Fourfold (doubled spin-1/2)	$(-1, 1) \times 2$	$19, 92, 96, 198, 212, 213$	$18, 19, 90, 92, 94, 96, 198, 212, 213$

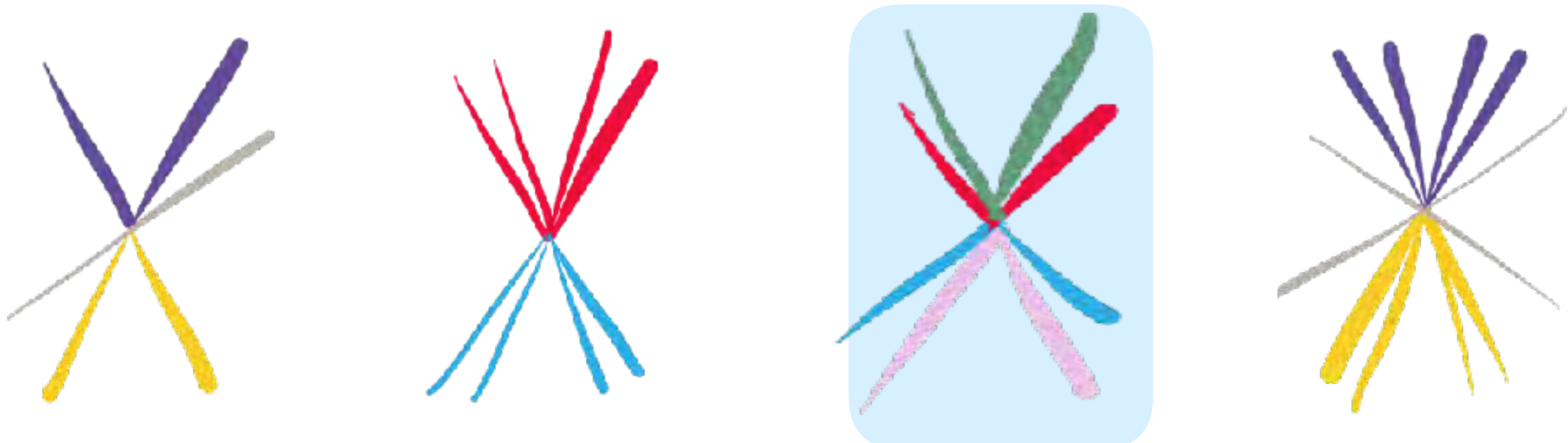

Space groups that host chiral multifold fermions

node	C_n	No SO	SO
Threefold (spin-1)	$-2, 0, 2$	$195-199,\ 207-214$	$199, 214$
Sixfold (doubled spin-1)	$(-2, 0, 2) \times 2$	–	$198, 212, 213$
Fourfold (spin-3/2)	$-3, -1, 1, 3$	–	$195-199\ ,\ 207-214$
Fourfold (doubled spin-1/2)	$(-1, 1) \times 2$	$19, 92, 96, 198, 212, 213$	$18, 19, 90, 92, 94, 96, 198, 212, 213$

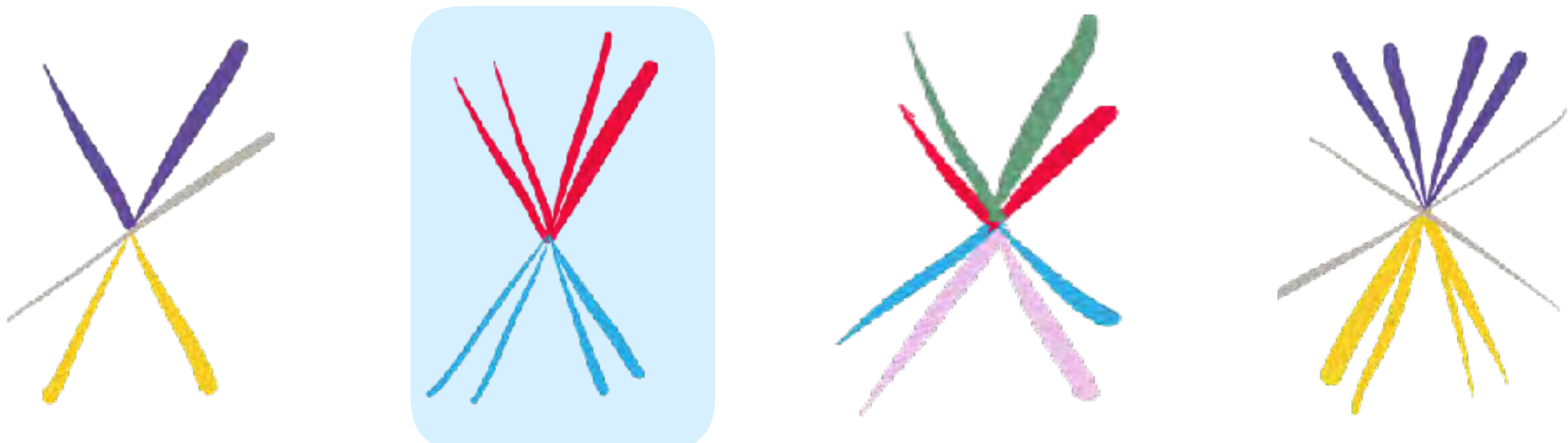

Space groups that host chiral multifold fermions

node	C_n	No SO	SO
Threefold (spin-1)	$-2, 0, 2$	$195-199,\ 207-214$	$199, 214$
Sixfold (doubled spin-1)	$(-2, 0, 2) \times 2$	–	$198, 212, 213$
Fourfold (spin-3/2)	$-3, -1, 1, 3$	–	$195-199\ ,\ 207-214$
Fourfold (doubled spin-1/2)	$(-1, 1) \times 2$	$19, 92, 96, 198, 212, 213$	$18, 19, 90, 92, 94, 96, 198, 212, 213$

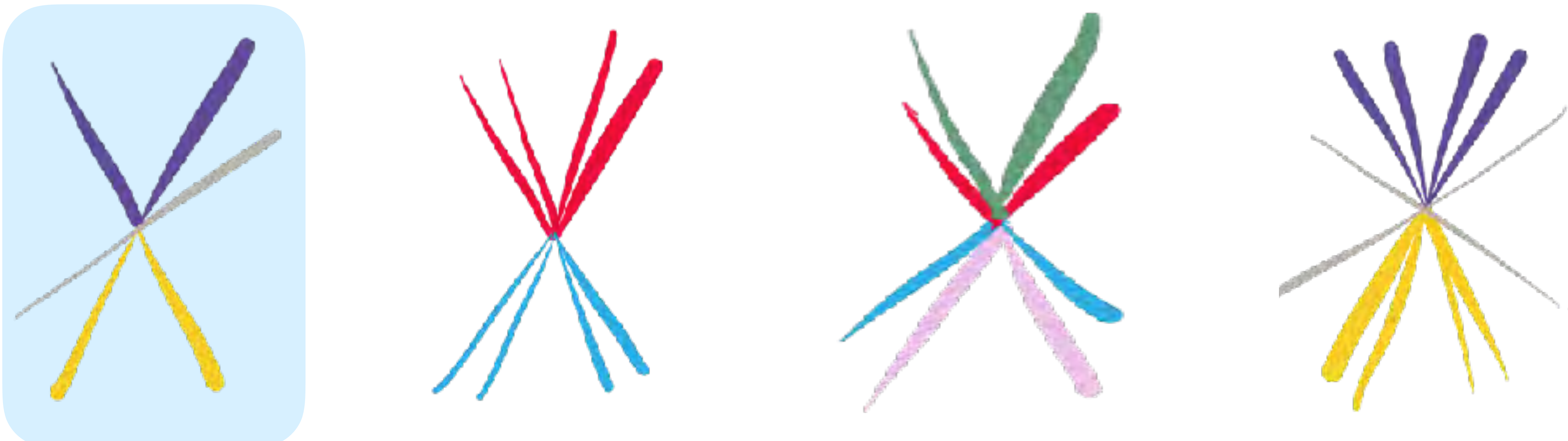

Three-fold fermion

node	C_n	No SO	SO
Threefold (spin-1)	$-2, 0, 2$	$195-199,\ 207-214$	$199, 214$

SG $195 - 199, 207 - 214$

Three-fold fermion

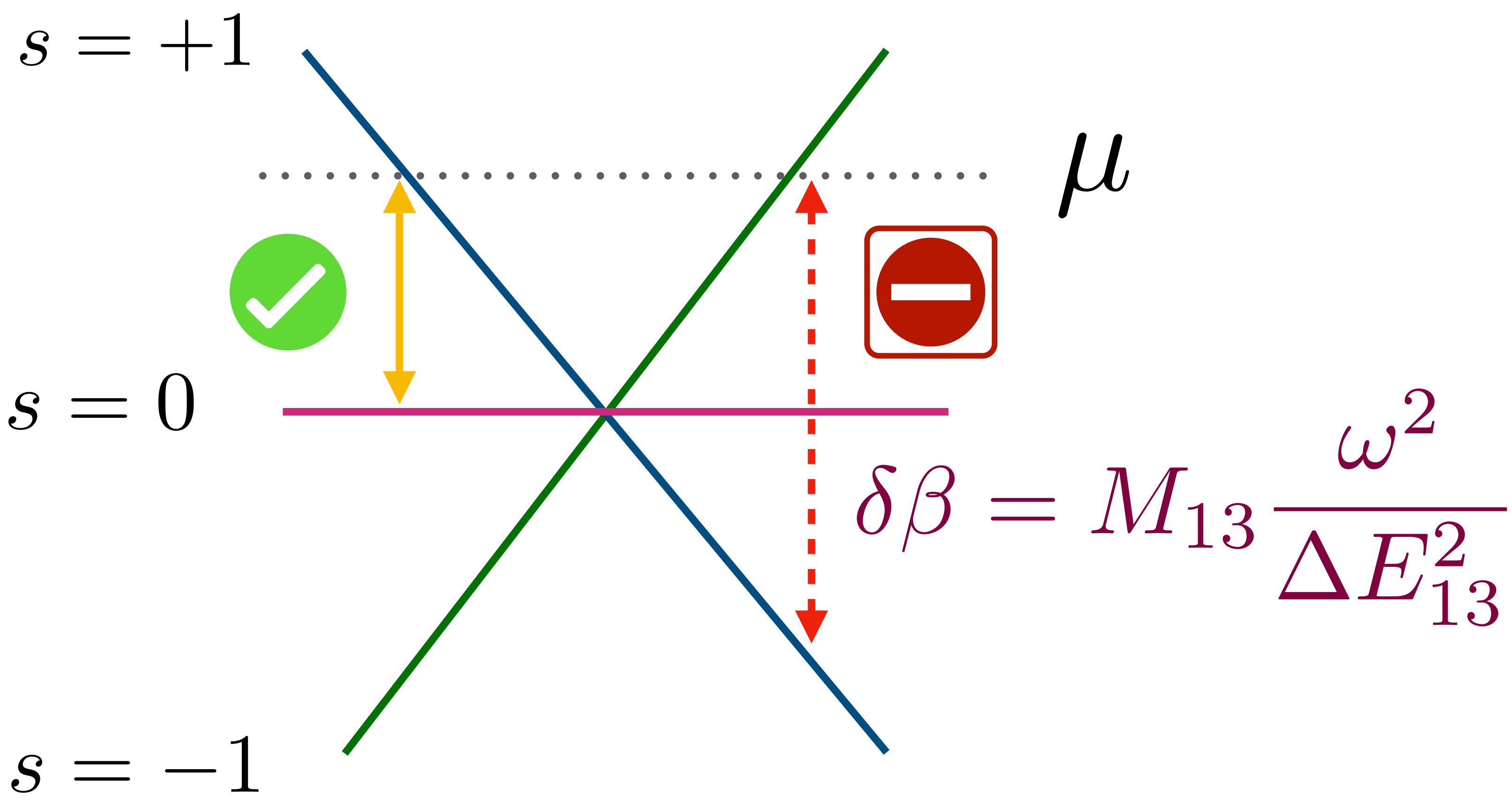

$$H = \mathbf{k} \cdot \boldsymbol{S}$$

e.g. SG 199 at the Γ point with no spin-orbit

Three-fold fermion

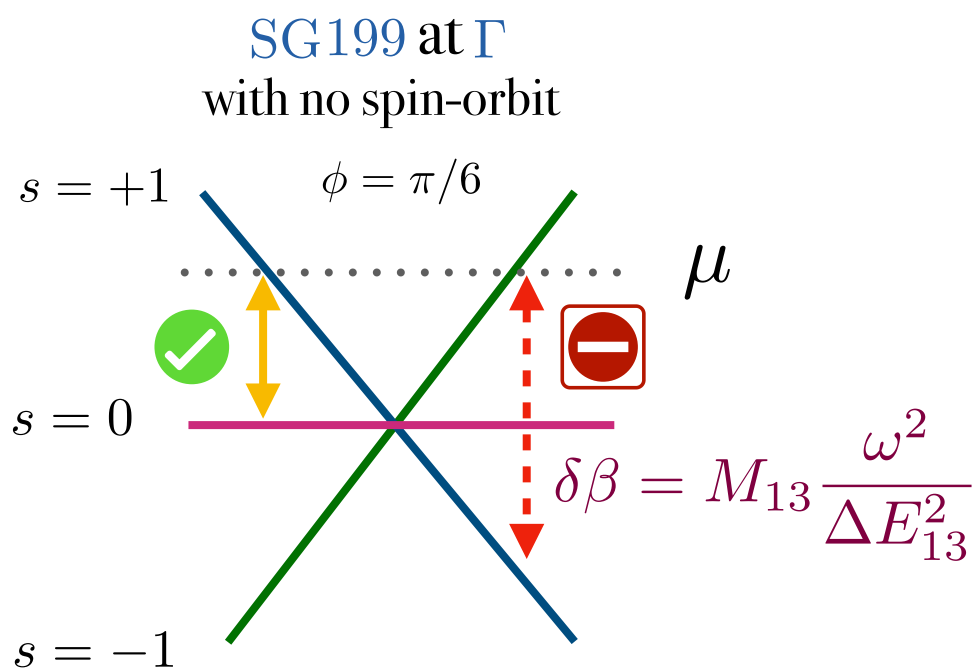

$$H = \mathbf{k} \cdot \boldsymbol{S}$$

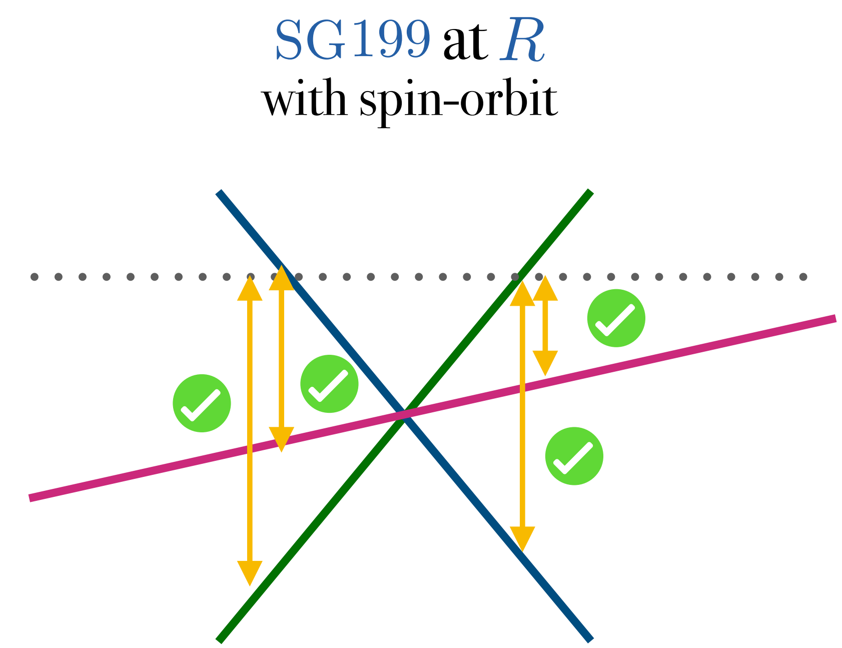

$$H \neq \mathbf{k} \cdot \boldsymbol{S}$$

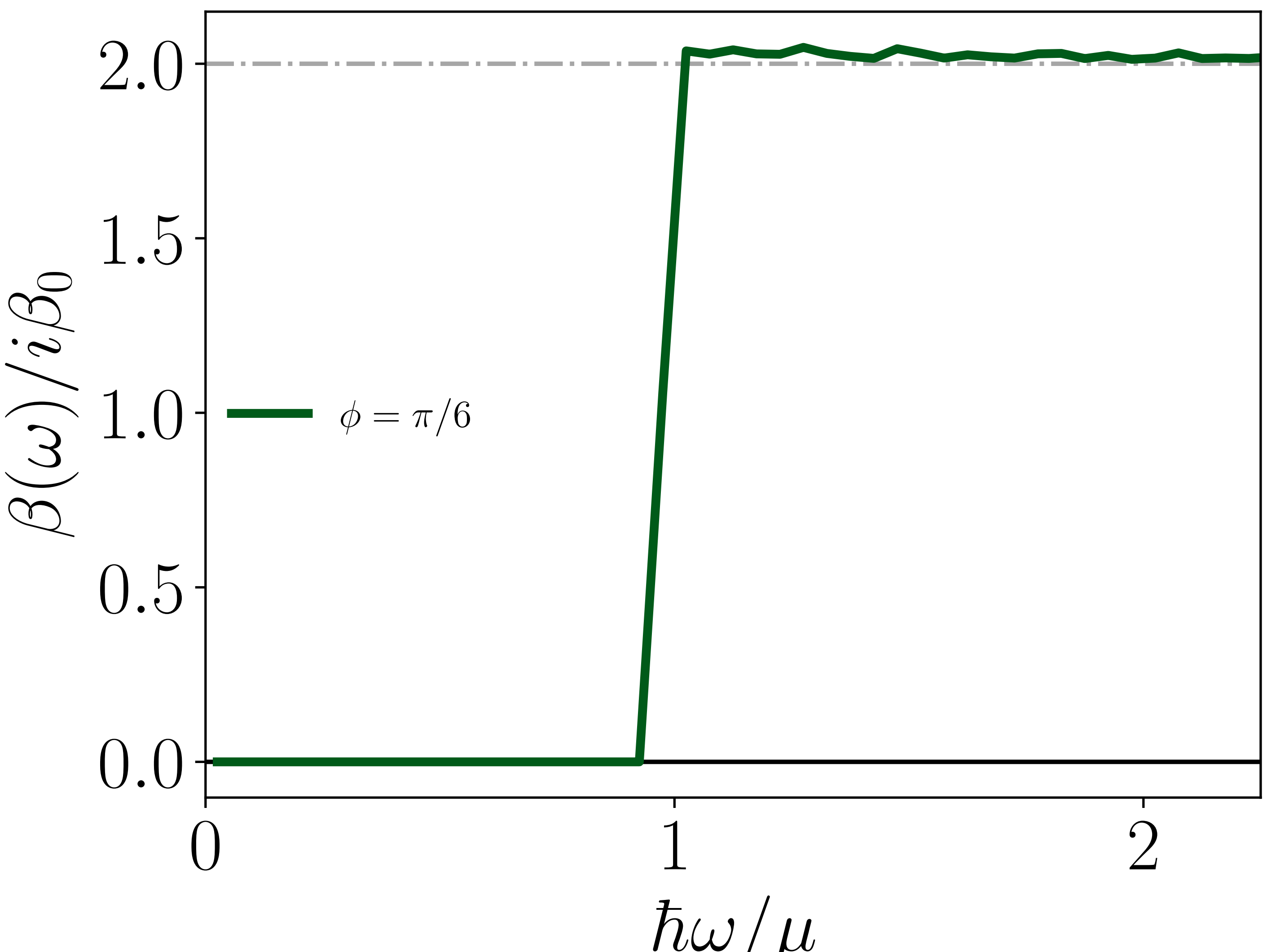

$$H_{3\mathrm{f}} = \begin{pmatrix} \mu & e^{i\phi}k_x & e^{-i\phi}k_y \\ e^{-i\phi}k_x & \mu & e^{i\phi}k_z \\ e^{i\phi}k_y & e^{-i\phi}k_z & \mu \end{pmatrix}$$

Three-fold fermion

SG199 at Γ
with no spin-orbit

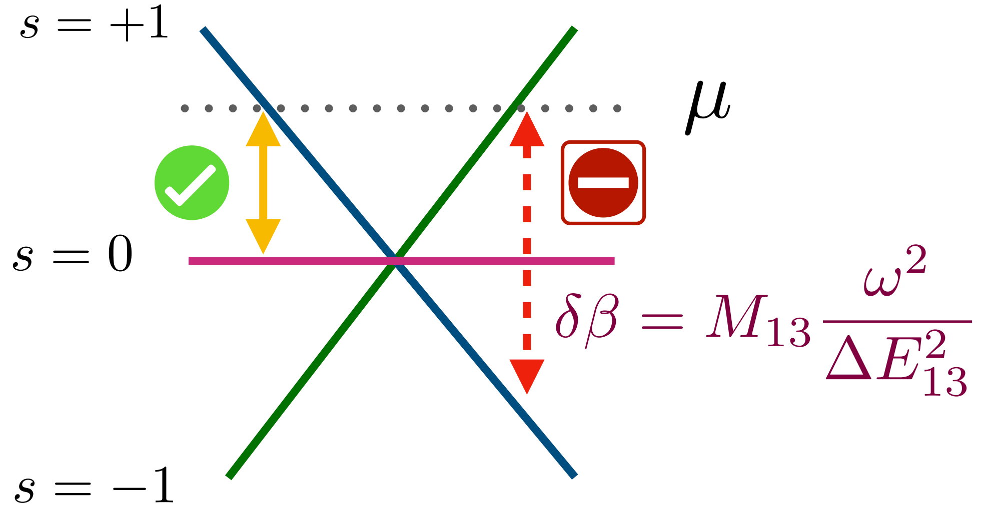

$$H = \mathbf{k}\cdot\boldsymbol{S}$$

SG199 at R
with spin-orbit

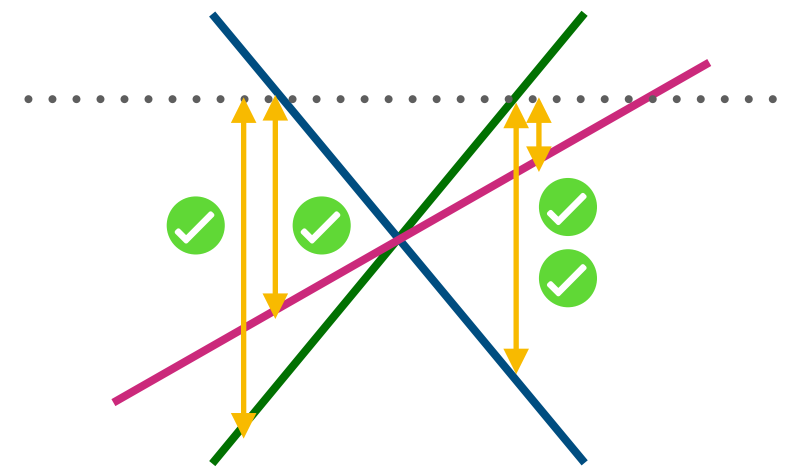

$$H \neq \mathbf{k}\cdot\boldsymbol{S}$$

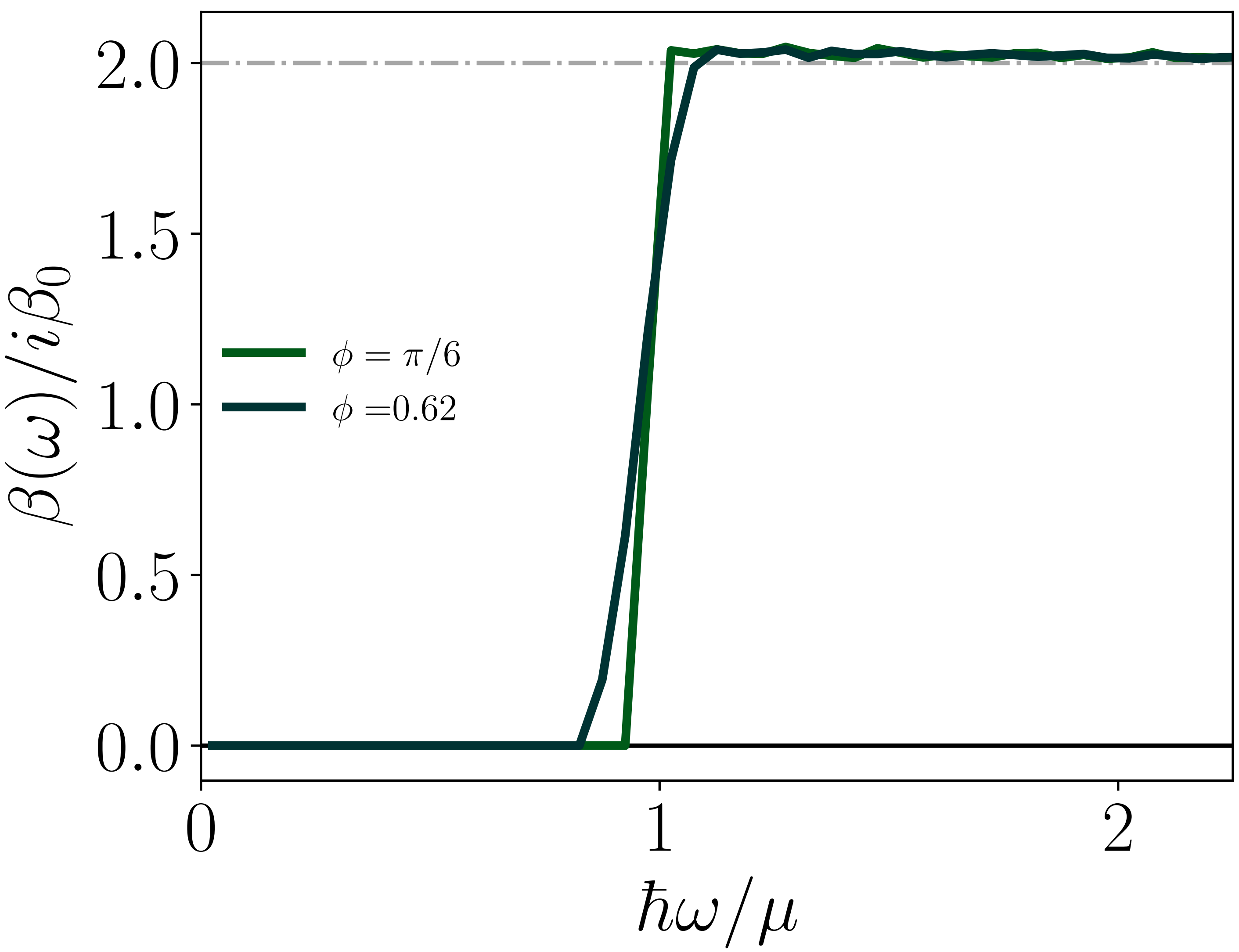

$$H_{3\mathrm{f}} = \begin{pmatrix} \mu & e^{i\phi}k_x & e^{-i\phi}k_y \\ e^{-i\phi}k_x & \mu & e^{i\phi}k_z \\ e^{i\phi}k_y & e^{-i\phi}k_z & \mu \end{pmatrix}$$

Three-fold fermion

SG199 at Γ
with no spin-orbit

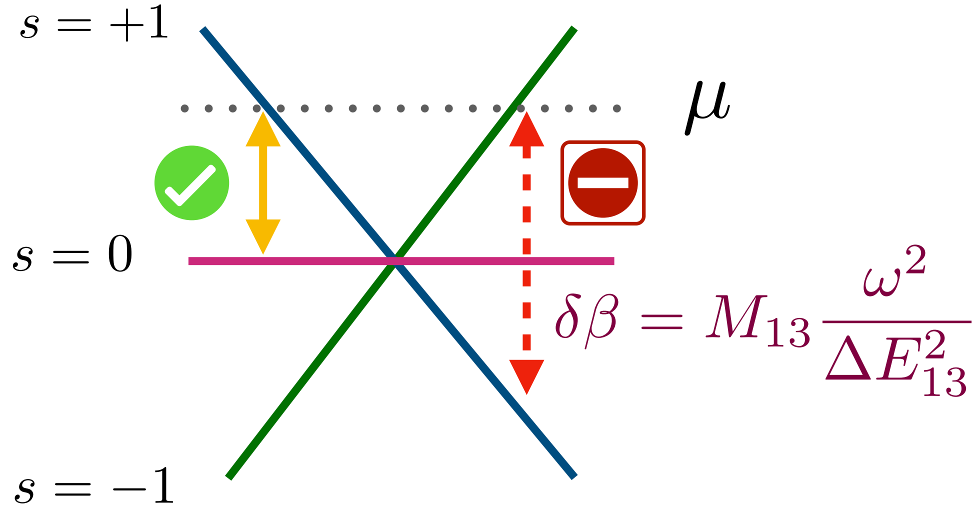

$$H = \mathbf{k} \cdot \boldsymbol{S}$$

SG199 at R
with spin-orbit

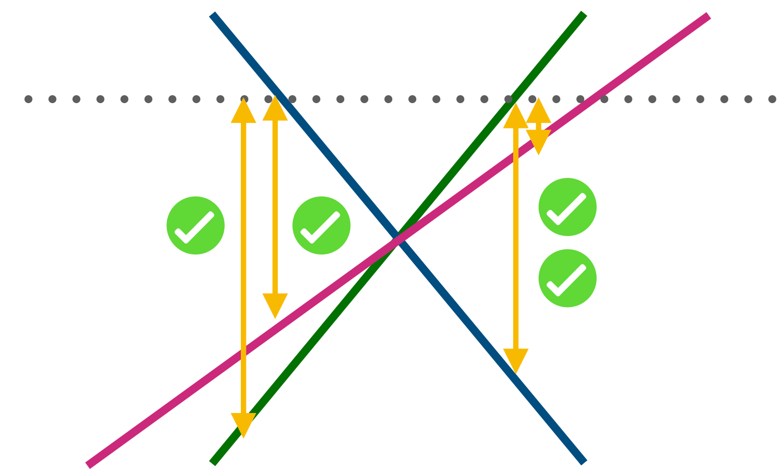

$$H \neq \mathbf{k} \cdot \boldsymbol{S}$$

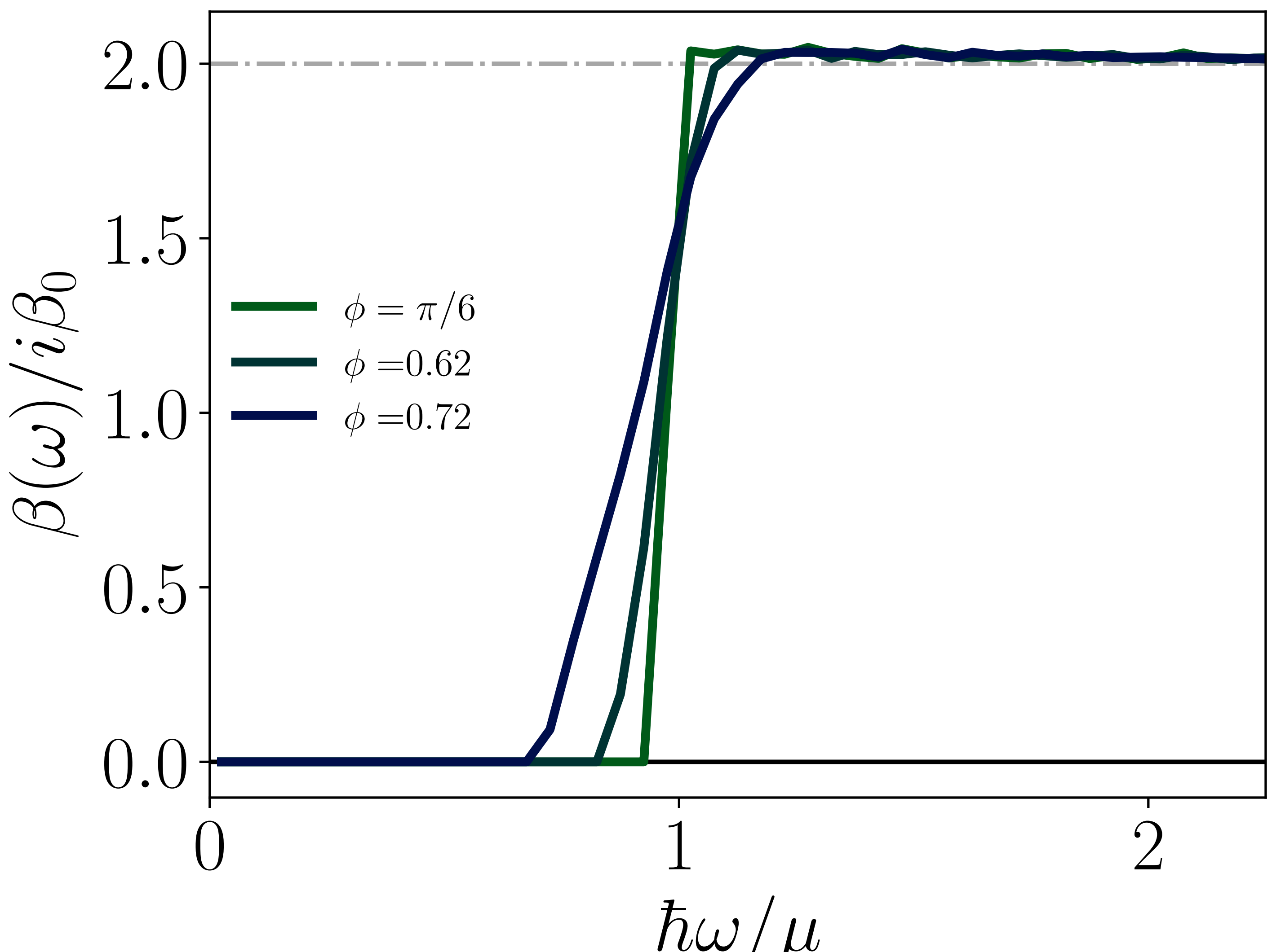

$$H_{3\mathrm{f}} = \begin{pmatrix} \mu & e^{i\phi}k_x & e^{-i\phi}k_y \\ e^{-i\phi}k_x & \mu & e^{i\phi}k_z \\ e^{i\phi}k_y & e^{-i\phi}k_z & \mu \end{pmatrix}$$

Three-fold fermion

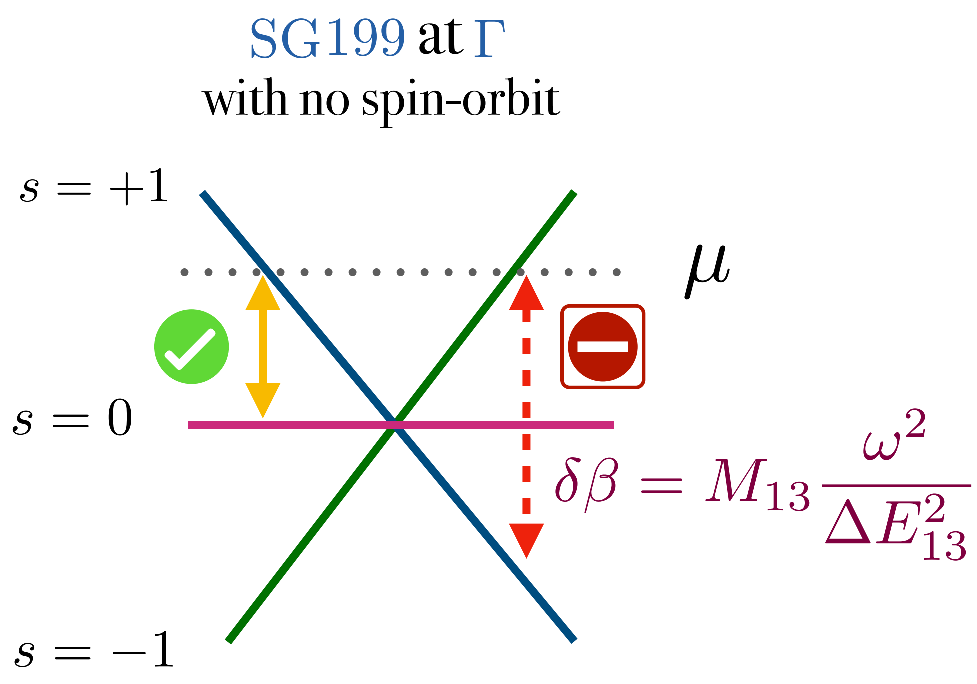

$$H = \mathbf{k} \cdot \boldsymbol{S}$$

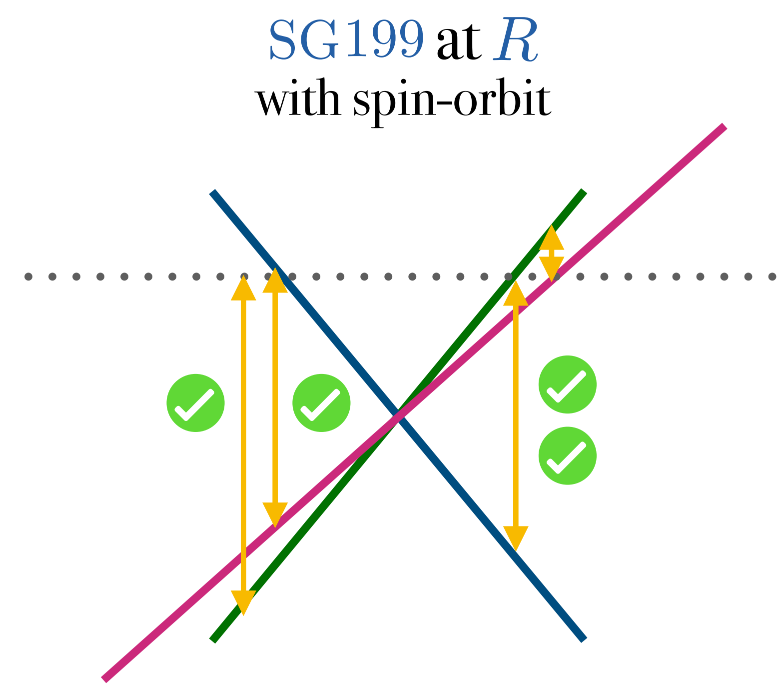

$$H \neq \mathbf{k} \cdot \boldsymbol{S}$$

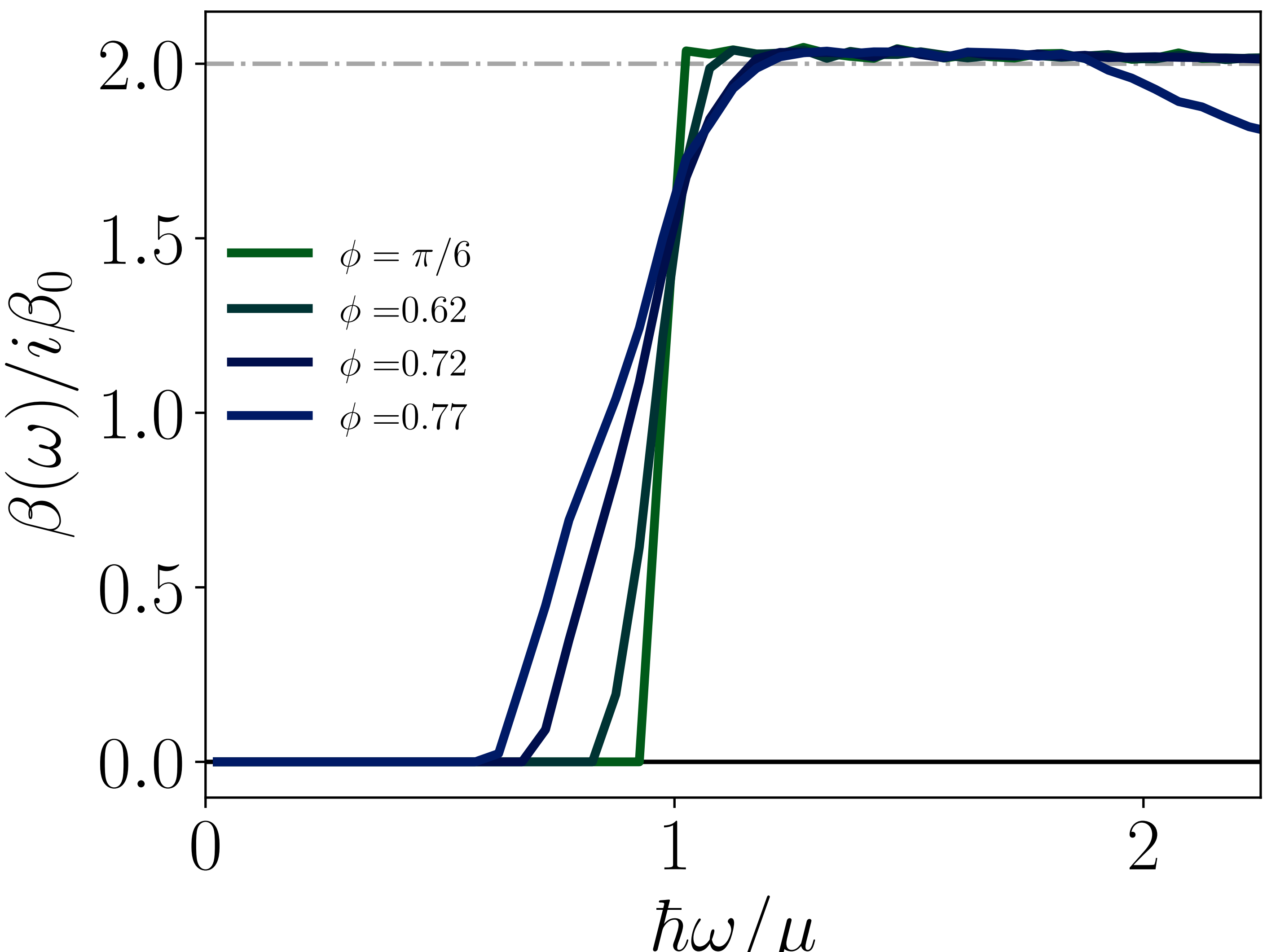

$$H_{3f} = \begin{pmatrix} \mu & e^{i\phi}k_x & e^{-i\phi}k_y \\ e^{-i\phi}k_x & \mu & e^{i\phi}k_z \\ e^{i\phi}k_y & e^{-i\phi}k_z & \mu \end{pmatrix}$$

Three-fold fermion

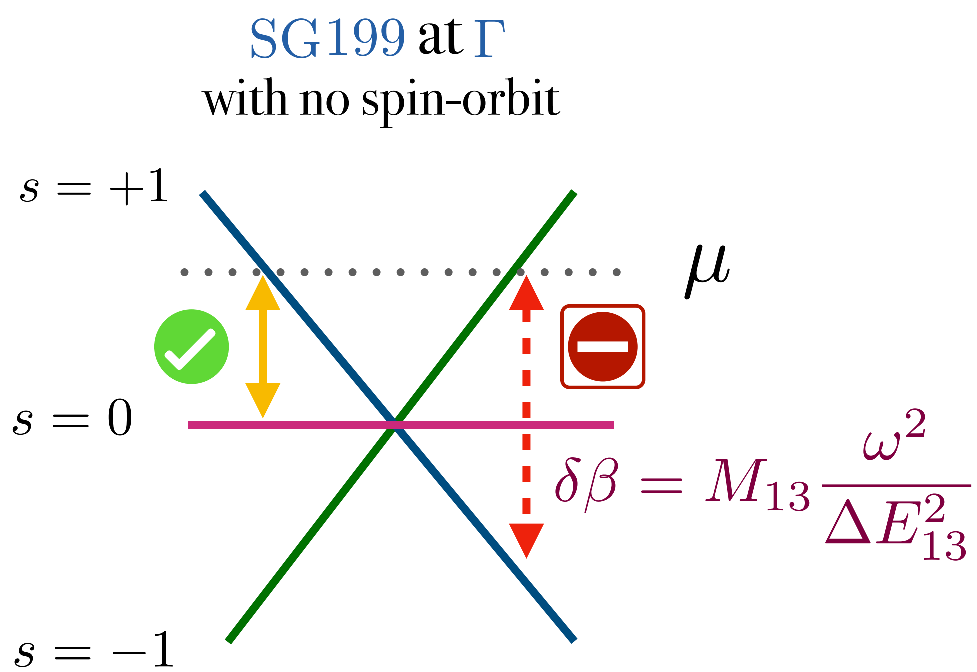

$$H = \mathbf{k}\cdot\boldsymbol{S}$$

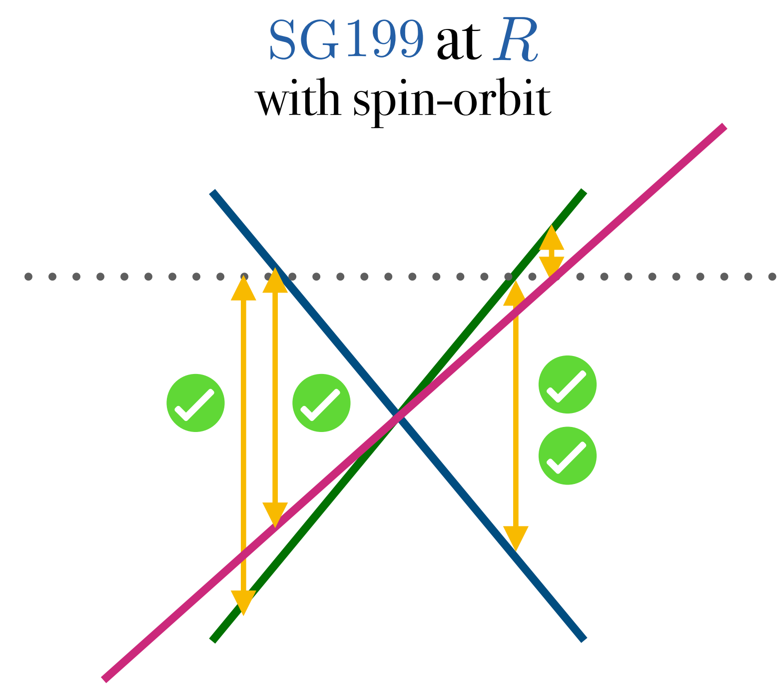

$$H \neq \mathbf{k}\cdot\boldsymbol{S}$$

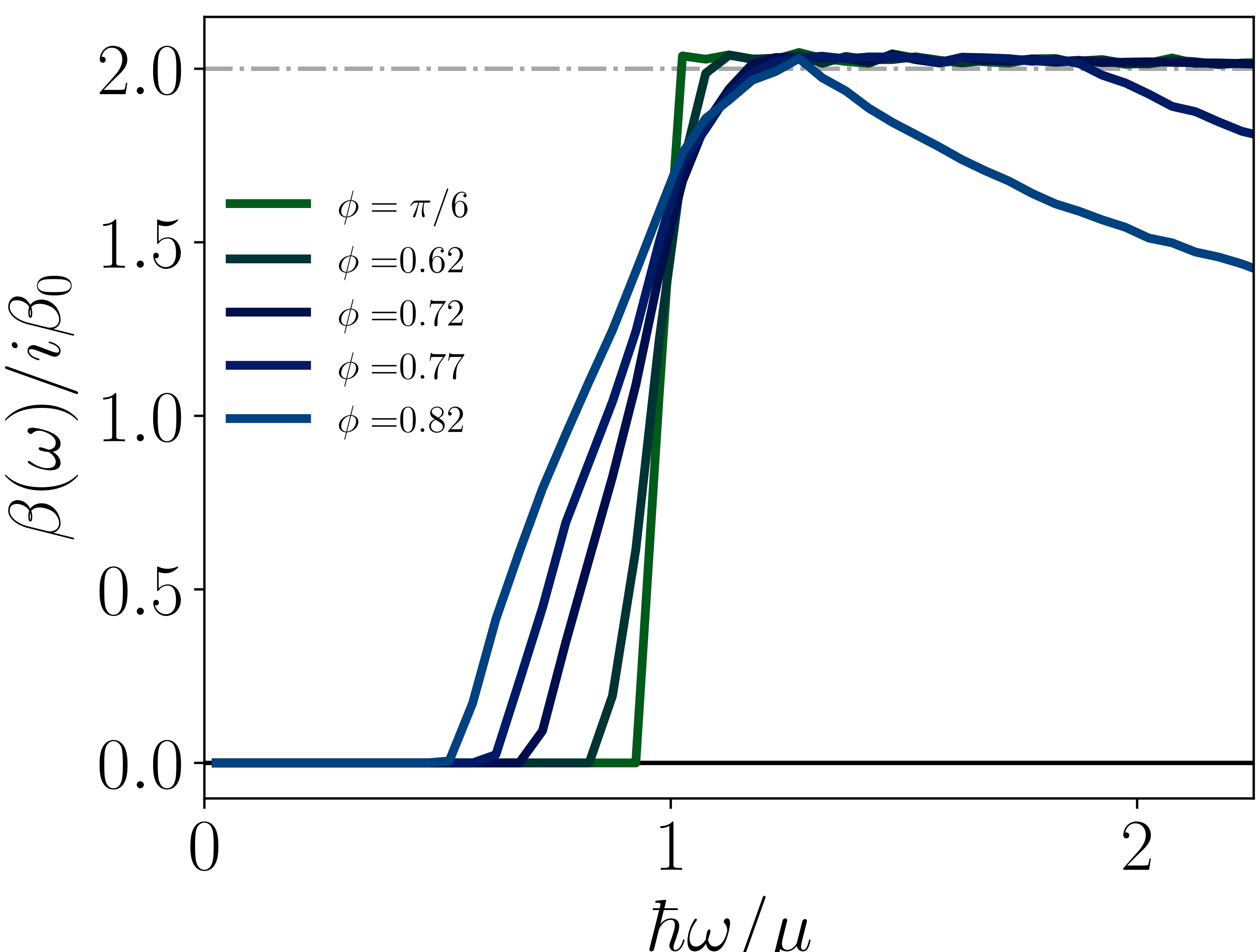

$$H_{3\mathrm{f}} = \begin{pmatrix} \mu & e^{i\phi}k_x & e^{-i\phi}k_y \\ e^{-i\phi}k_x & \mu & e^{i\phi}k_z \\ e^{i\phi}k_y & e^{-i\phi}k_z & \mu \end{pmatrix}$$

Three-fold fermion

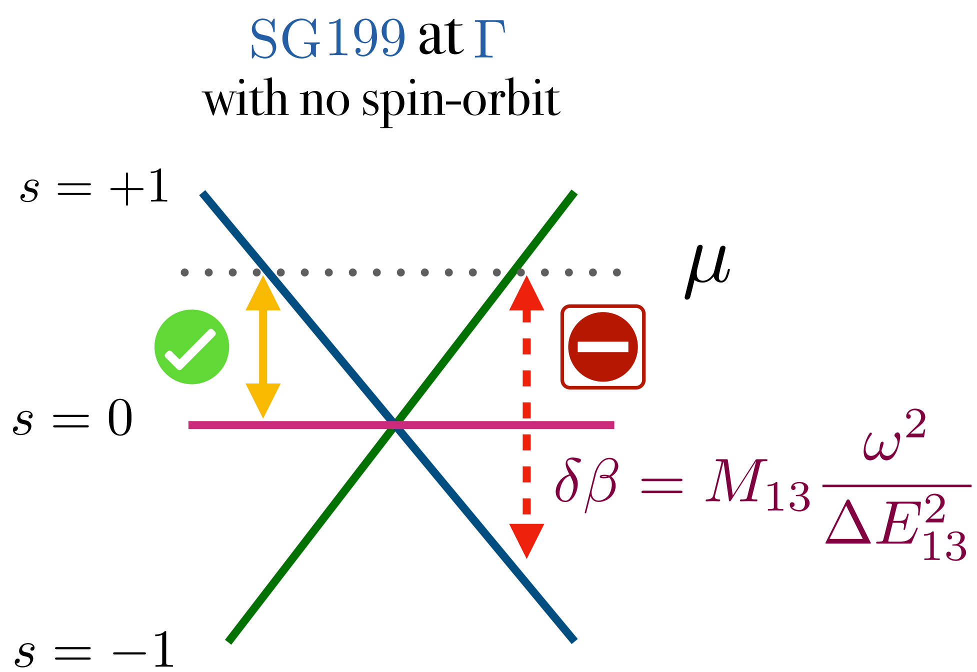

$$H = \mathbf{k}\cdot\boldsymbol{S}$$

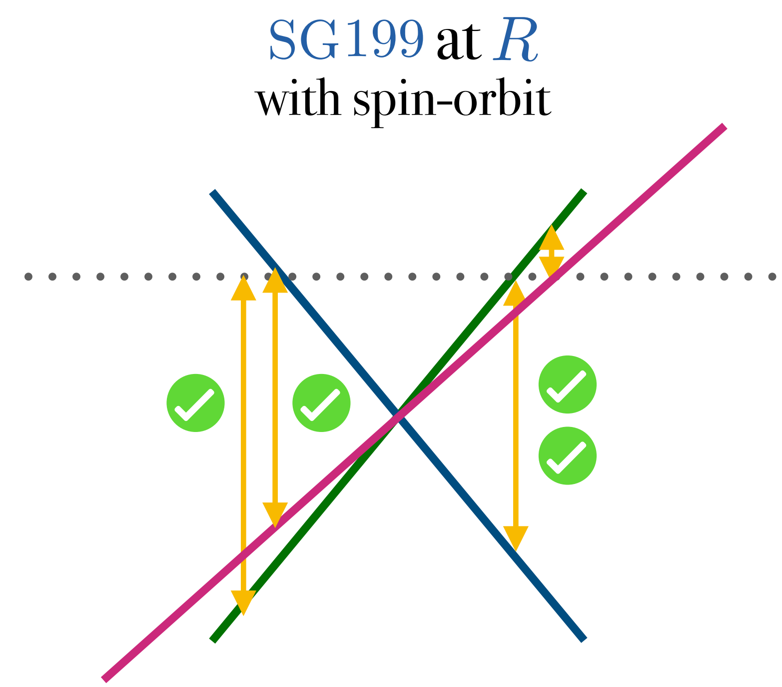

$$H \neq \mathbf{k}\cdot\boldsymbol{S}$$

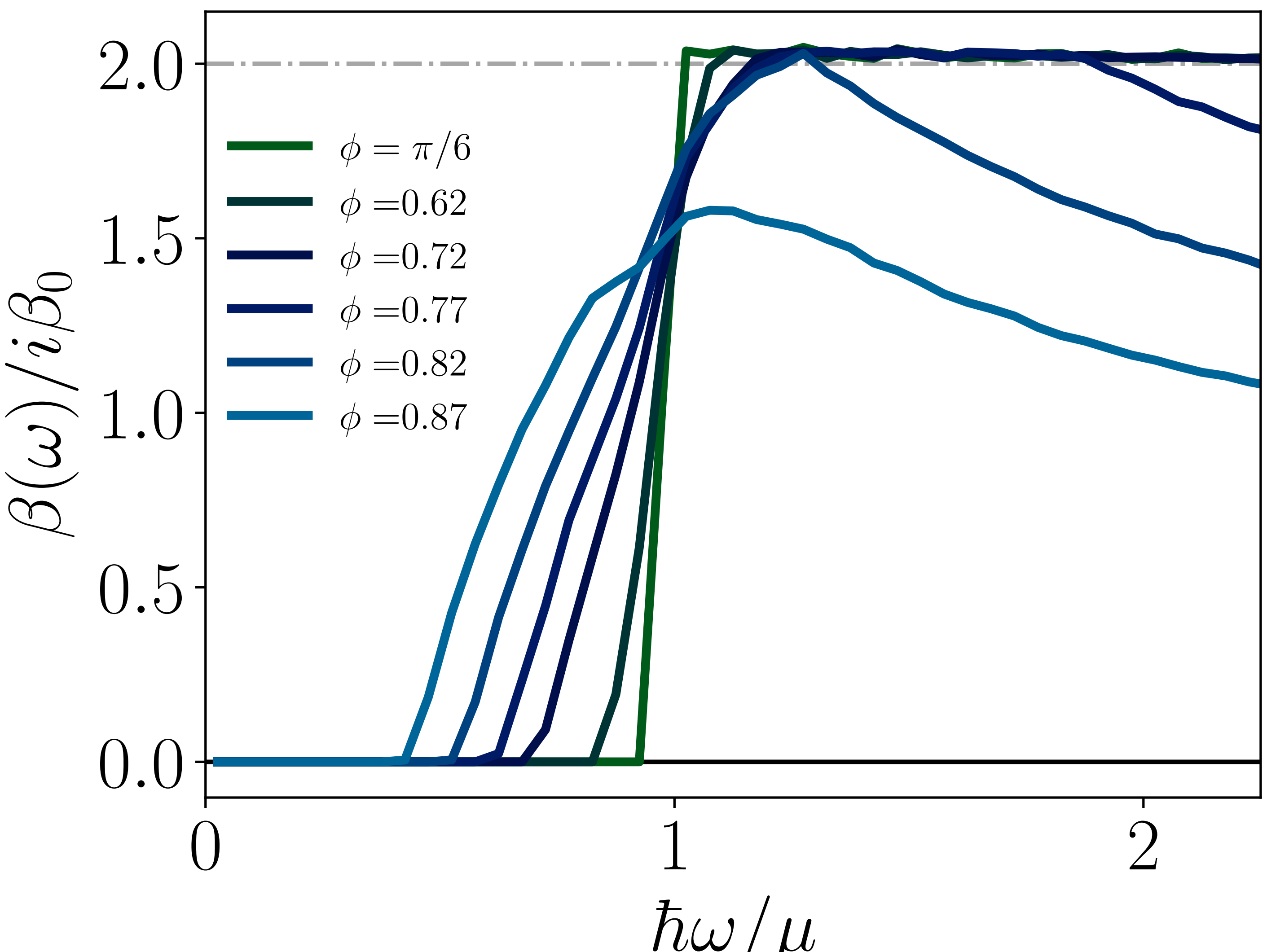

$$H_{3\mathrm{f}} = \begin{pmatrix} \mu & e^{i\phi}k_x & e^{-i\phi}k_y \\ e^{-i\phi}k_x & \mu & e^{i\phi}k_z \\ e^{i\phi}k_y & e^{-i\phi}k_z & \mu \end{pmatrix}$$

Three-fold fermion

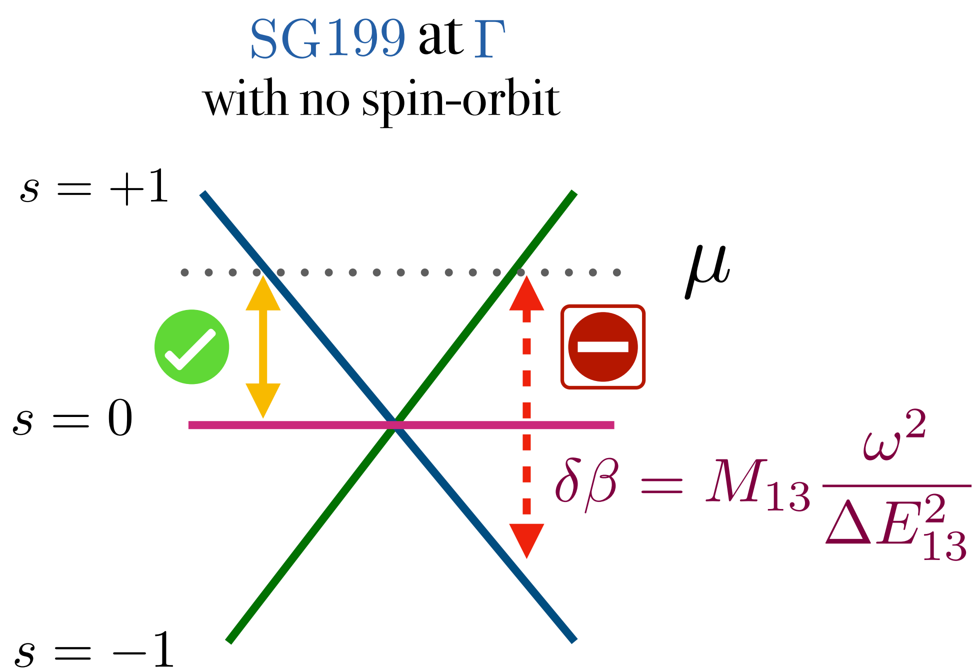

$$H = \mathbf{k}\cdot\boldsymbol{S}$$

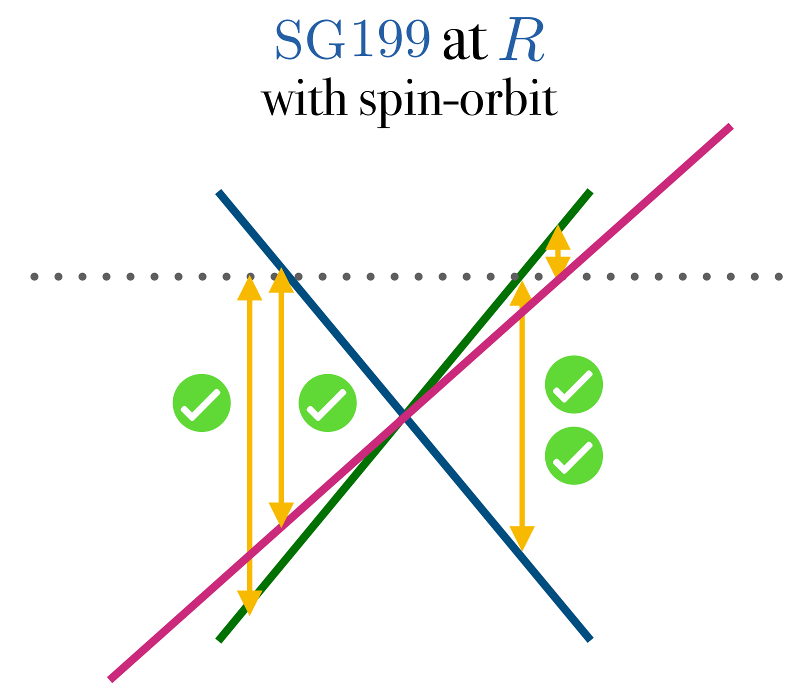

$$H \neq \mathbf{k}\cdot\boldsymbol{S}$$

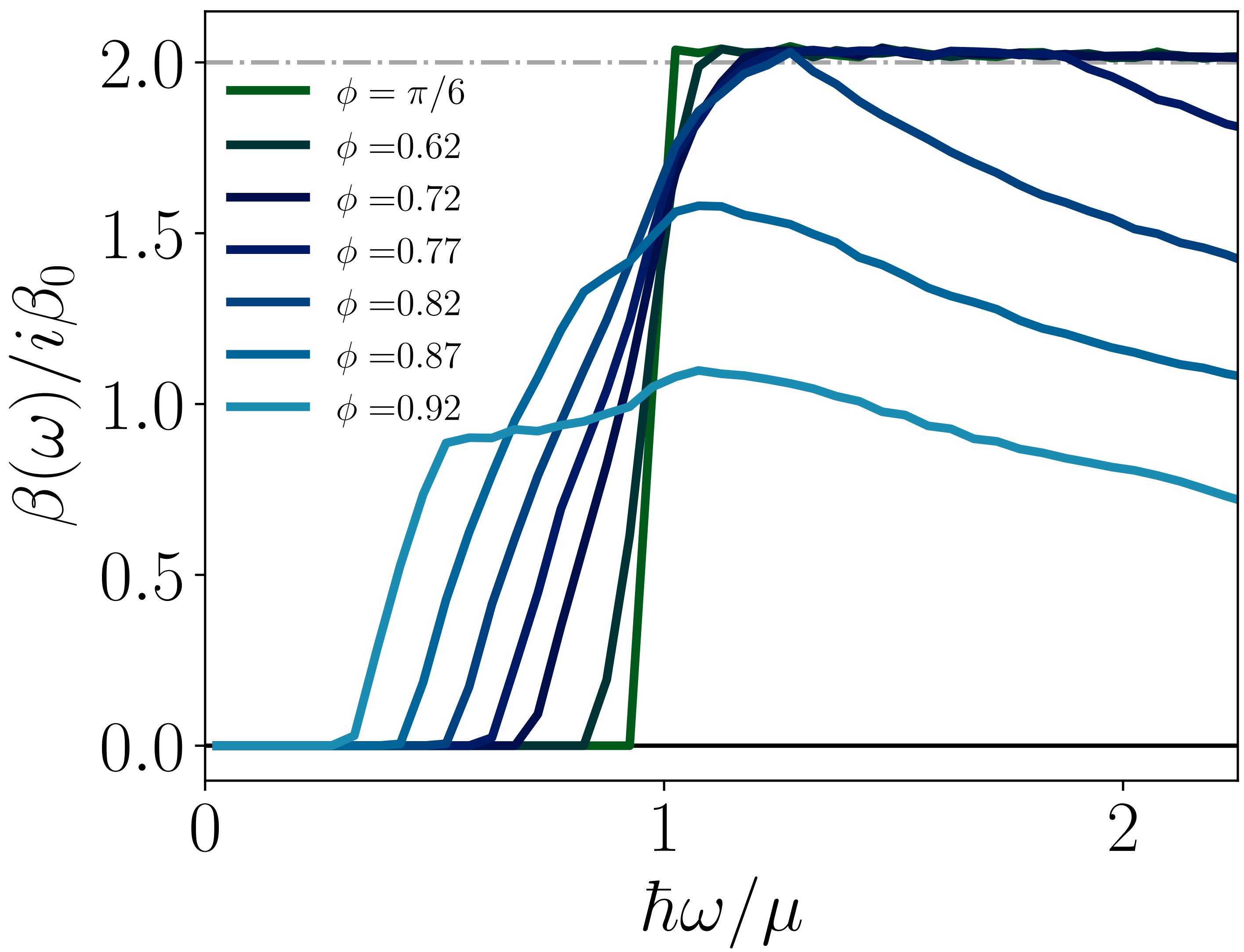

$$H_{3\mathrm{f}} = \begin{pmatrix} \mu & e^{i\phi}k_x & e^{-i\phi}k_y \\ e^{-i\phi}k_x & \mu & e^{i\phi}k_z \\ e^{i\phi}k_y & e^{-i\phi}k_z & \mu \end{pmatrix}$$

Conditions for plateaus and quantization

$$\frac{dj_i}{dt} = \beta_{ij}(\omega)(\mathbf{E} \times \mathbf{E}^*)_j$$

– the magic –

$$\mathrm{Tr}[\beta] = 4\pi^2\beta_0 \sum_{n,m} \int d\vec{S}_{nm} \cdot \vec{R}_{nm}$$

$$R^j_{nm} = \epsilon_{jkl} r^k_{nm} r^l_{mn}$$

$$\mathbf{r}_{\mathbf{k},nm} = i \langle n | \partial_{\mathbf{k}} | m \rangle$$

linear model + closed surfaces

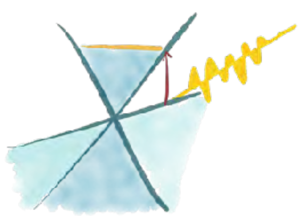

+

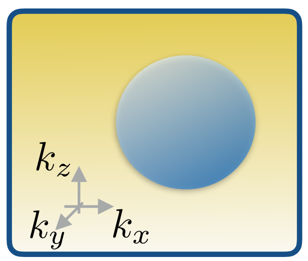

$$= 4\pi^2\beta_0 \int \frac{d\Omega}{(2\pi)^3} \bar{R}_{nm}$$

plateau (non-universal)

Sum rule

$$\Omega^c_n = i \sum_{m \neq n} R^c_{nm}$$

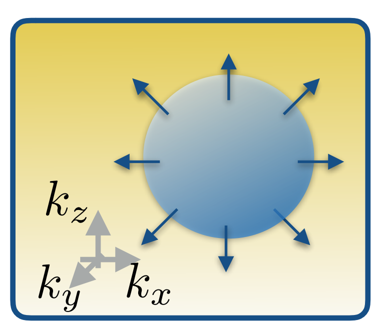

Sipe, Shkrebtii, PRB (2000)

plateau (universal)

$$\beta(\omega) = 4\pi^2\beta_0 C_\Sigma$$

Three-fold fermion

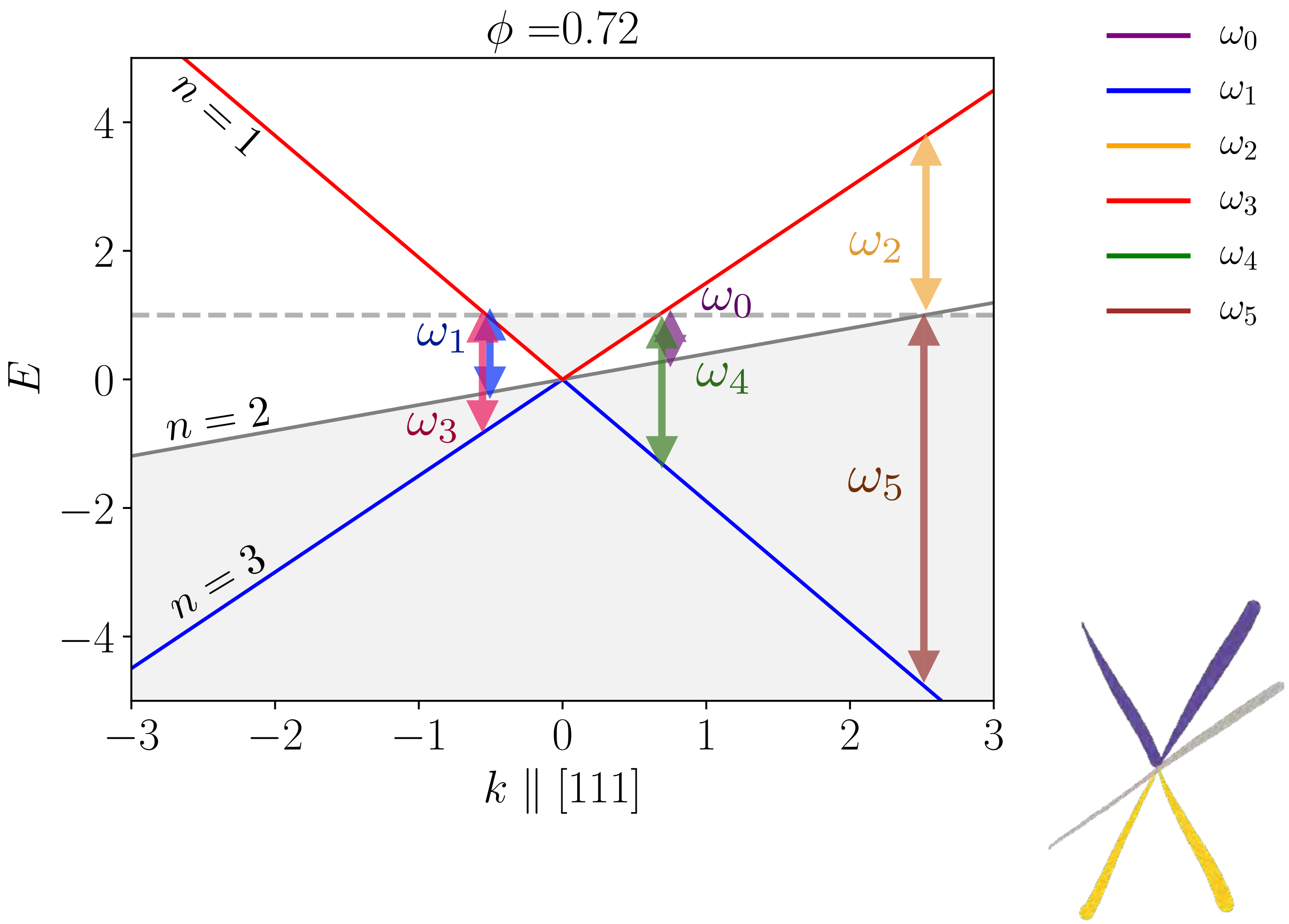

Three-fold fermion

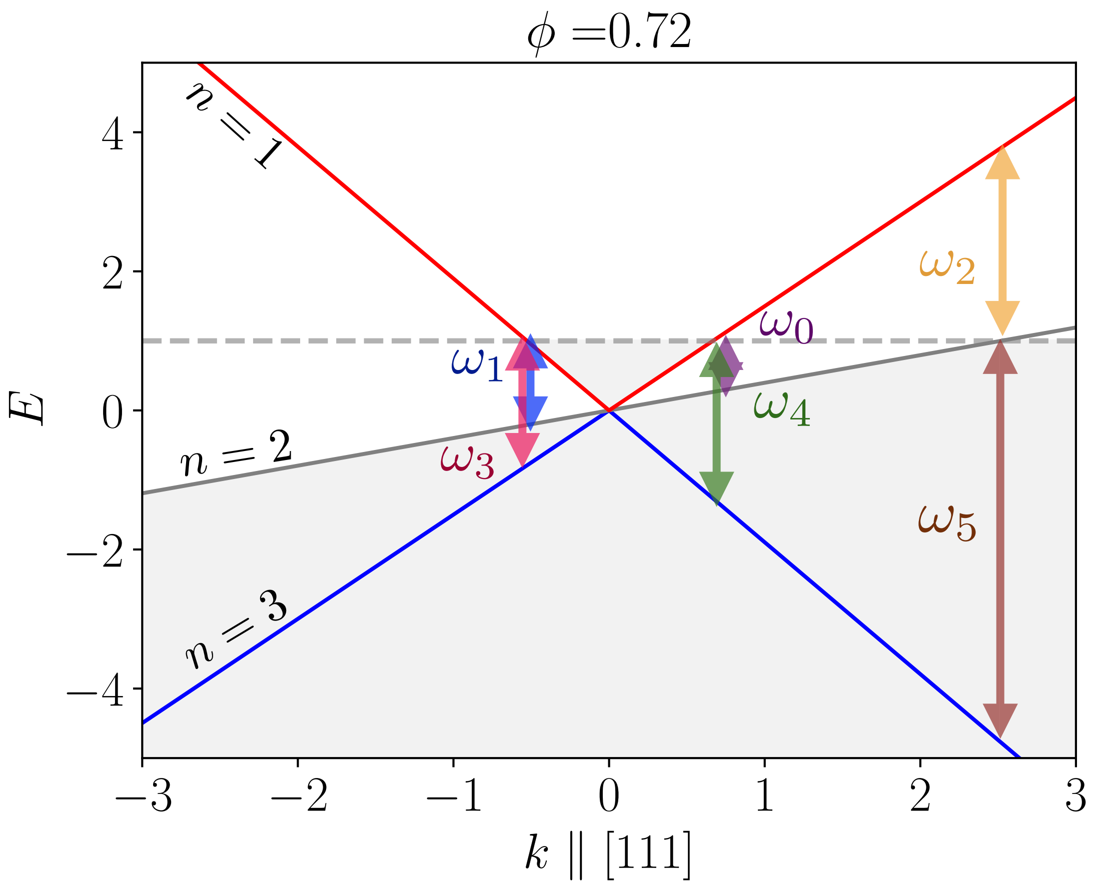

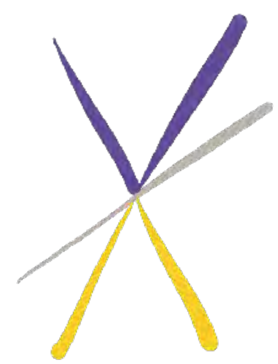

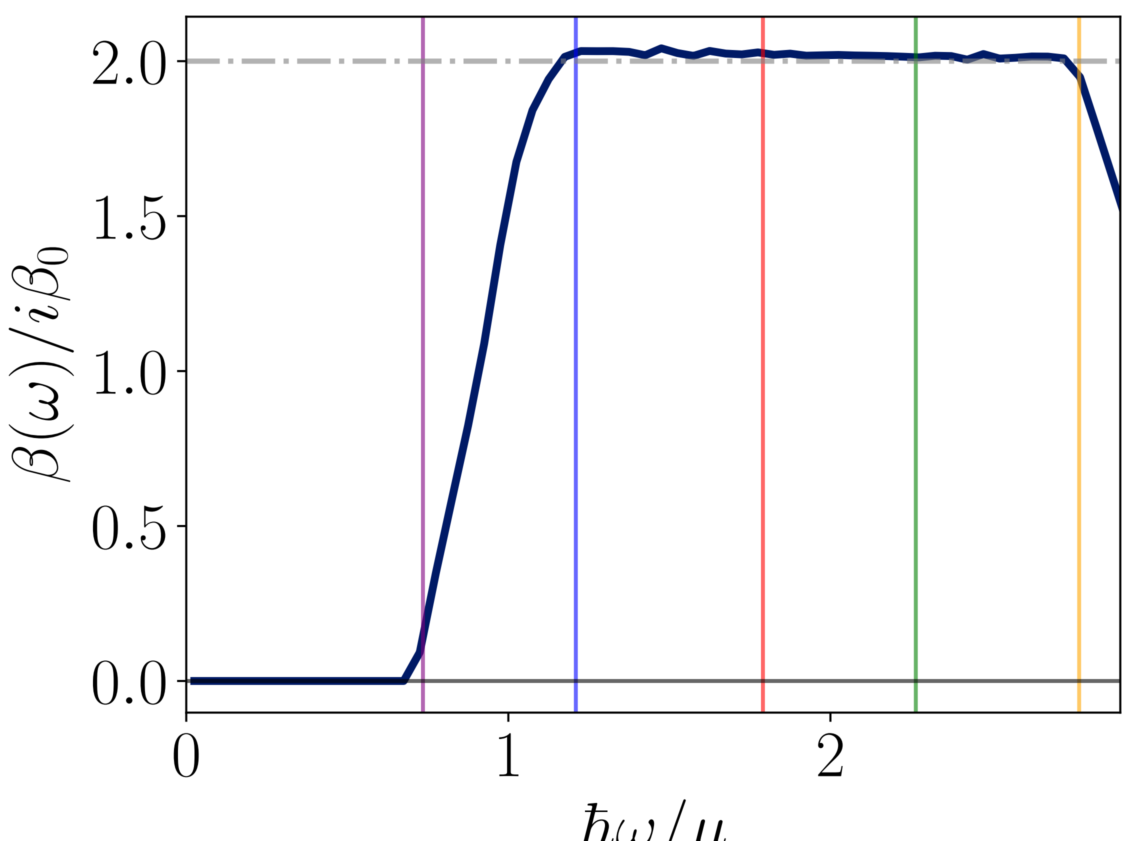

Three-fold fermion

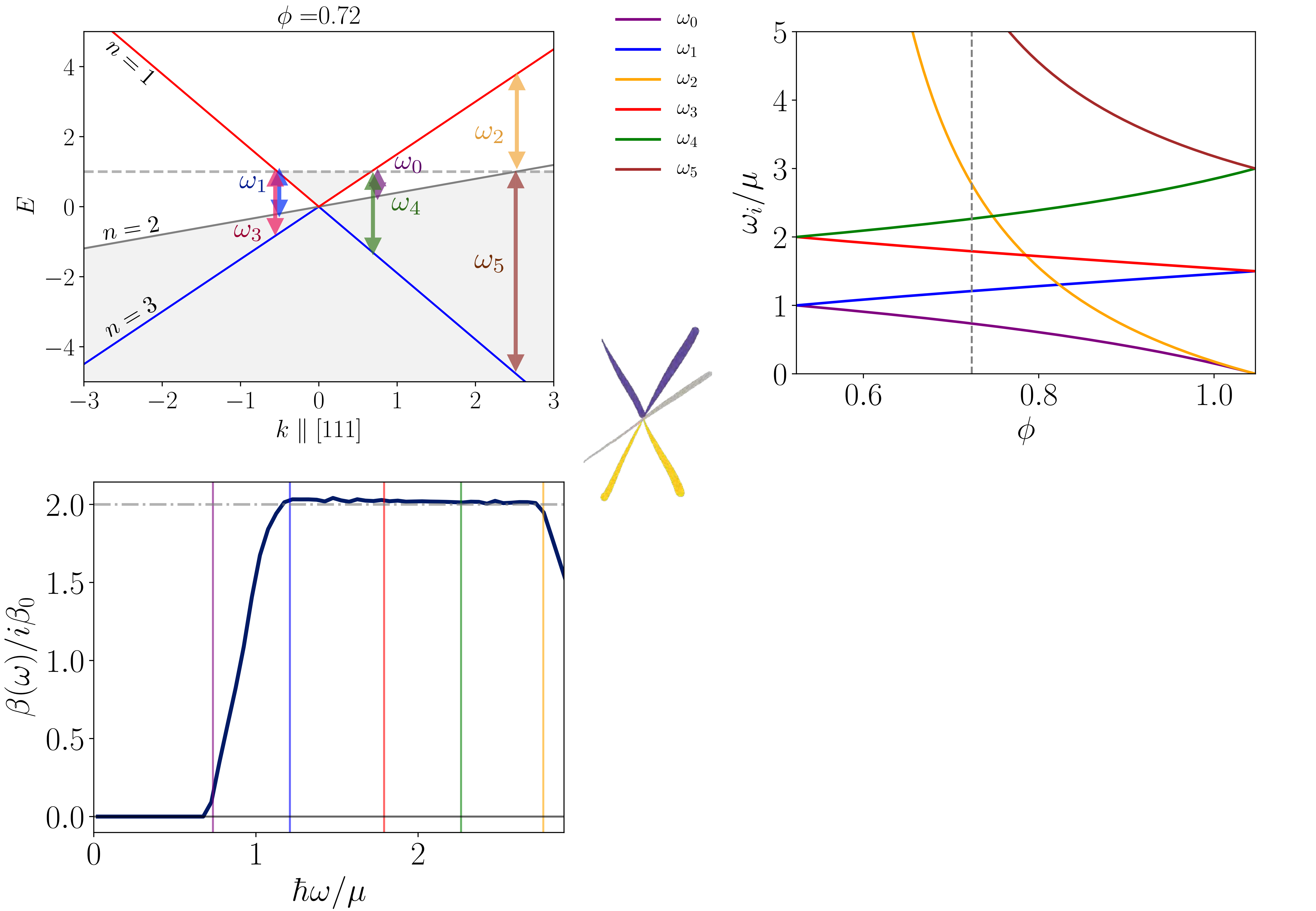

Three-fold fermion

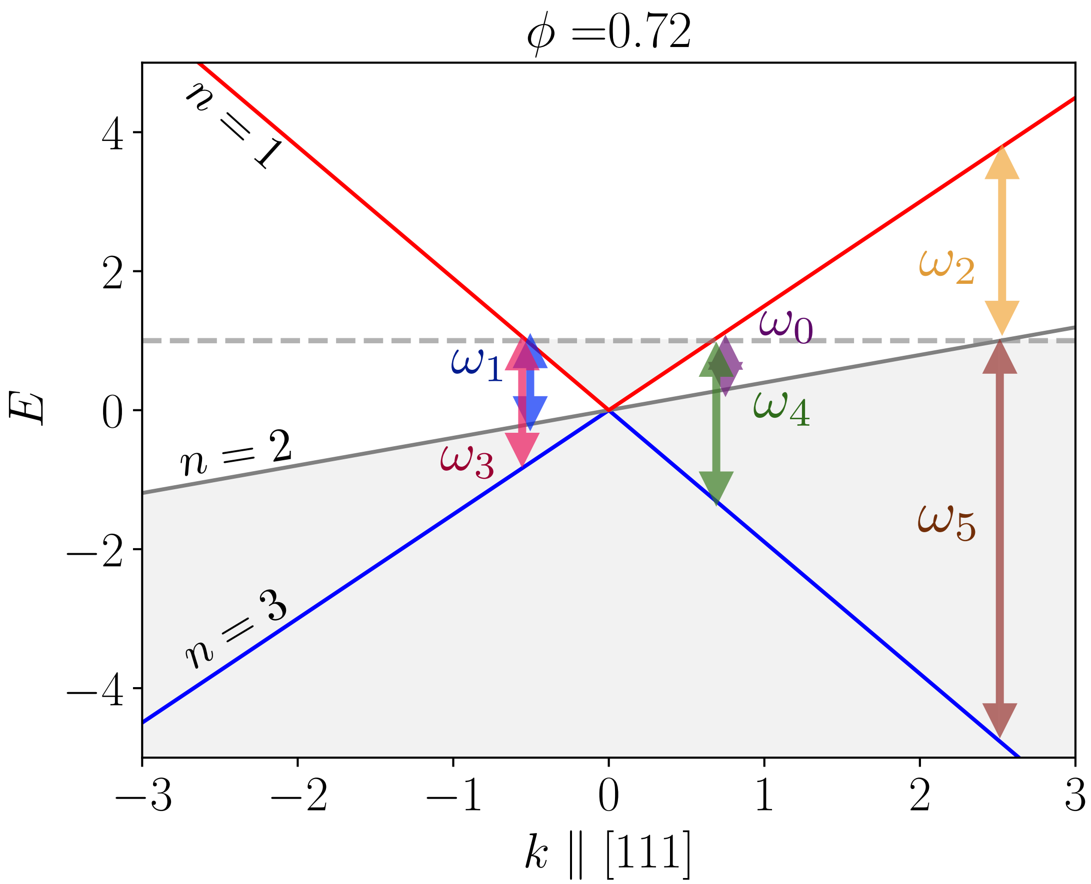

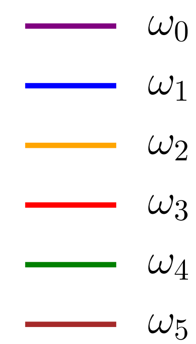

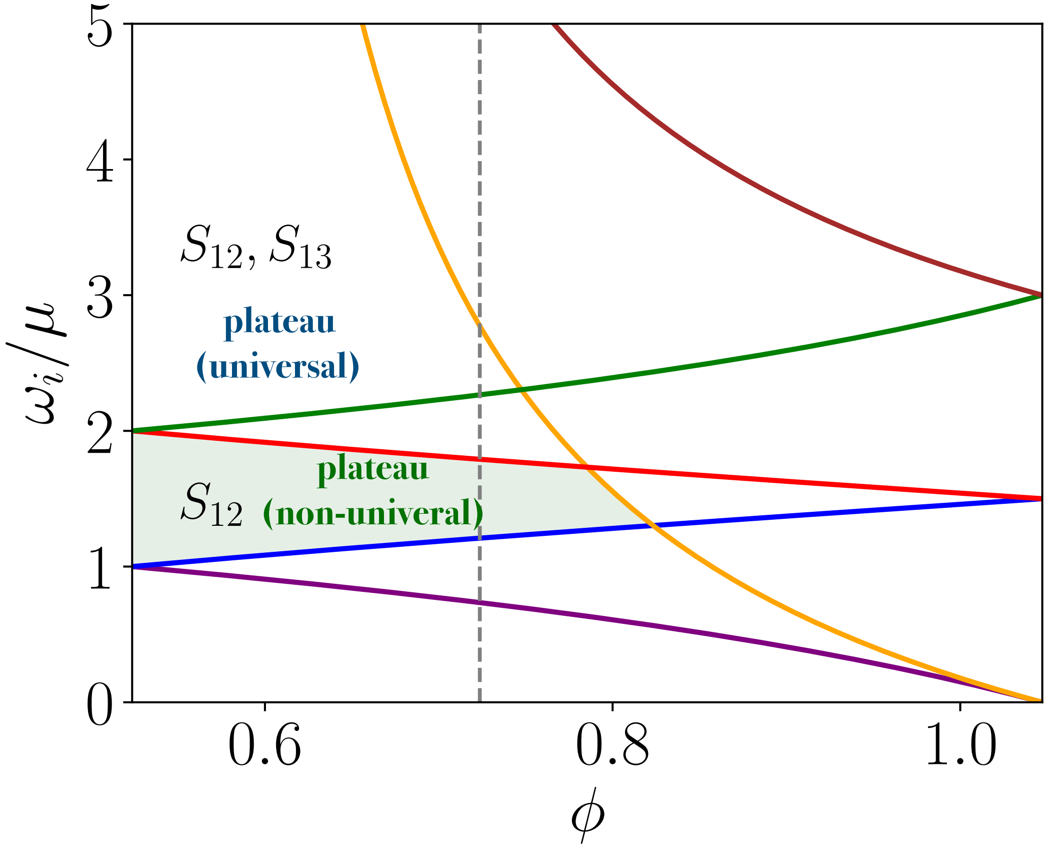

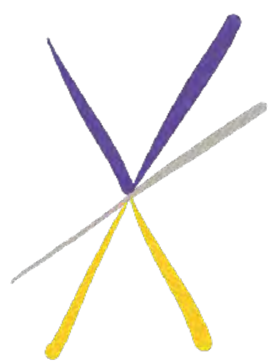

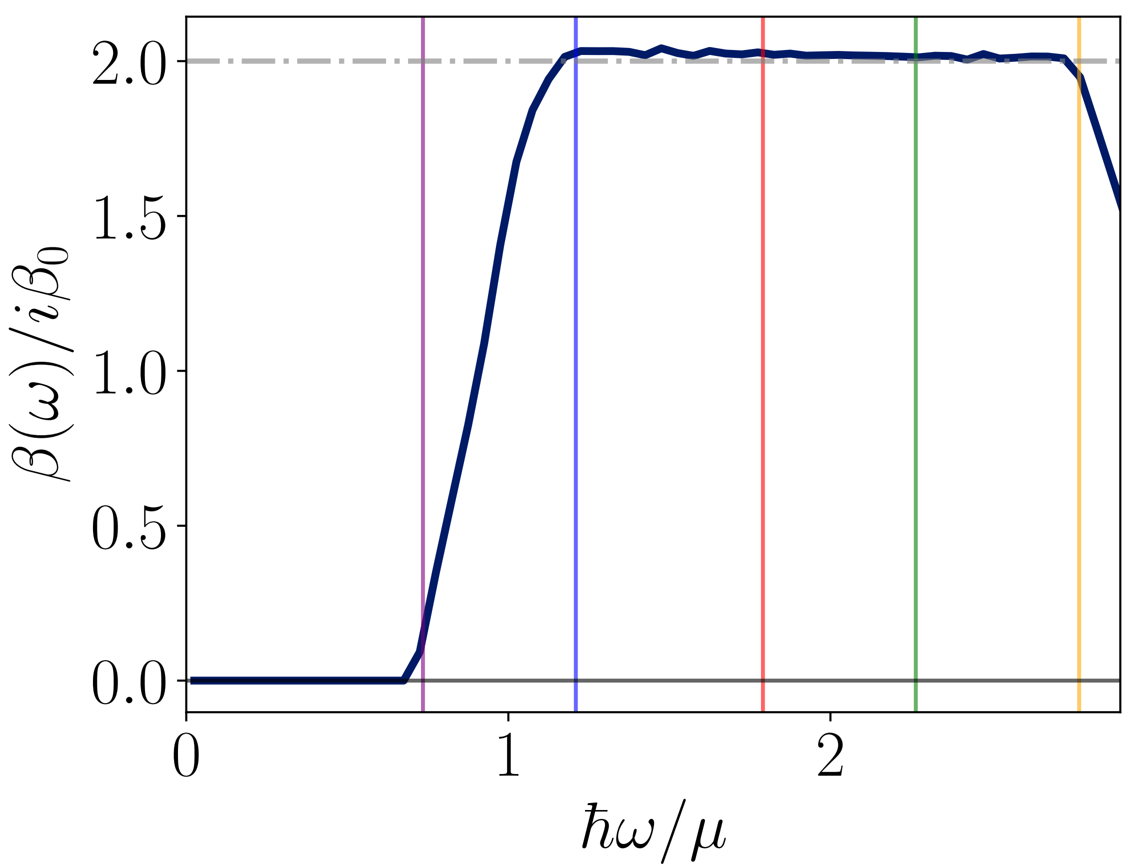

Three-fold fermion

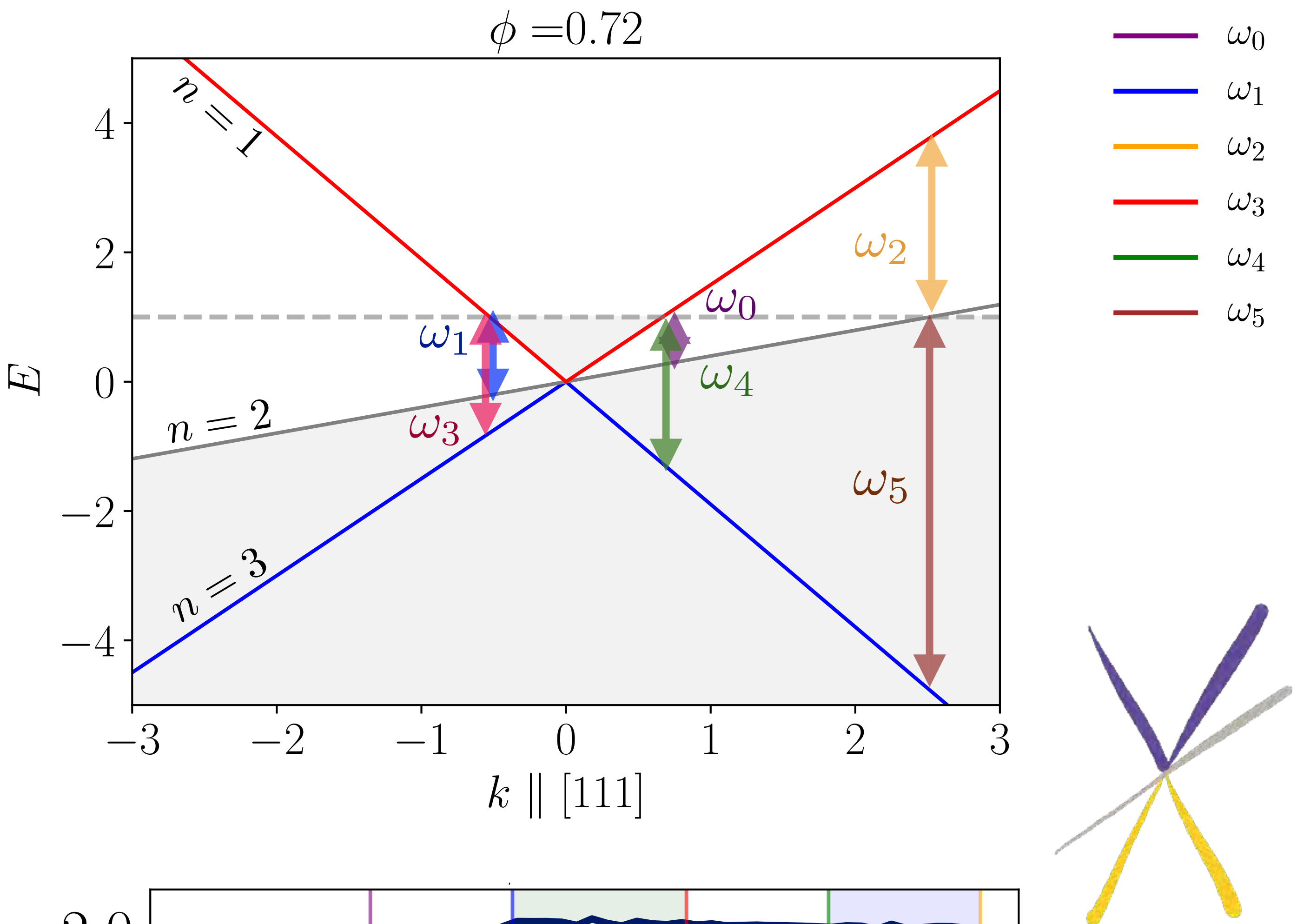

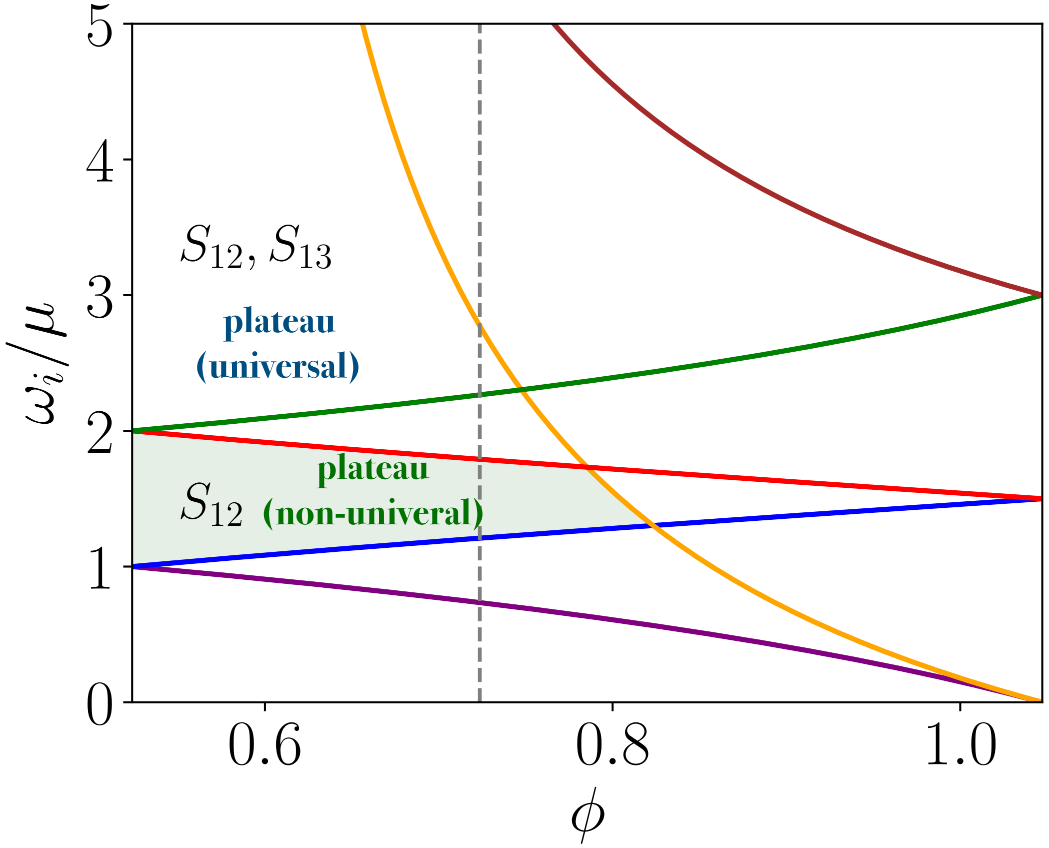

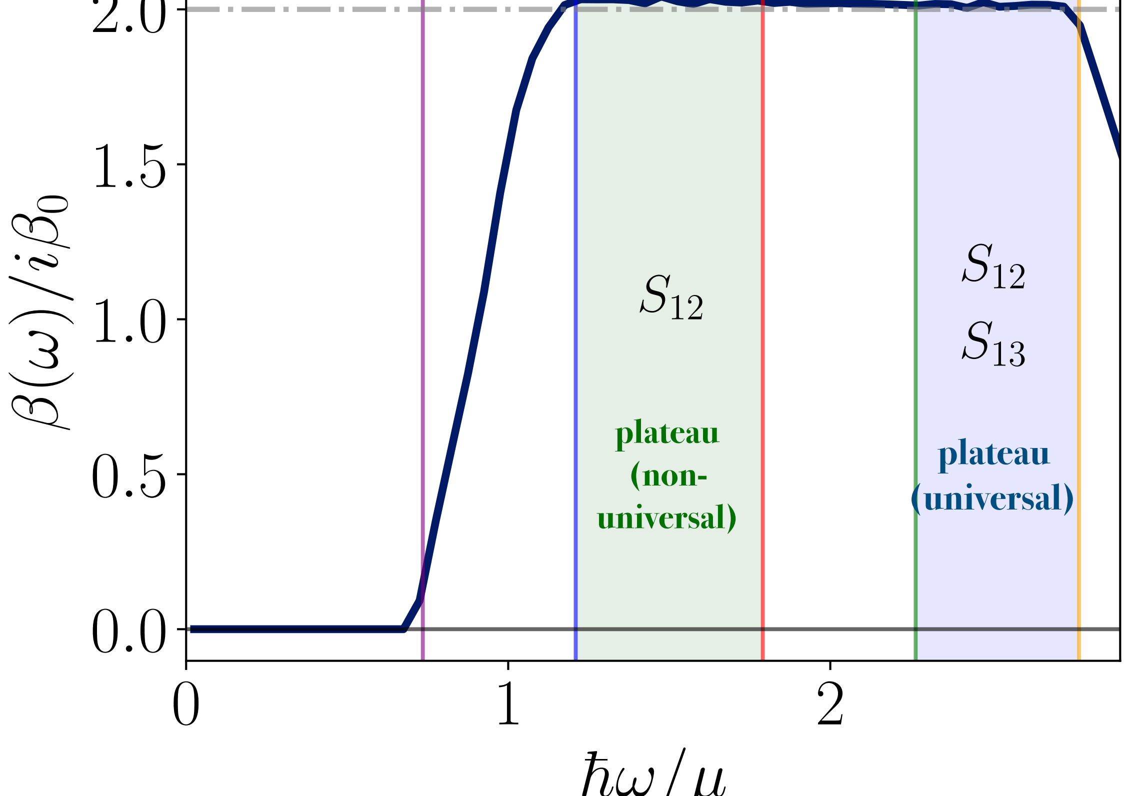

Three-fold fermion

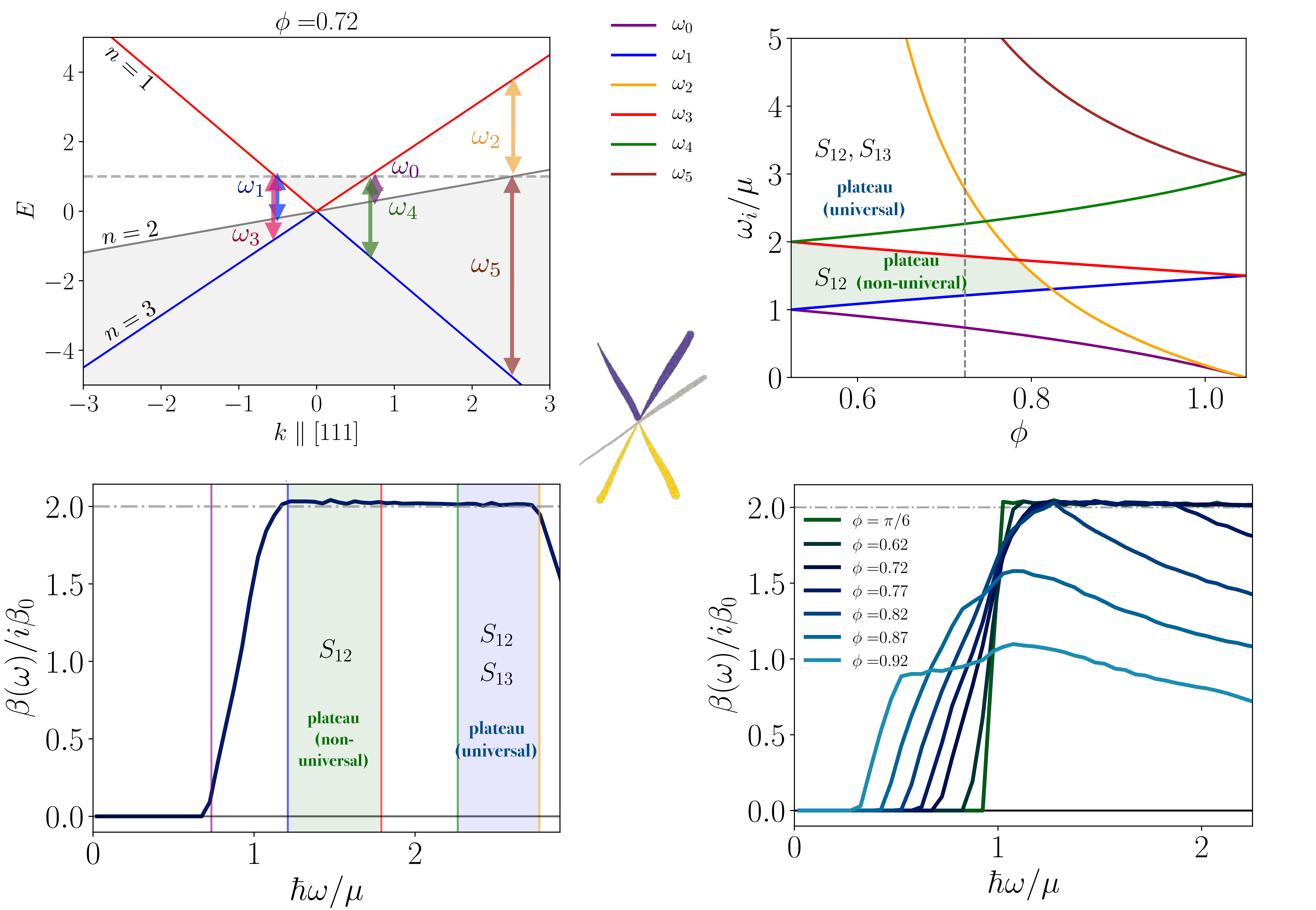

Four-fold fermion

node	C_n	No SO	SO
Fourfold (spin-3/2)	$-3, -1, 1, 3$	–	$195-199$, $207-214$

$$H = \mathbf{k} \cdot \boldsymbol{S}$$

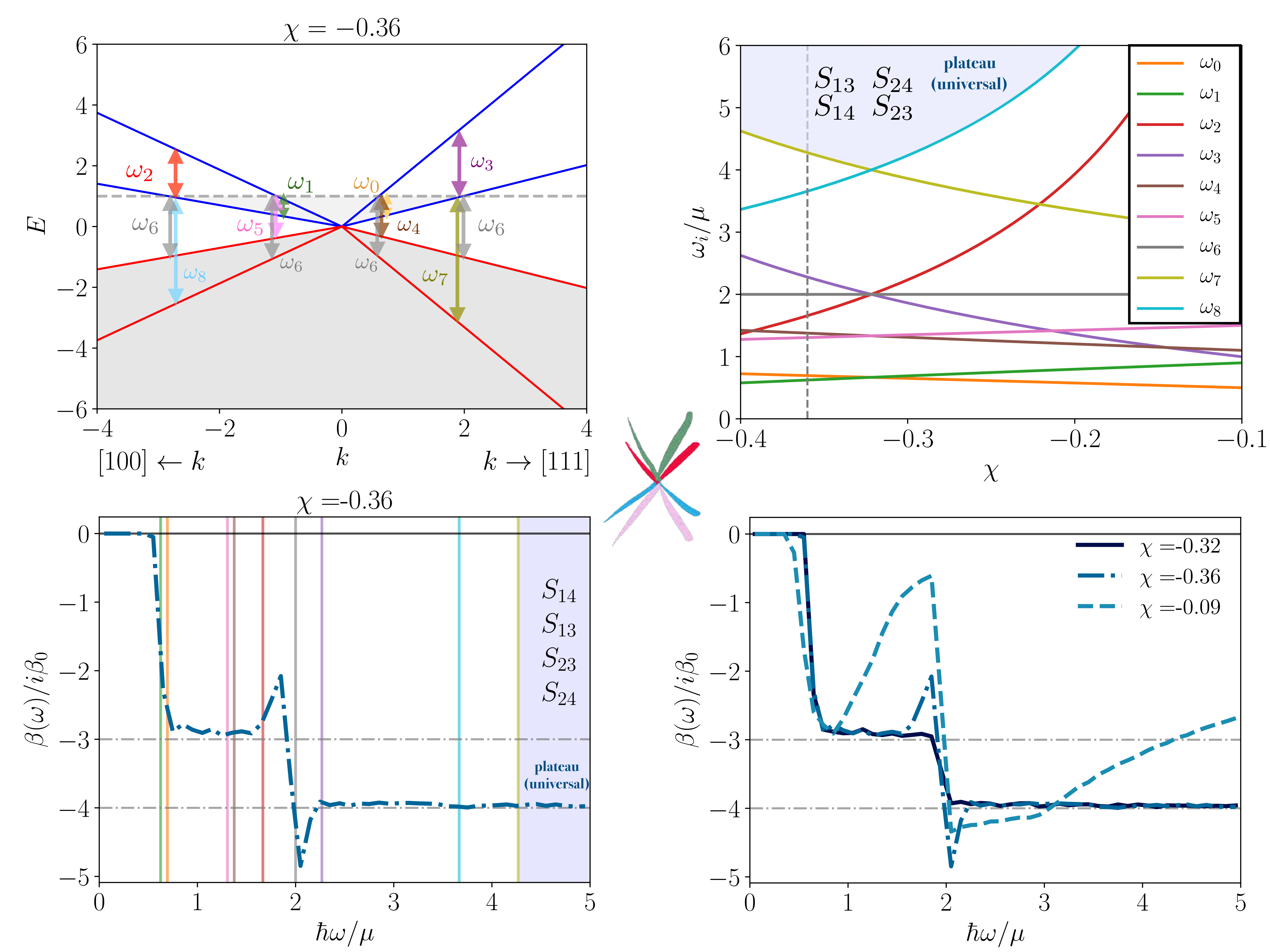

χ = −0.36
E
k
[100] ← k
k → [111]
ω0
ω1
ω2
ω3
ω4
ω5
ω6
ω7
ω8
ωi/μ
χ
plateau
(universal)
S13 S24
S14 S23
χ =-0.36
β(ω)/iβ0
ħω/μ
S14
S13
S23
S24
χ =-0.32
χ =-0.36
χ =-0.09

The rest of chiral multifolds

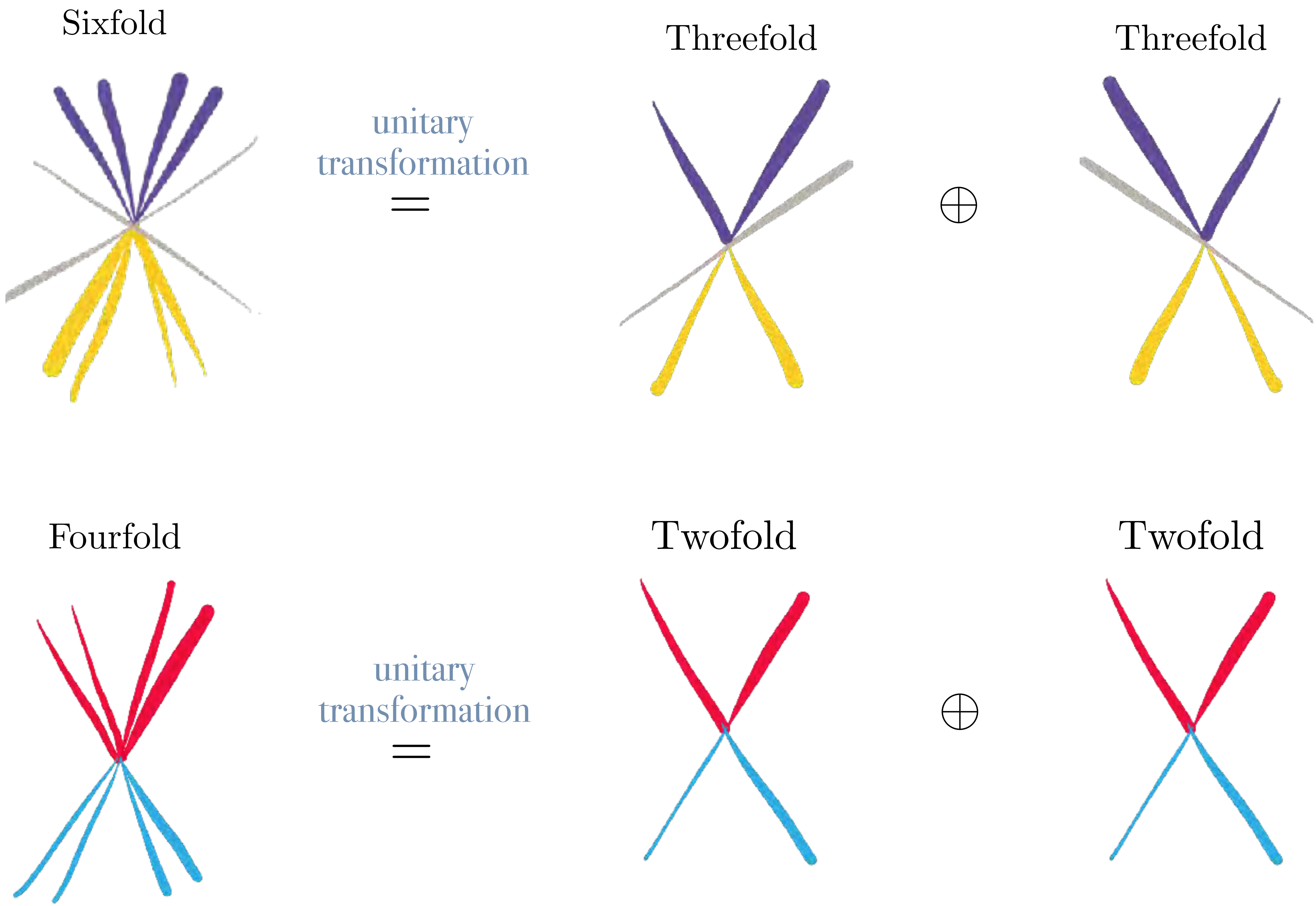

Conditions for plateaus quantization

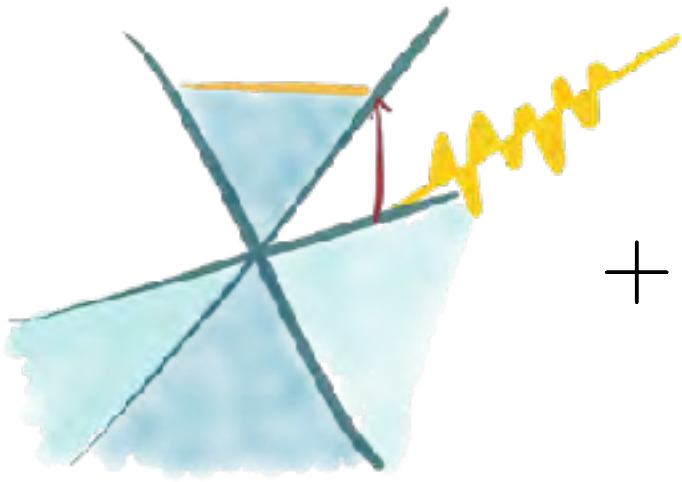

+

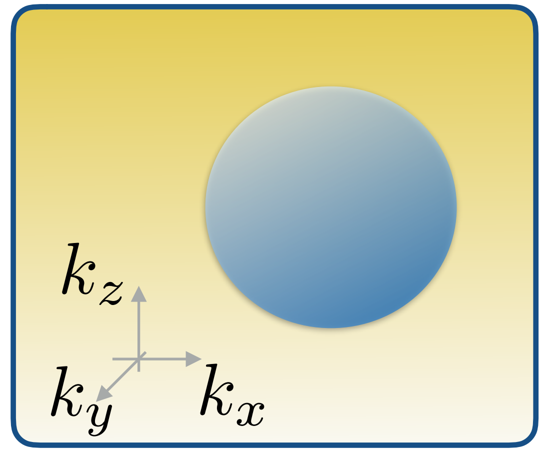

A chiral topological metal

Closed optical surfaces

plateau (non-universal)

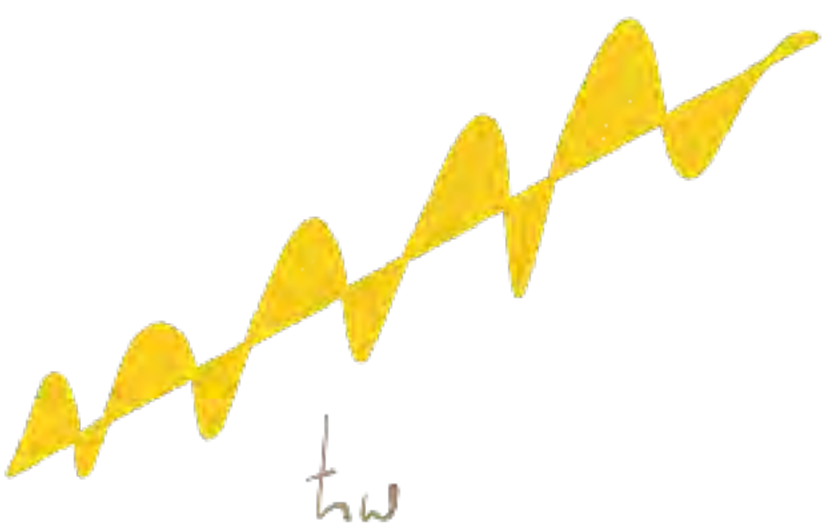

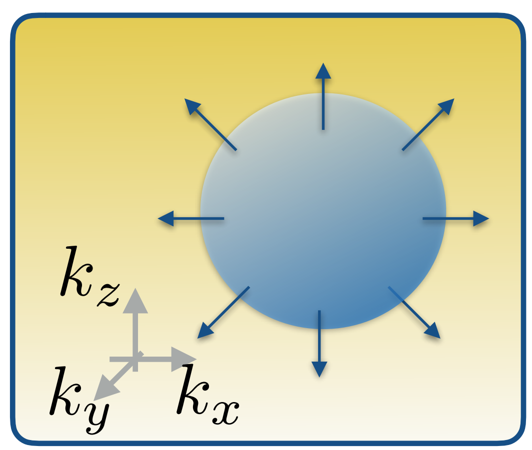

A closed form of the sum rule for the involved closed surfaces

plateau (universal)

$$\beta(\omega) = 4\pi^2 \beta_0 C_\Sigma$$

All chiral topological metals have quantized ($\frac{e^3}{h^2}$) injection currents

Real materials with quantized injection

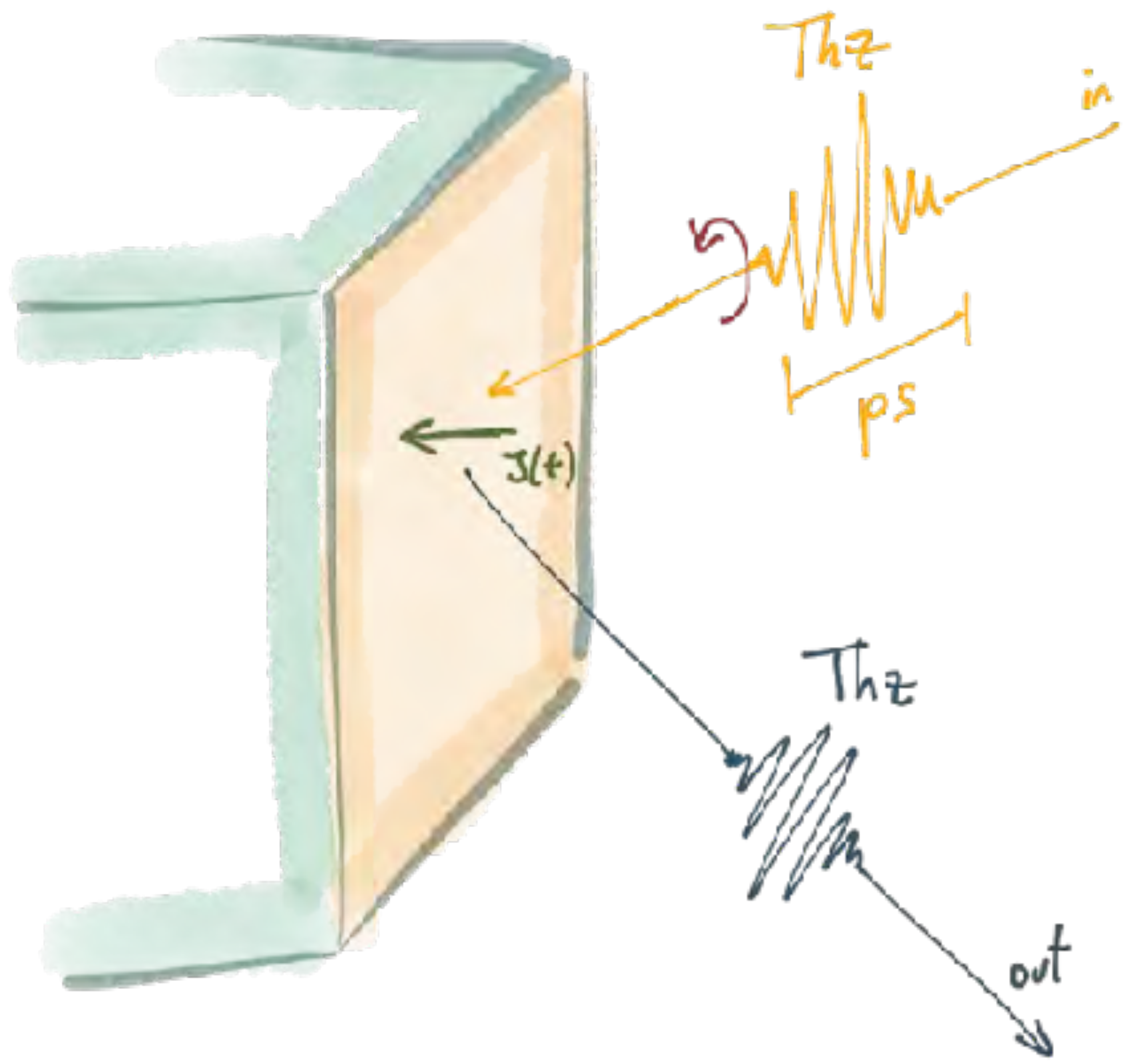

Real materials with quantized injection

node	C_n	No SO	SO
Threefold (spin-1)	$-2, 0, 2$	$195-199, 207-214$	$199, 214$
Sixfold (doubled spin-1)	$(-2, 0, 2) \times 2$	–	$198, 212, 213$
Fourfold (spin-3/2)	$-3, -1, 1, 3$	–	$195-199, 207-214$
Fourfold (doubled spin-1/2)	$(-1, 1) \times 2$	$19, 92, 96, 198, 212, 213$	$18, 19, 90, 92, 94, 96, 198, 212, 213$

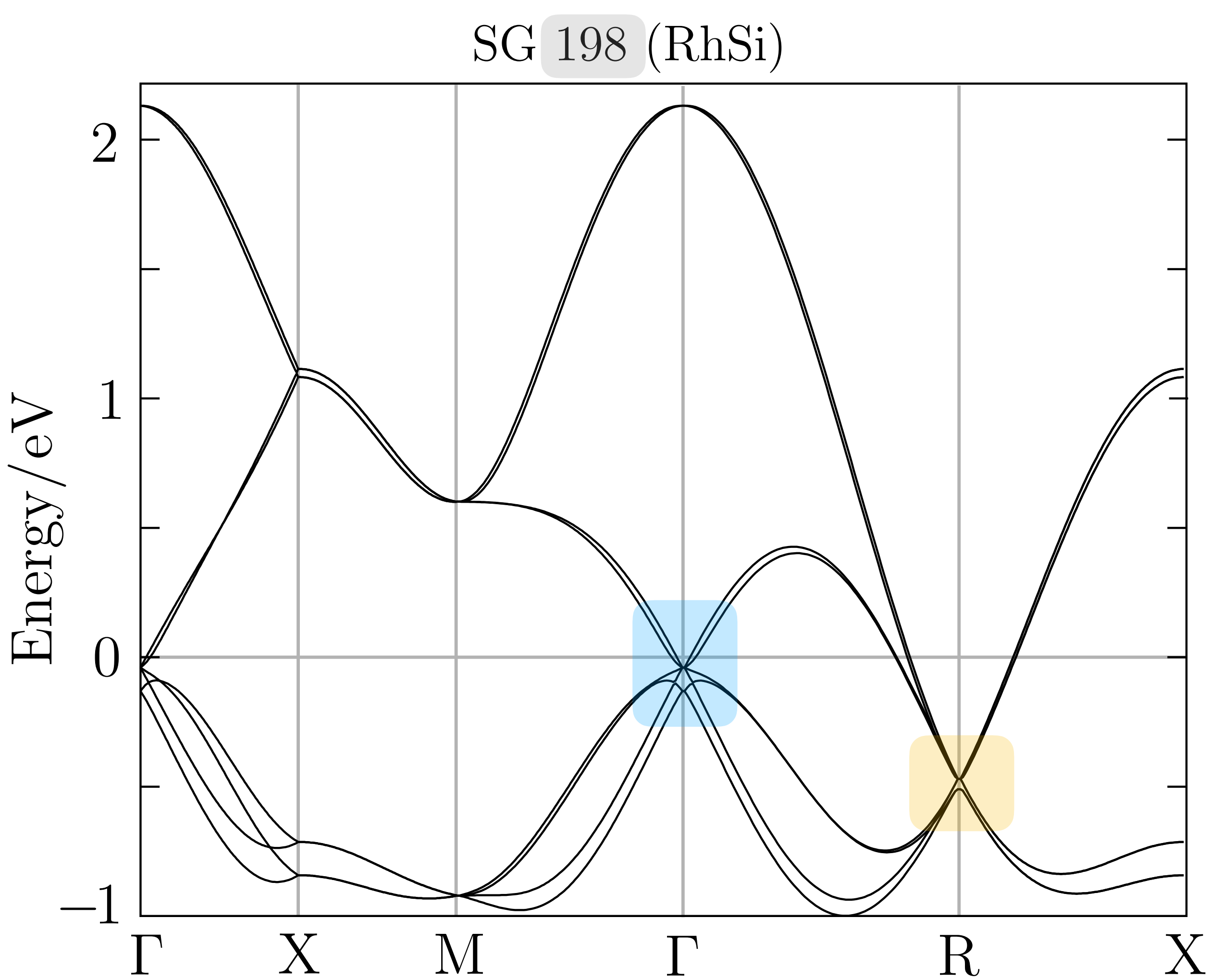

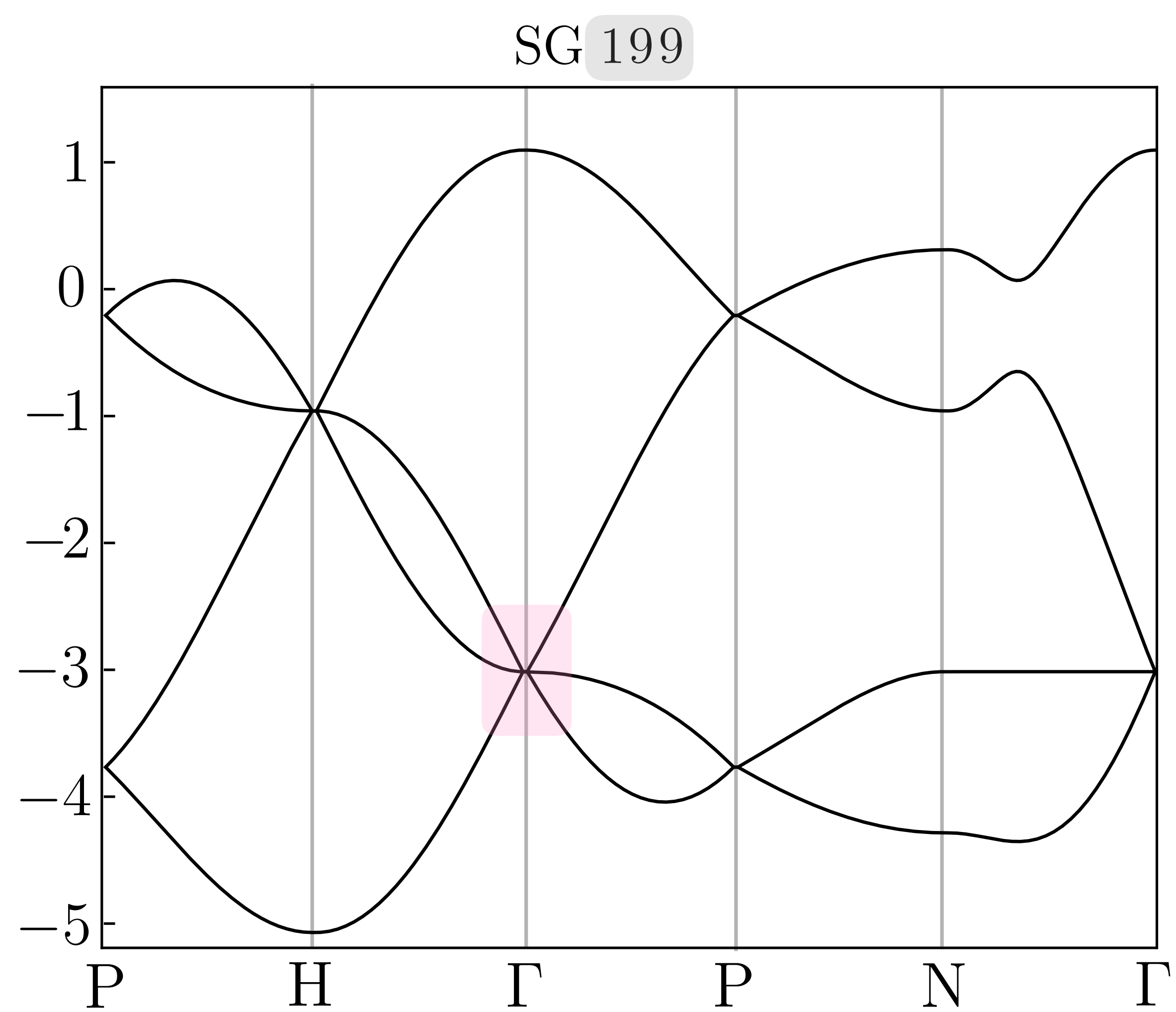

Real materials with quantized injection

node	C_n	No SO	SO
Threefold (spin-1)	$-2, 0, 2$	$195-199,\ 207-214$	$199, 214$
Sixfold (doubled spin-1)	$(-2, 0, 2)\times 2$	–	$198, 212, 213$
Fourfold (spin-3/2)	$-3, -1, 1, 3$	–	$195-199\ ,\ 207-214$
Fourfold (doubled spin-1/2)	$(-1, 1)\times 2$	$19, 92, 96, 198, 212, 213$	$18, 19, 90, 92, 94, 96, 198, 212, 213$

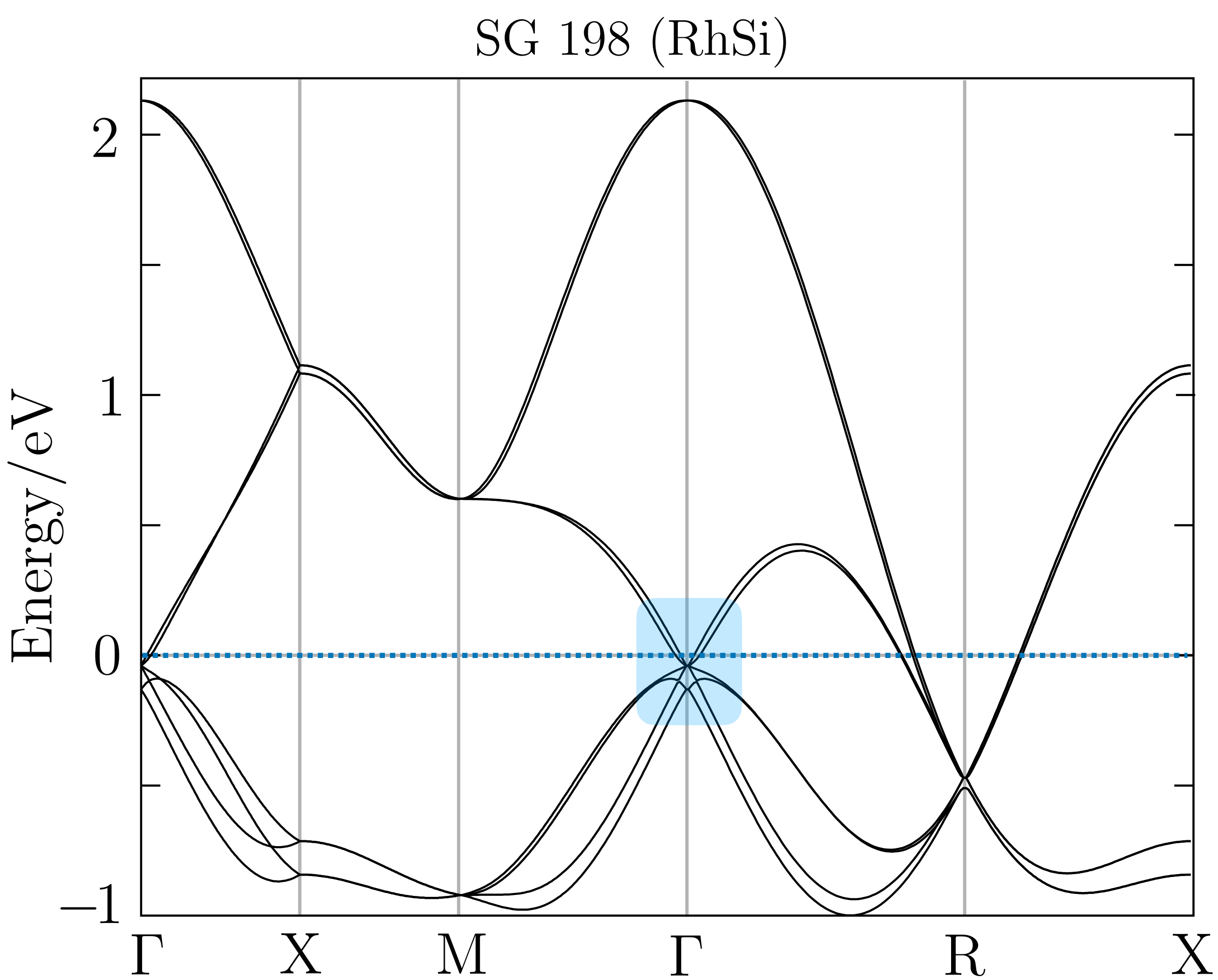

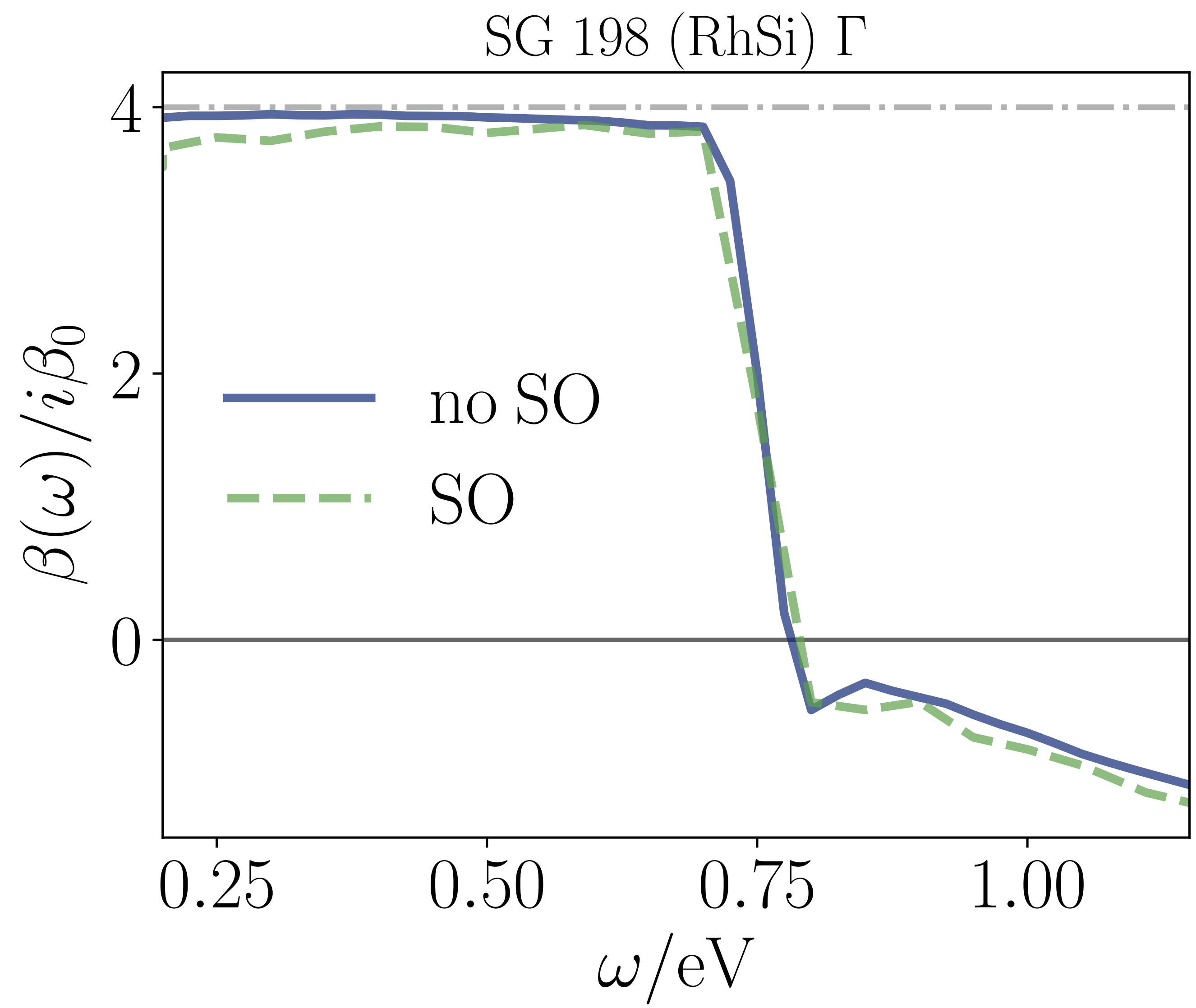

Real materials with quantized injection

node	C_n	No SO	SO
Threefold (spin-1)	$-2, 0, 2$	$195-199,\ 207-214$	$199, 214$
Sixfold (doubled spin-1)	$(-2, 0, 2) \times 2$	–	$198, 212, 213$
Fourfold (spin-3/2)	$-3, -1, 1, 3$	–	$195-199\ ,\ 207-214$
Fourfold (doubled spin-1/2)	$(-1, 1) \times 2$	$19, 92, 96, 198, 212, 213$	$18, 19, 90, 92, 94, 96, 198, 212, 213$

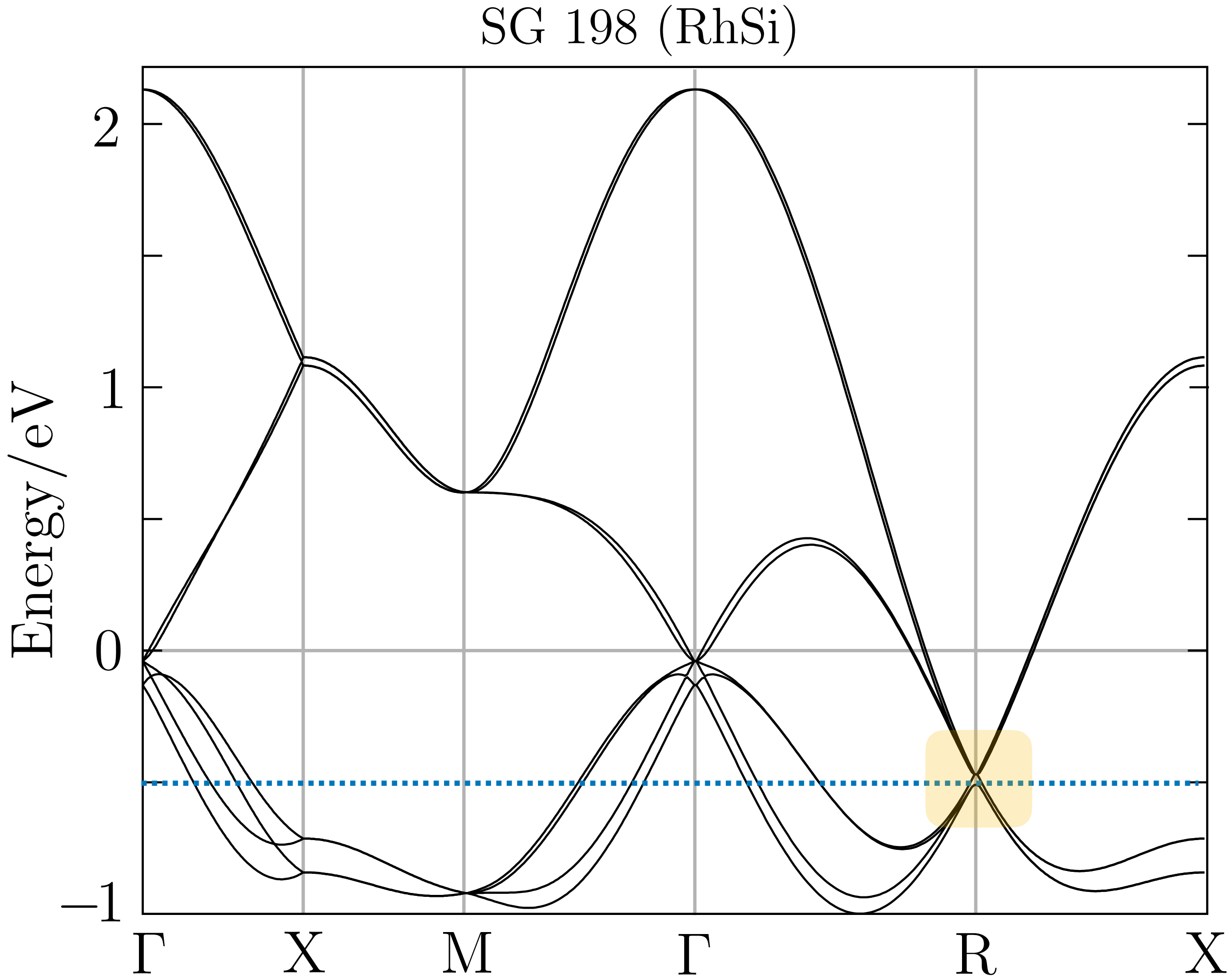

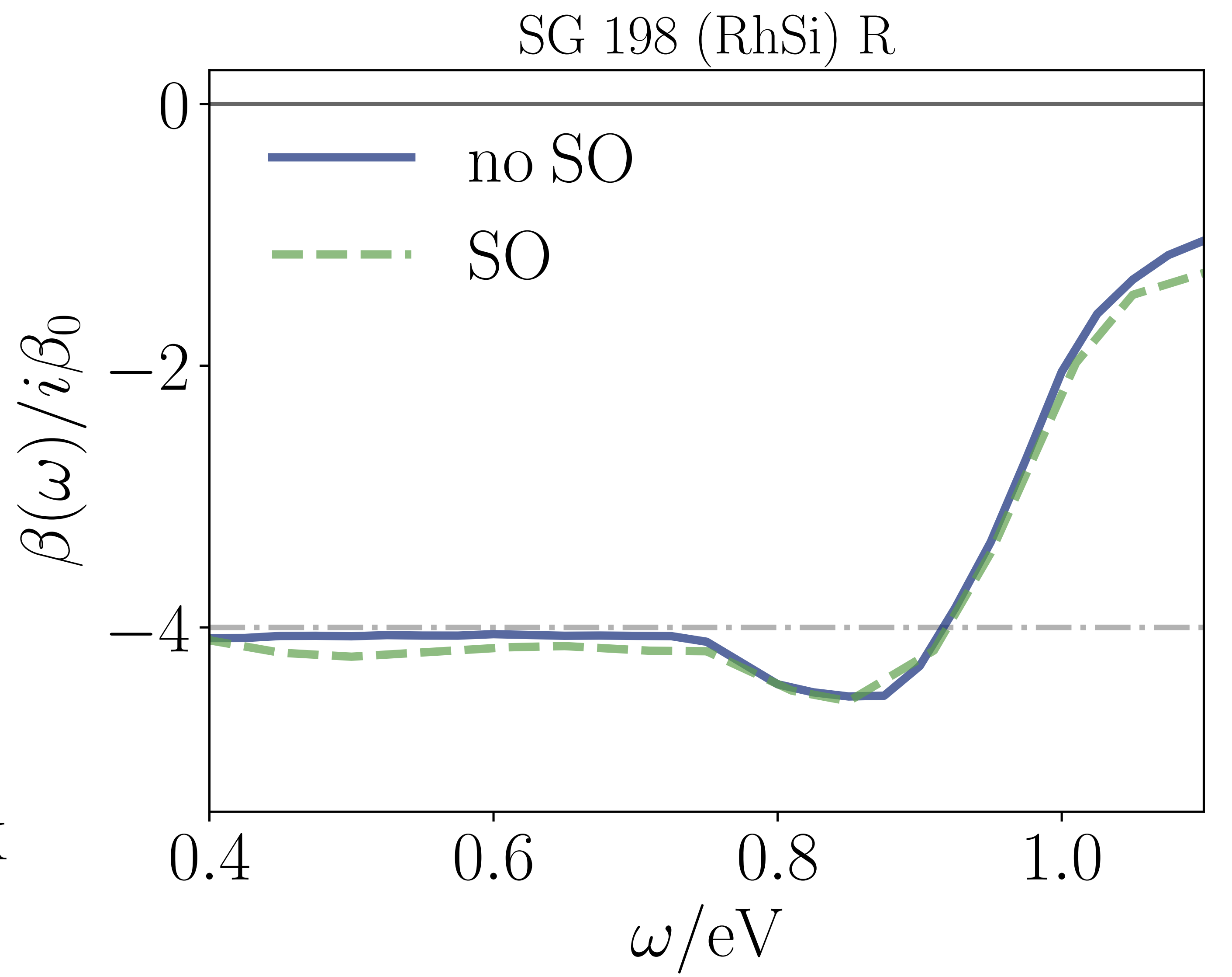

Real materials with quantized injection

node	C_n	No SO	SO
Threefold (spin-1)	$-2, 0, 2$	$195 - 199, 207 - 214$	$199, 214$
Sixfold (doubled spin-1)	$(-2, 0, 2) \times 2$	–	$198, 212, 213$
Fourfold (spin-3/2)	$-3, -1, 1, 3$	–	$195 - 199\ ,\ 207 - 214$
Fourfold (doubled spin-1/2)	$(-1, 1) \times 2$	$19, 92, 96, 198, 212, 213$	$18, 19, 90, 92, 94, 96, 198, 212, 213$

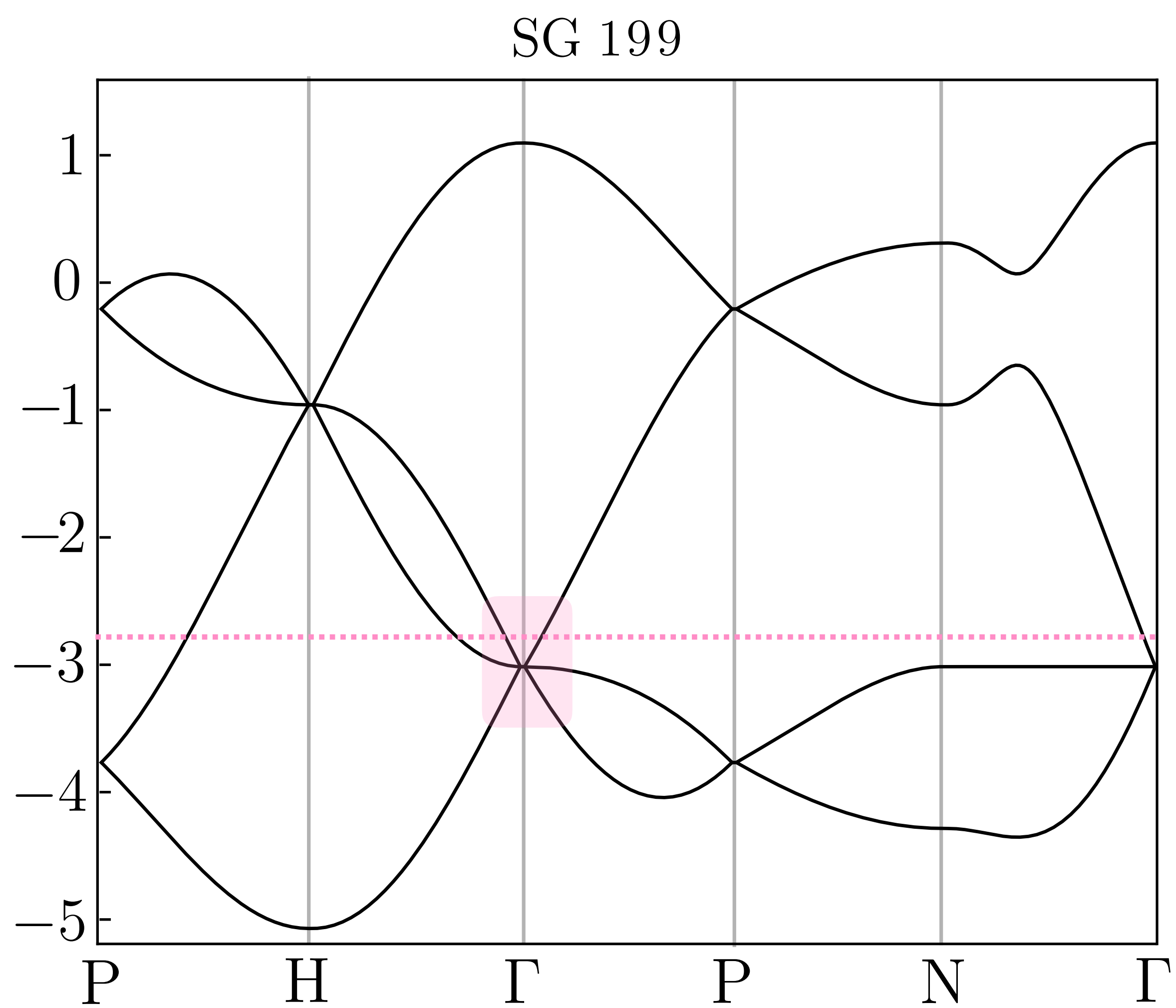

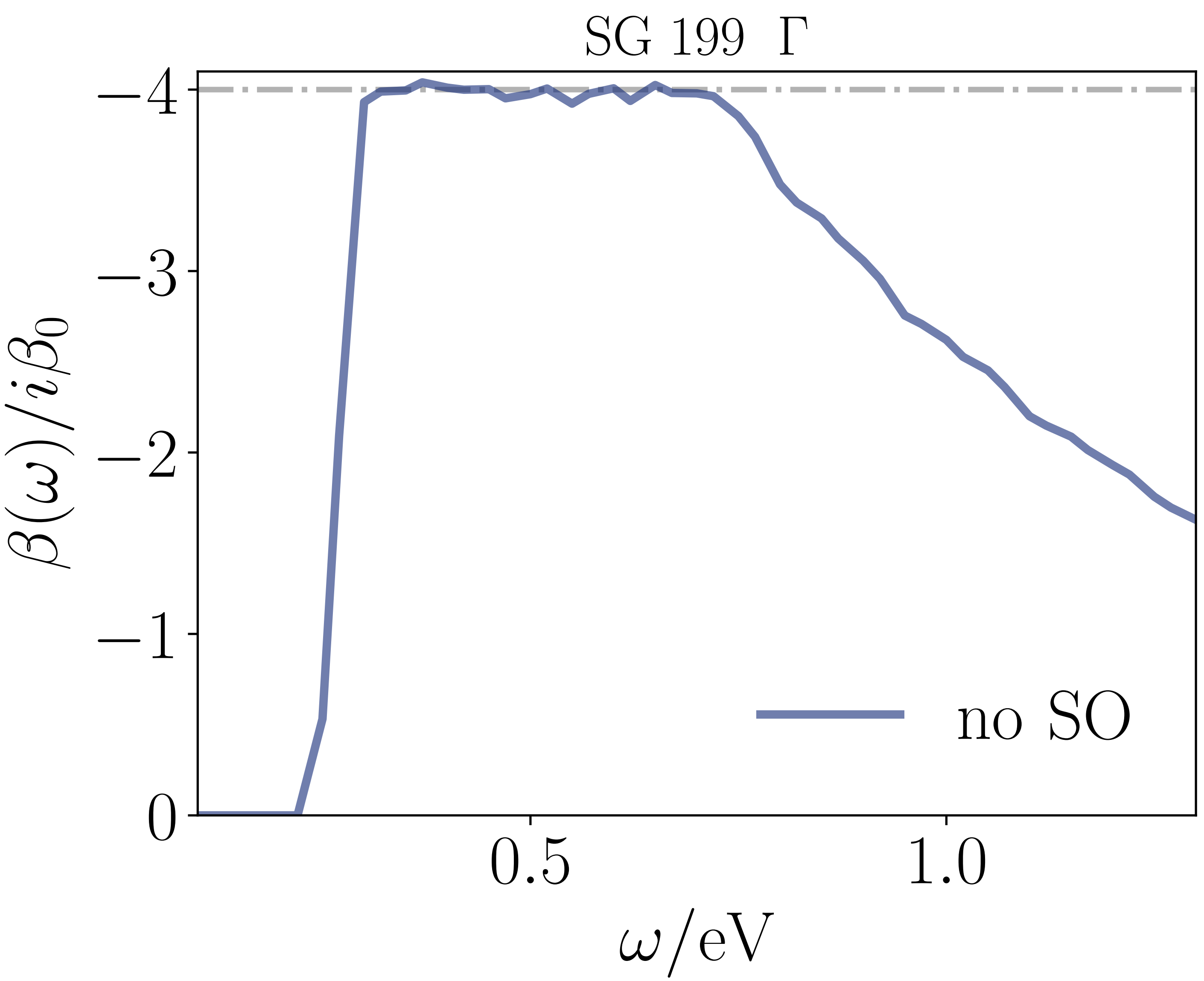

Real materials with quantized injection

SG214

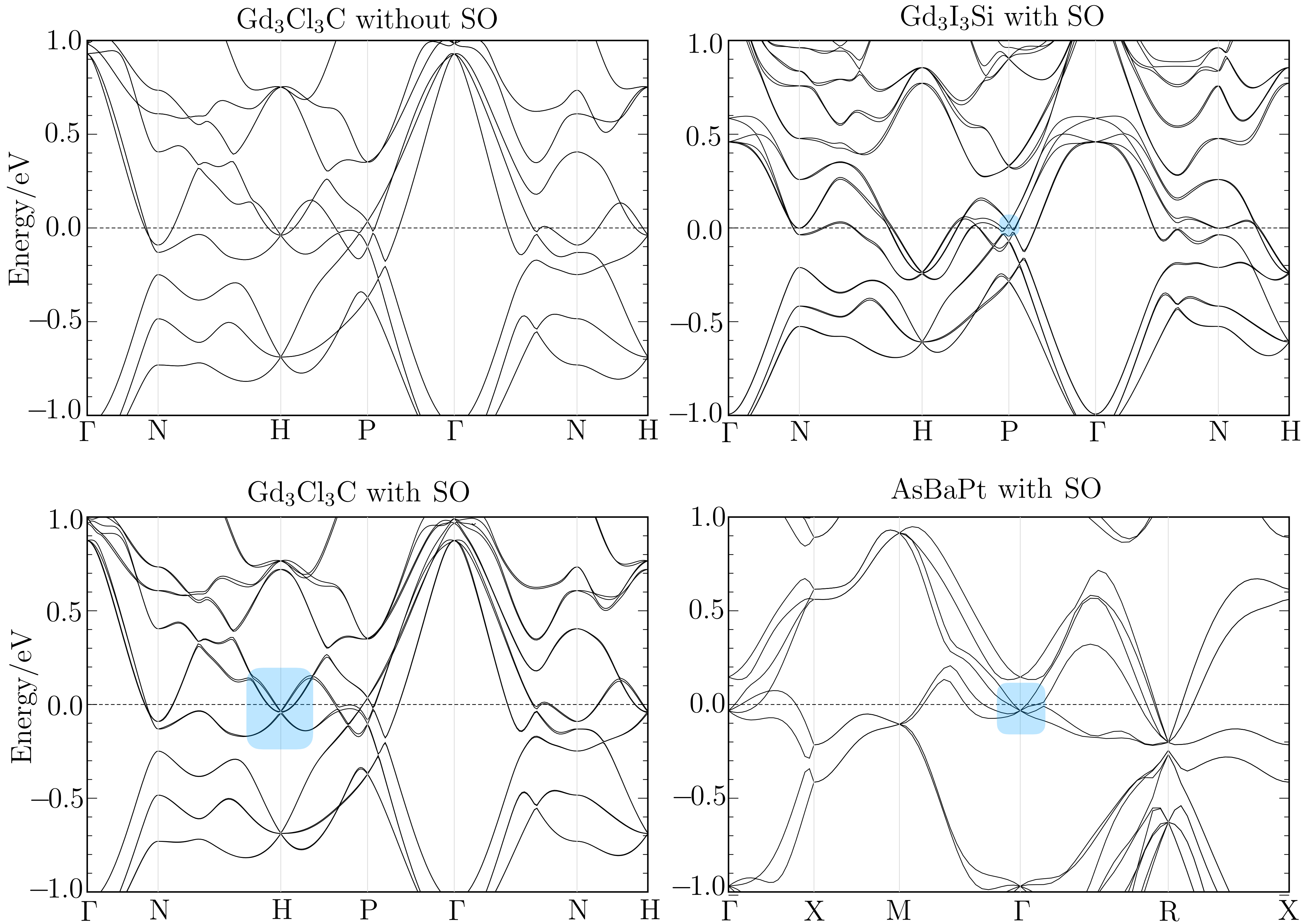

Maia Vergniory (DIPC)

Measurement

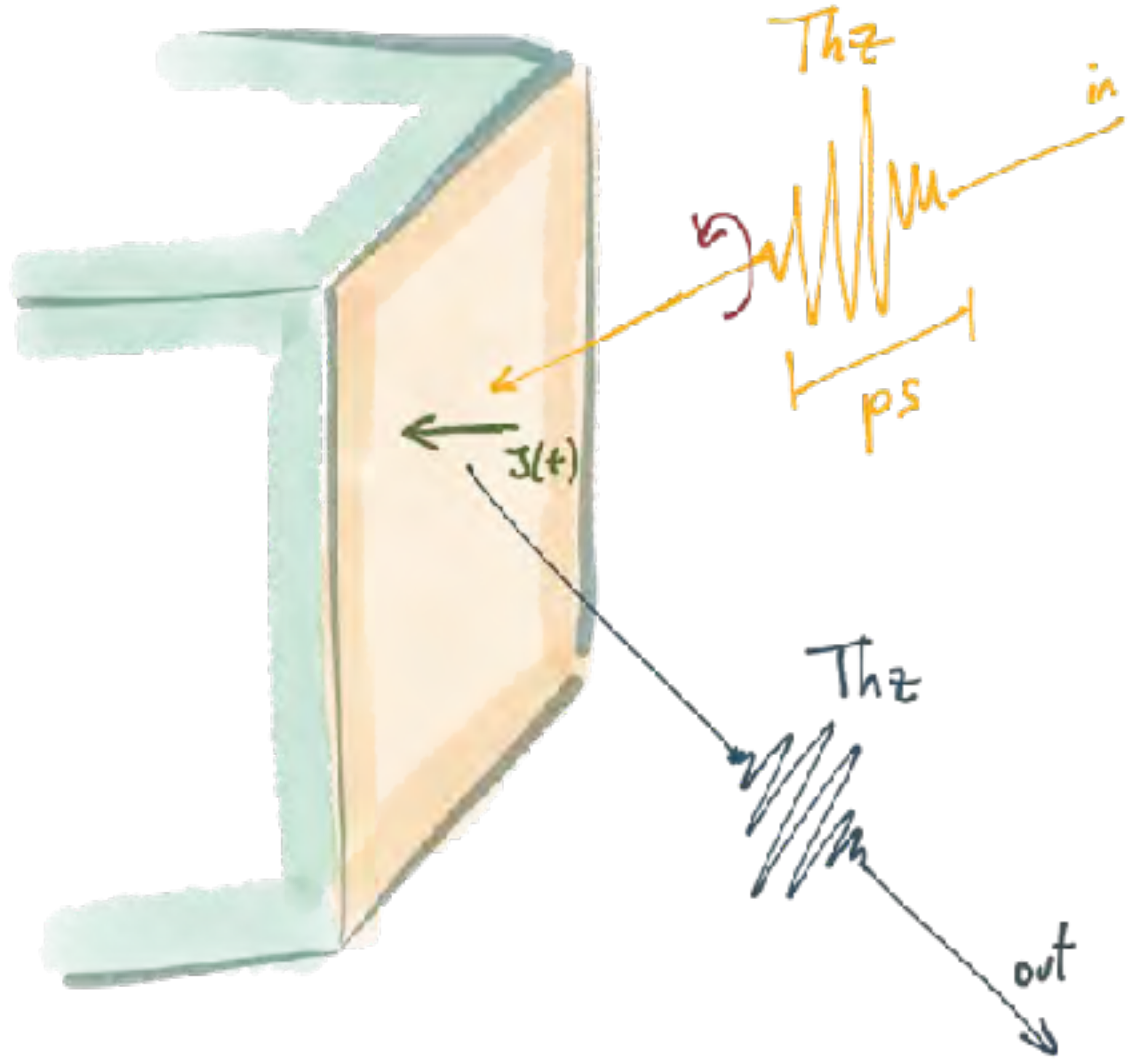

Time scales

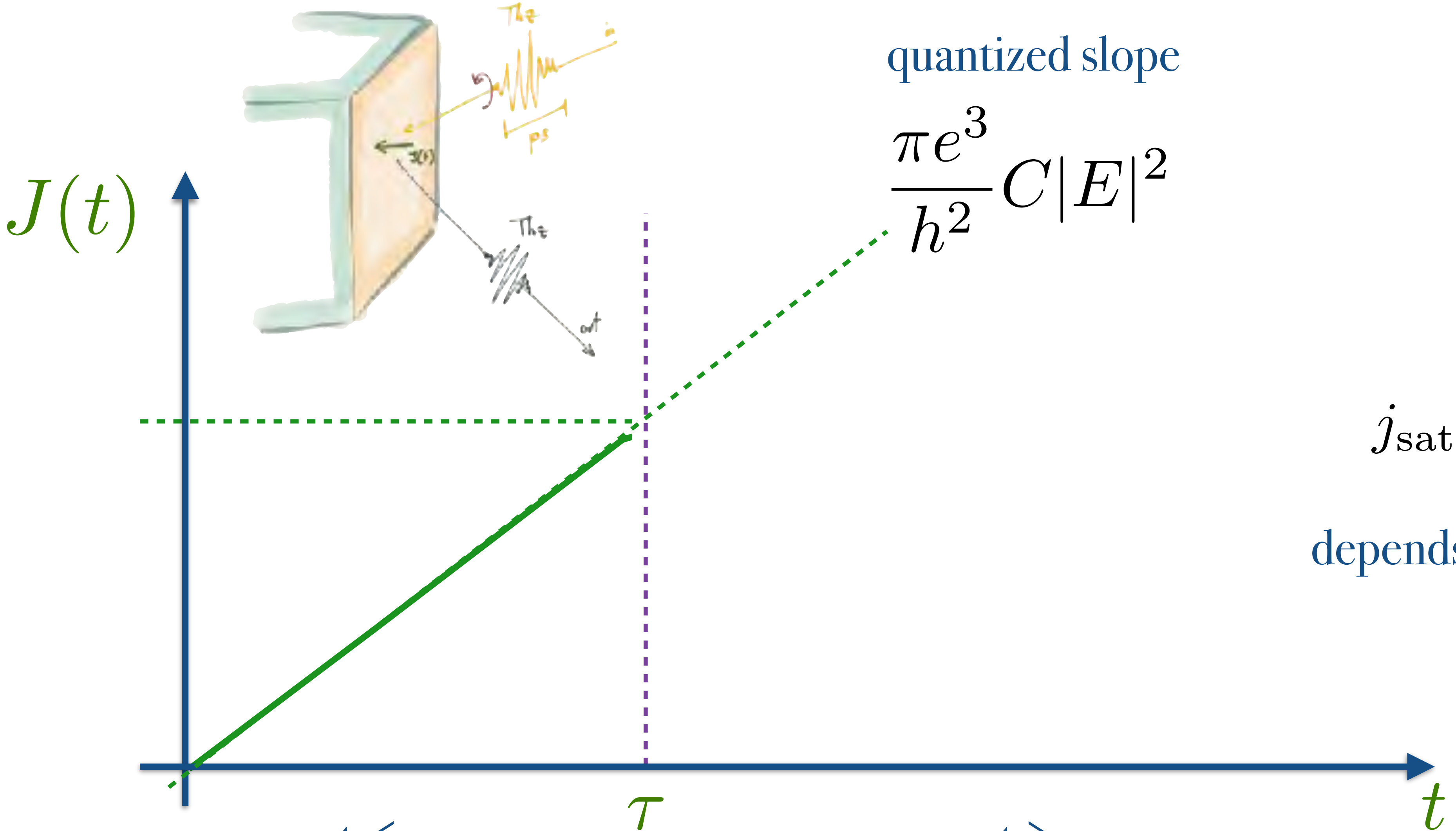

quantized slope

$$\frac{\pi e^3}{h^2} C |E|^2$$

$$j_{\text{sat}} = \tau \frac{\pi e^3}{h^2} C |E|^2$$

depends on scattering time

E. J. König et al. PRB'17

t < ps

all optical

t > ps

transport

How large?

$$j^{\text{sat}} = 22\,\frac{\text{A}}{\text{cm}^2}\,\frac{\tau}{\text{ps}}\,\frac{\text{I}}{\text{W}/\text{cm}^2}$$

$$\xrightarrow[\tau\,\sim\,\text{ps}]{10\text{nm}\,\times\,1\mu\text{m}}\ \frac{2\text{nA}}{\text{W}/\text{cm}^2} \gg \text{Fermi surface contribution}\ \frac{\text{pA}}{\text{W}/\text{cm}^2}$$

Moore Orenstein PRL 2005

Okada et al PRB 2016 (TI exp)

Very large!

$$\frac{2\,\mathrm{nA}}{\mathrm{W}/\mathrm{cm}^2}$$

Symmetries help

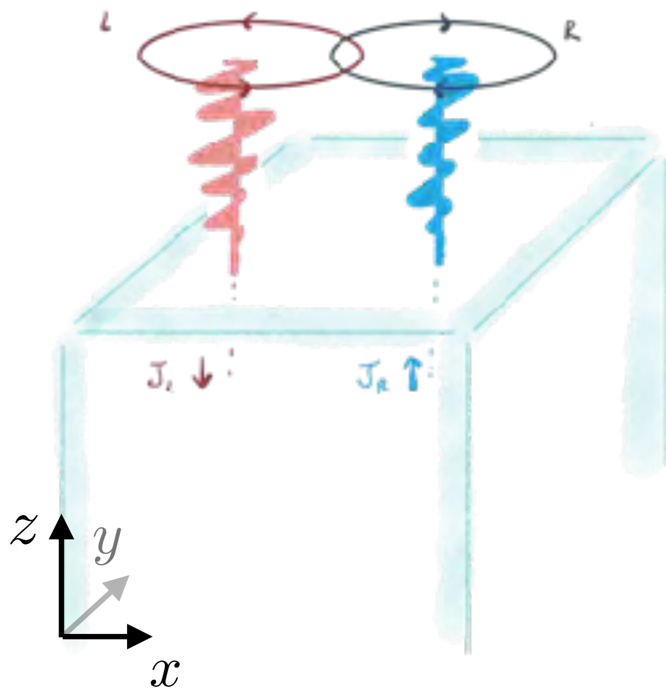

$$\frac{dj_i}{dt} = \beta_{ij}(\omega)(\mathbf{E} \times \mathbf{E}^*)_j$$

Need to measure in all polarization planes

True for chiral Weyls

Multifold are realized only in cubic space-groups

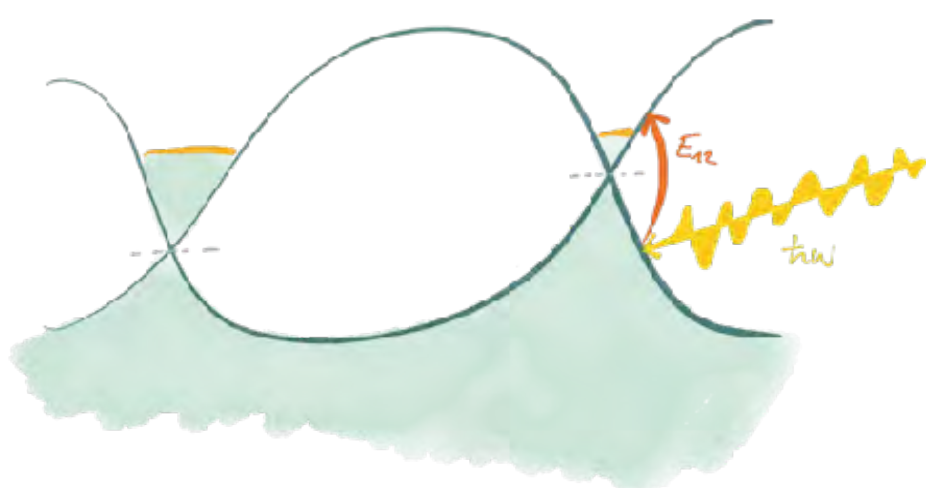

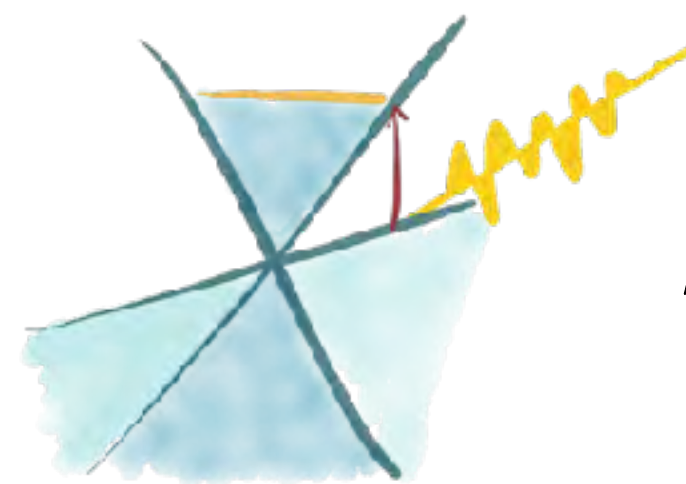

$$\beta_{ij} = \beta(\omega)\delta_{ij}$$

So one component is enough!

Gyrotropic magnetic effect

$$j_i(\omega) = \alpha_{ij}(\omega) B^j(\omega)$$



Felix Flicker, Fernando de Juan, Takahiro Morimoto


Maia Vergniory, Barry Bradlyn

Topological metals have large and anisotropic 2nd harmonic generation

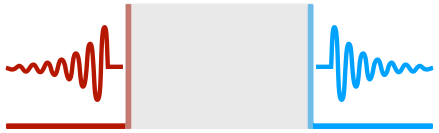

S. Pakantar et al. 1804.06973

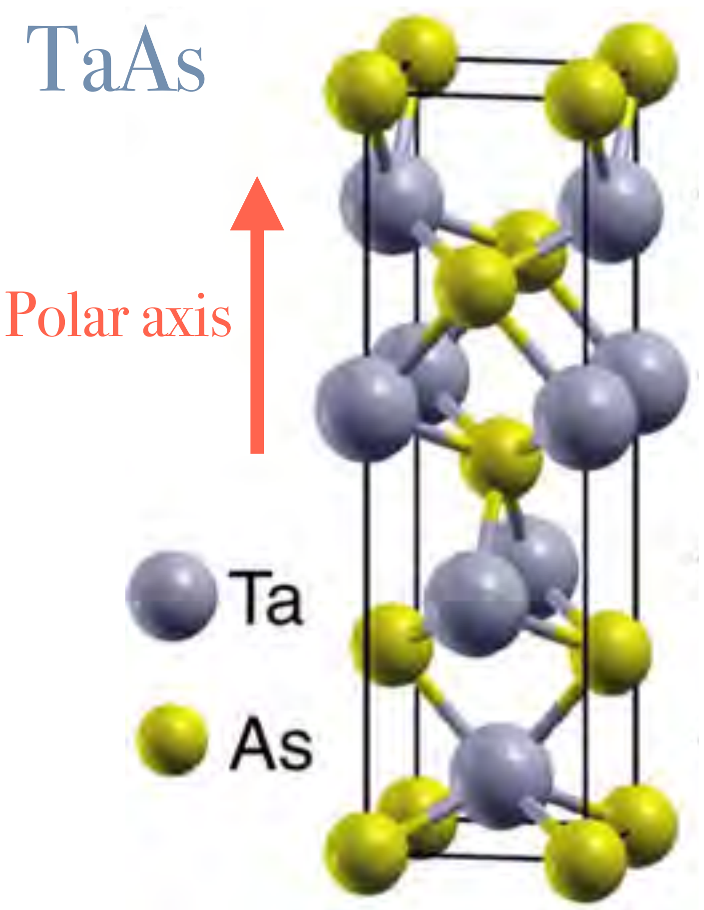

Weyl semimetal
ferroelectric point group 4mm (P=0)

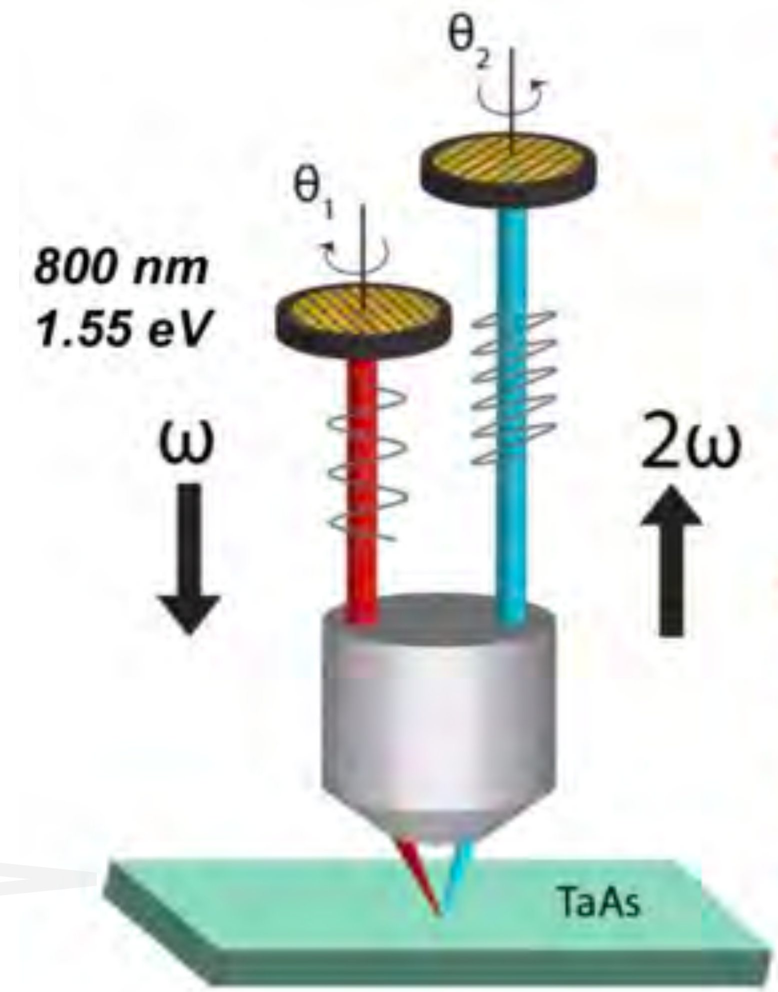

Second harmonic generation by reflection

James Analytis

Nityian Nair

Shreyas Patankar

Liang Wu

Darius Torchinsky

Joseph Orenstein

Second order zoo

$$j_i \propto \sigma_{ijl} E_j E_l$$

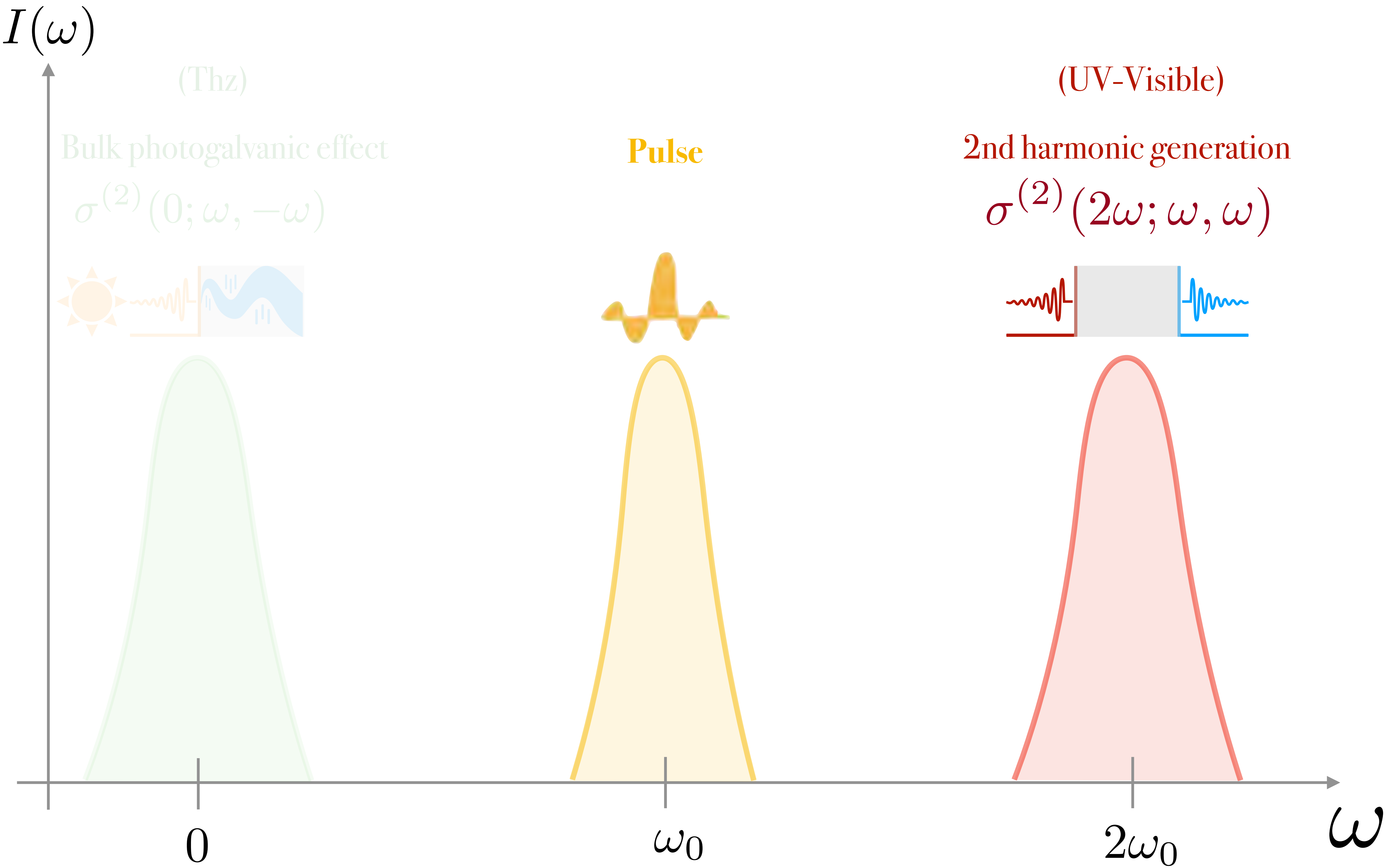

Resonant enhancement of second harmonic generation

2nd harmonic generation amplitude

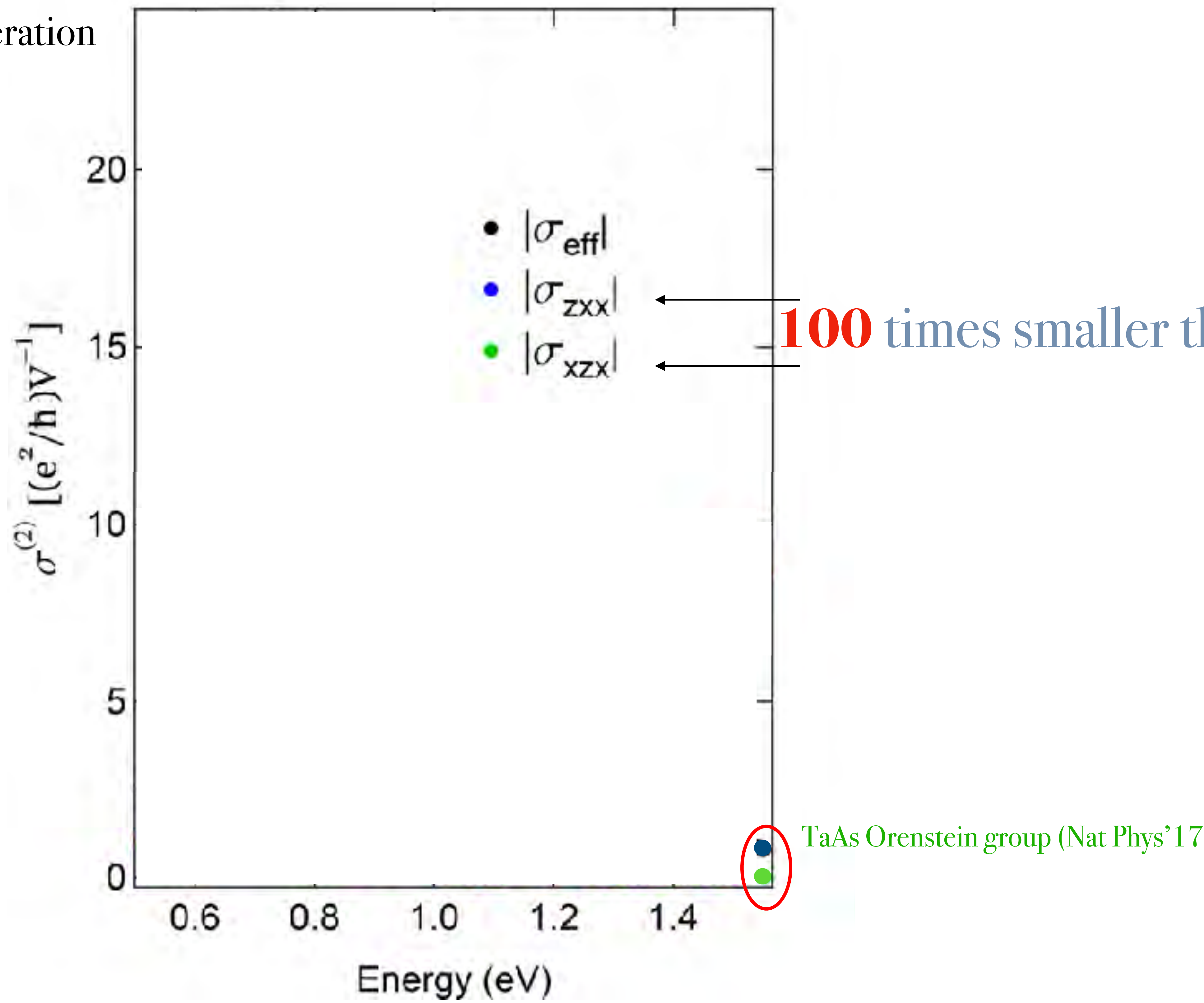

100 times smaller than ●

Resonant enhancement of second harmonic generation

2nd harmonic generation amplitude

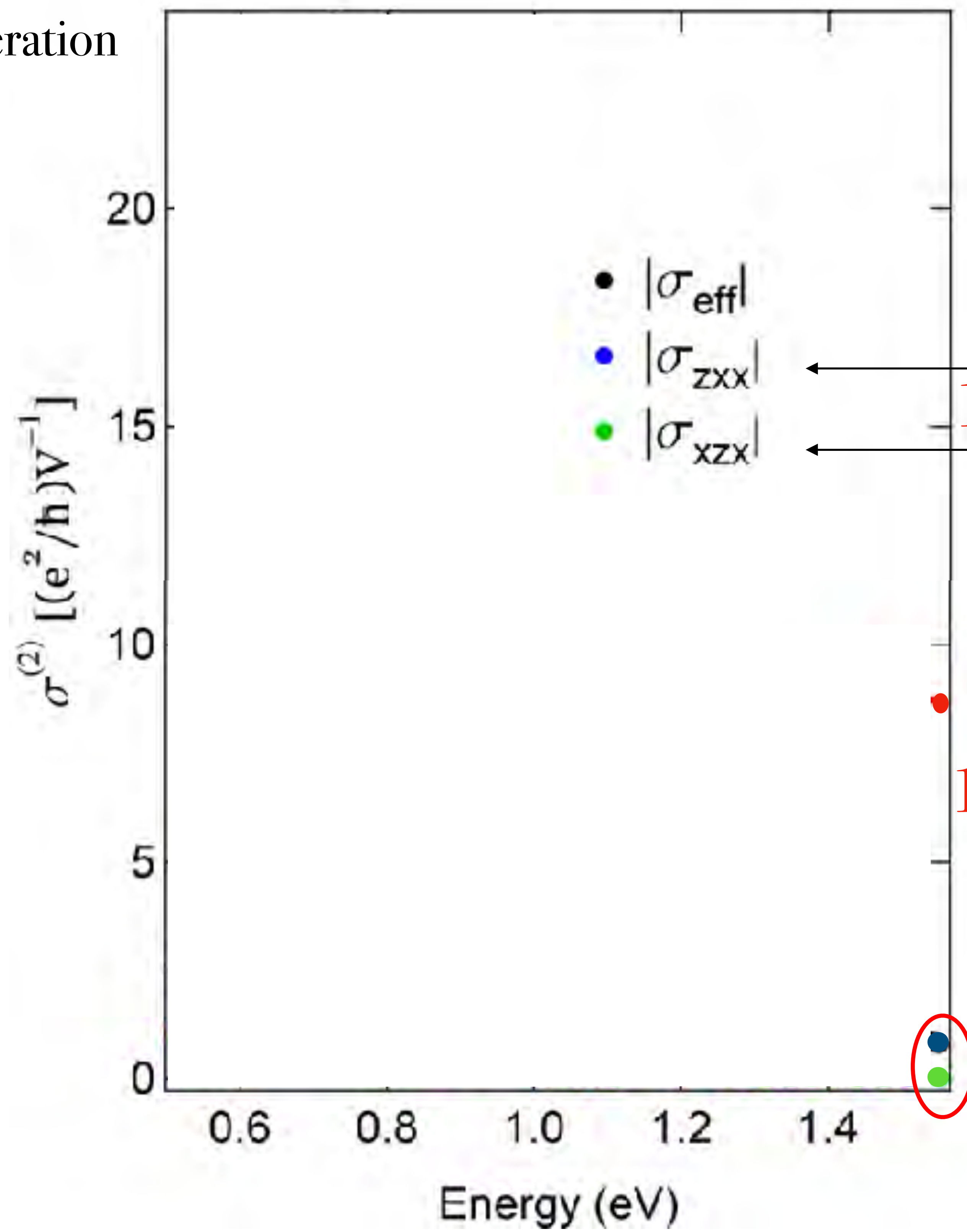

100 times smaller than ●

GaAs Bergfeld and Daum PRL '99 **x100 (!)**

10 times larger than GaAs

TaAs Orenstein group (Nat Phys'17)

Resonant enhancement of second harmonic generation

2nd harmonic generation amplitude

x16 increase in 0.7 - 1.5 eV

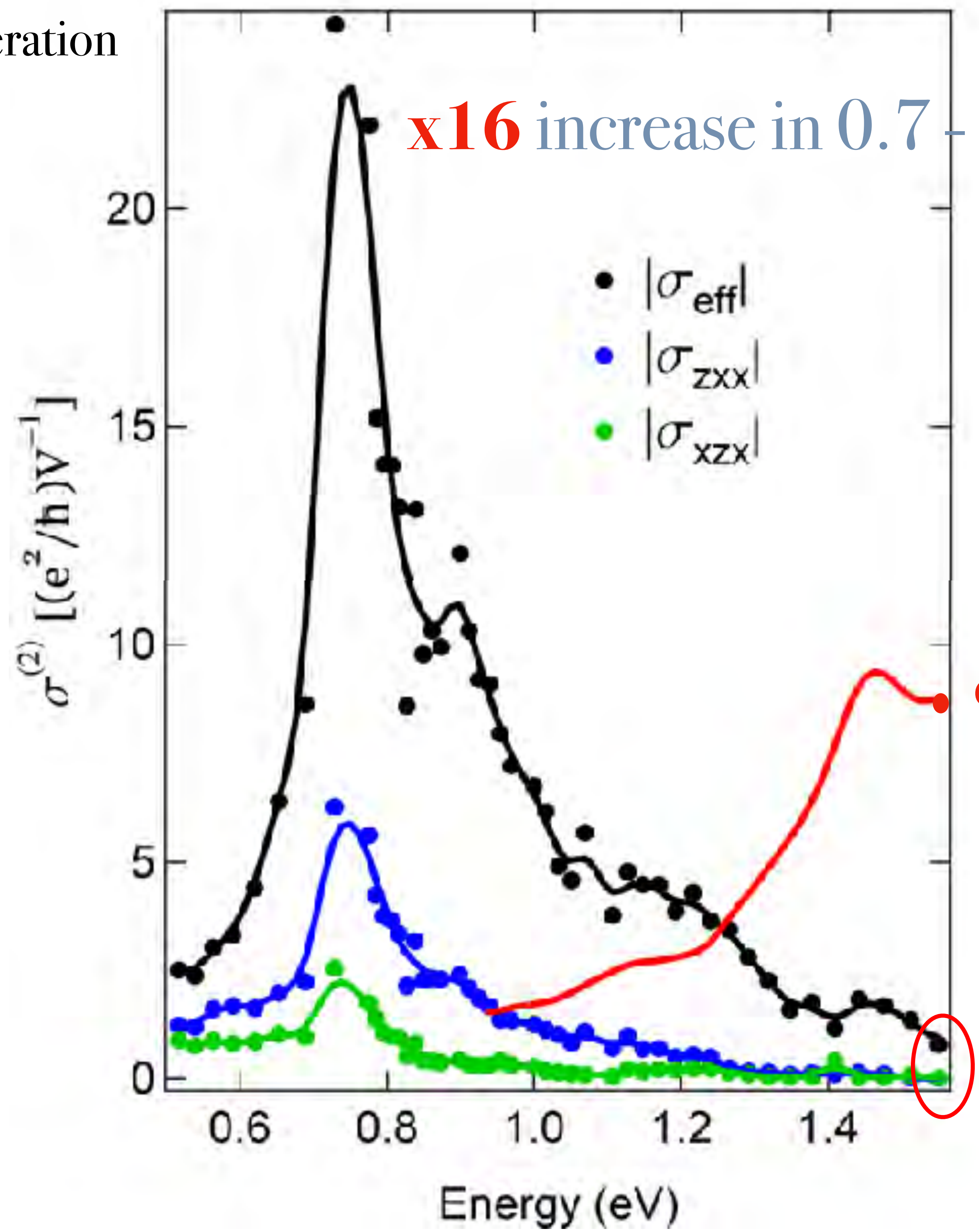

$$\frac{\sigma^{(2)}(\omega_{max})_{TaAs}}{\sigma^{(2)}(\omega_{max})_{GaAs}} \sim 200$$

GaAs Bergfeld and Daum PRL '99 **x100 (!)**

TaAs Orenstein group (Nat Phys'17)

Questions!

Bound?

Anisotropy?

Topology?

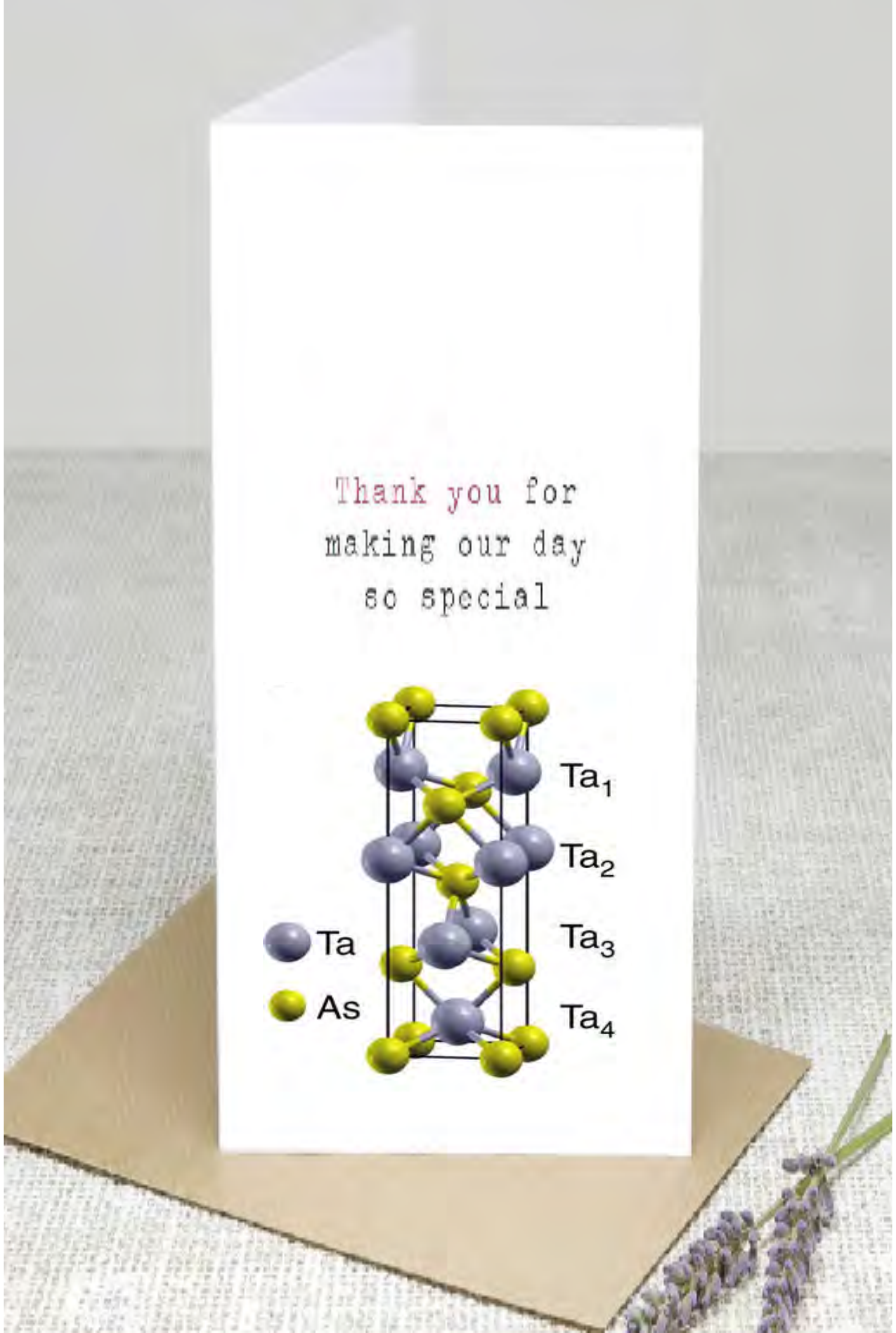

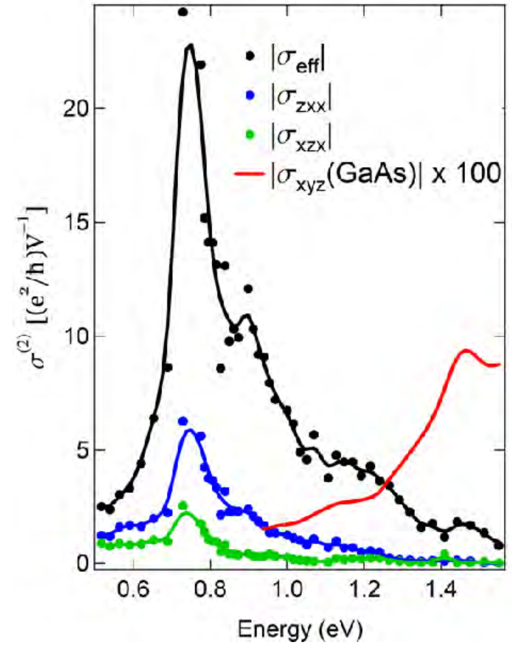

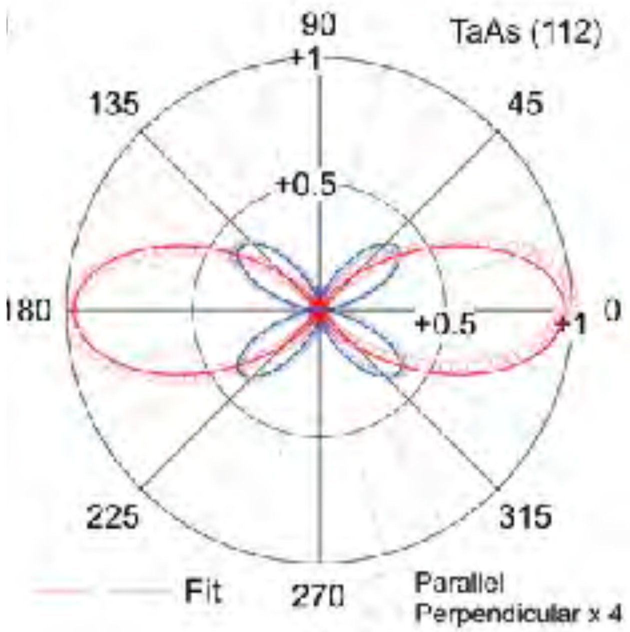

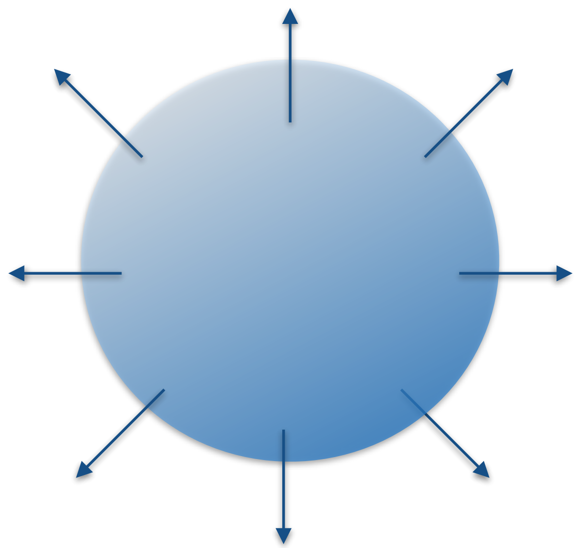

Second order zoo

$$j_i \propto \sigma_{ijl} E_j E_l$$

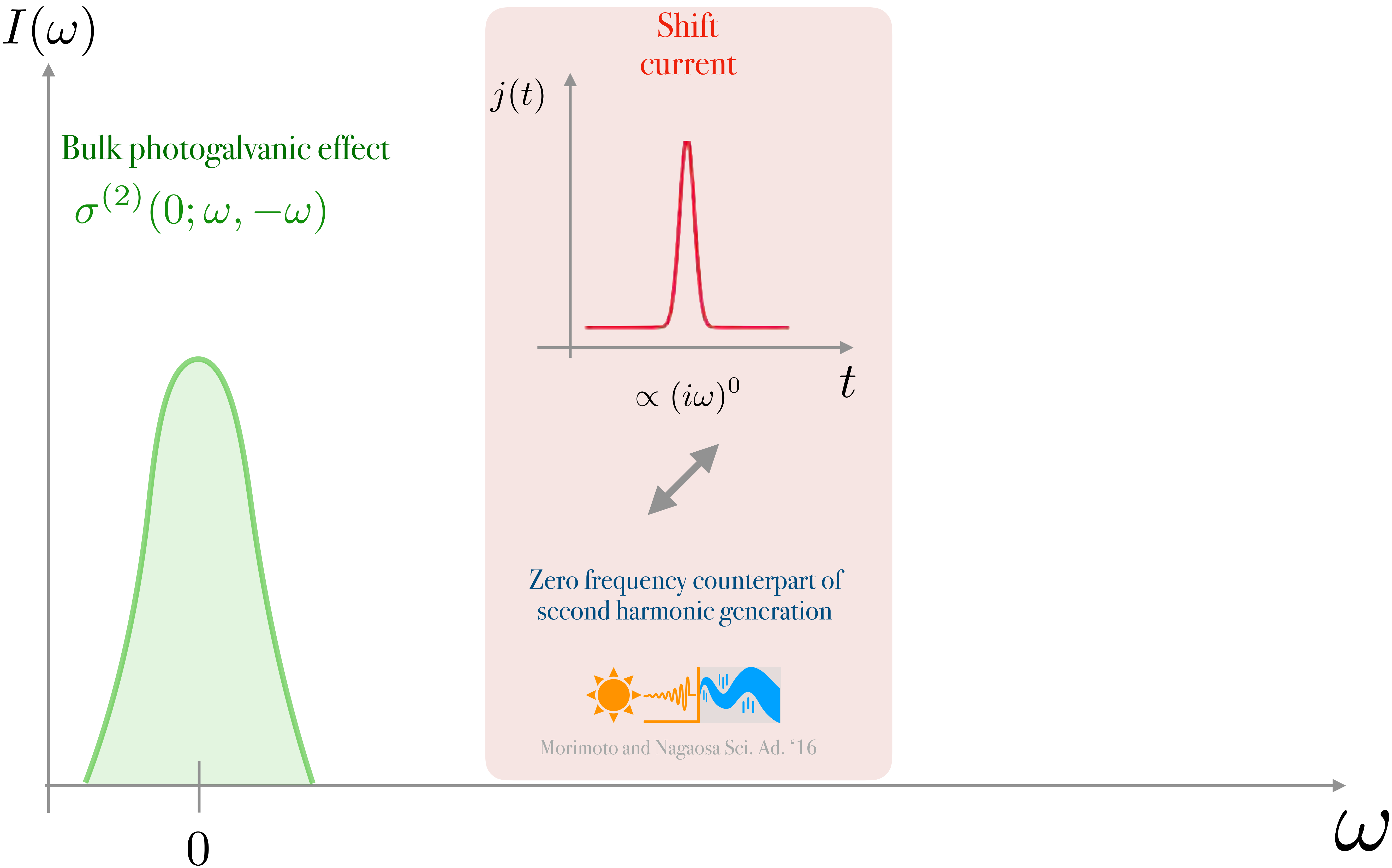

The shift vector

k-space

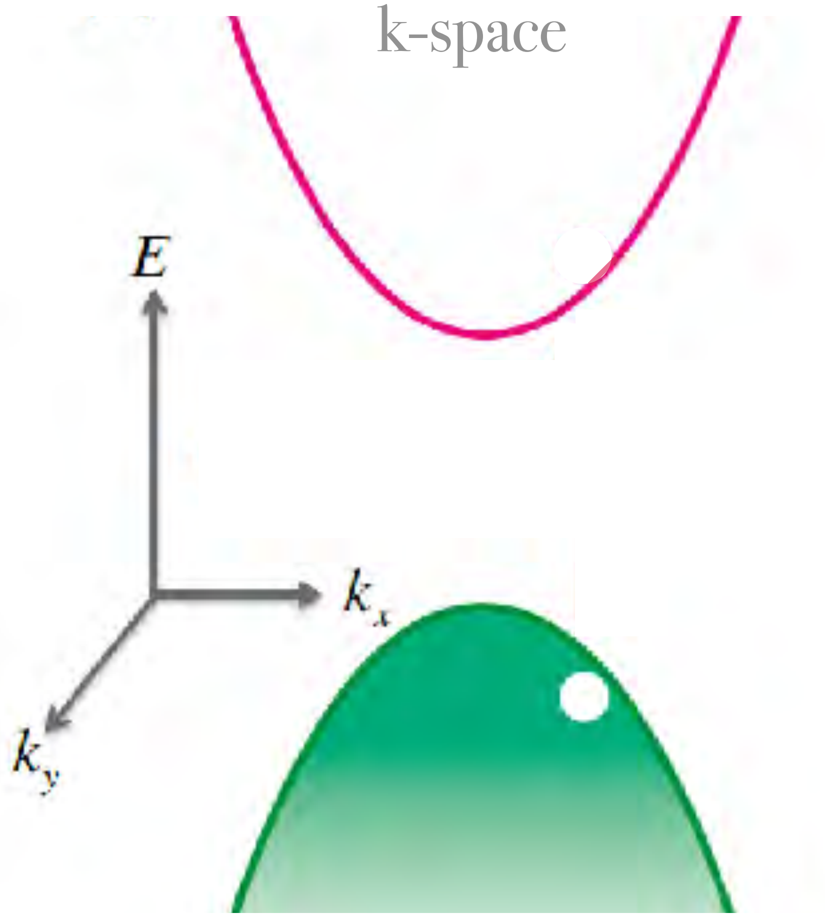

real space

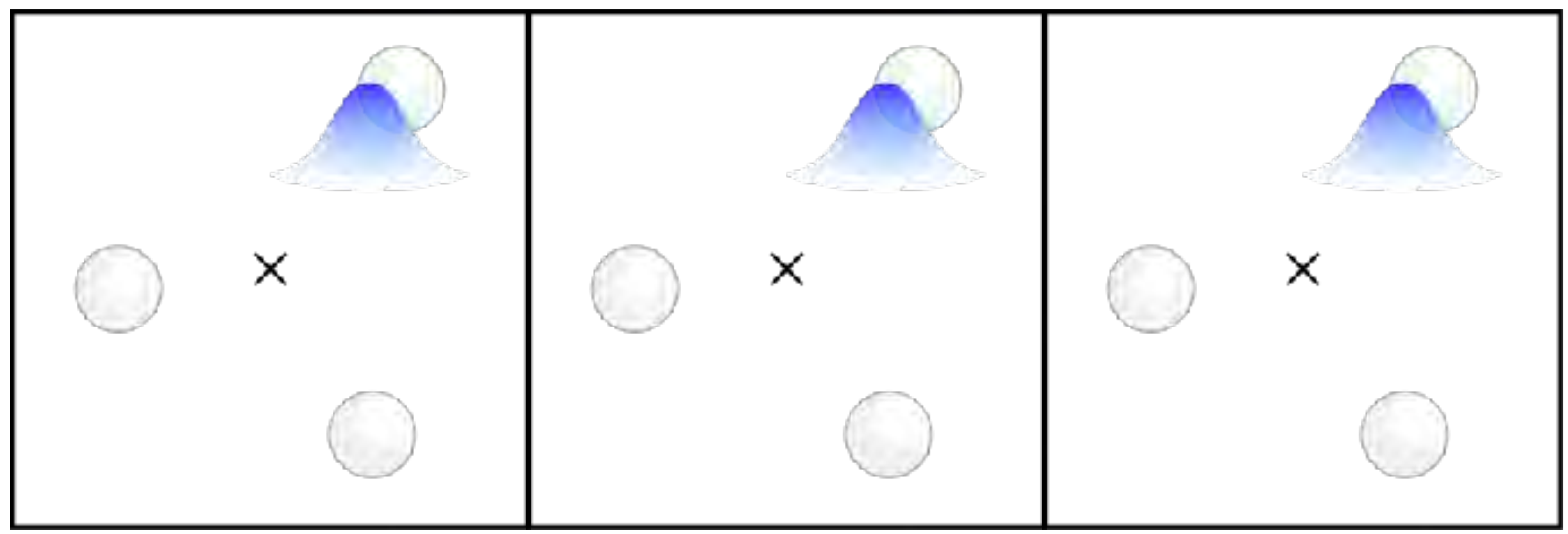

The shift vector

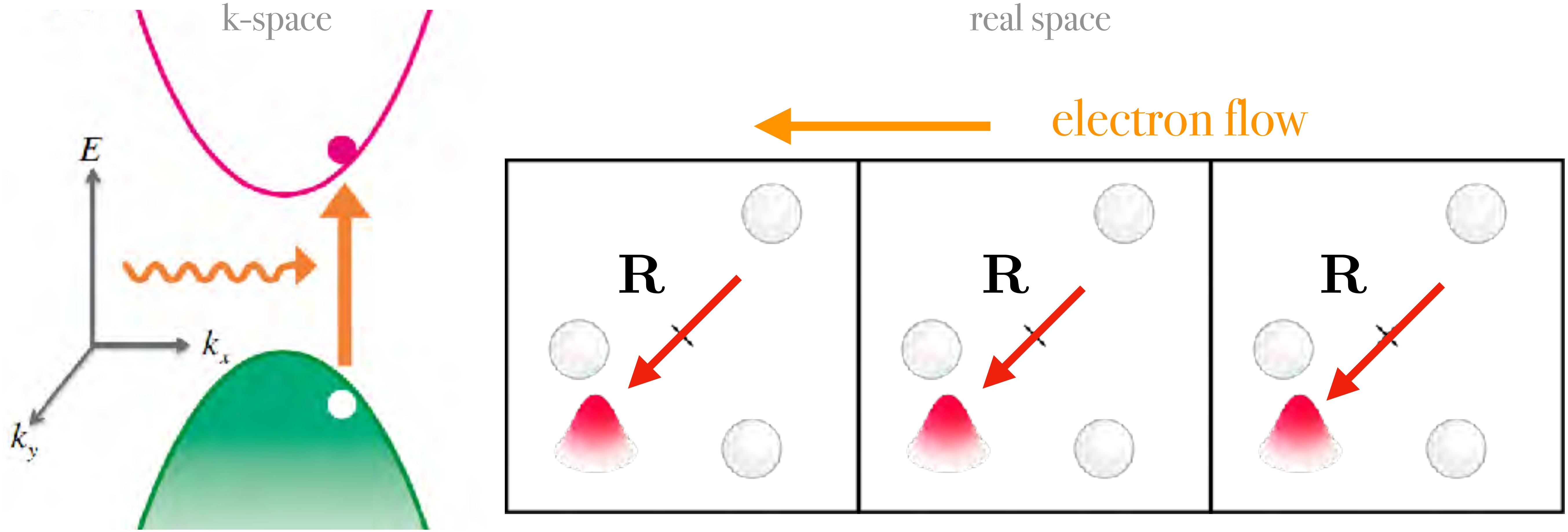

$$\partial_{\mathbf{k}}\varphi_{12} + \mathbf{a}_1 - \mathbf{a}_2 \quad = \quad \mathbf{R} \sim$$ displacement of an e-h pair

$$\sim \Delta\mathbf{P}$$ polarization difference of e-h pair

Shift current = Absorption × Rate $\sim$ $\mathbf{R} \times |v|^2\mathrm{JDOS}$

$$J_{\mathrm{SHG}} = -\frac{1}{2} J_{\mathrm{shft}}(\omega) + J_{\mathrm{shft}}(2\omega)$$

Morimoto and Nagaosa Sci. Ad. ‘16

1D model with large polarization (ferroelectric)

Rice-Mele model

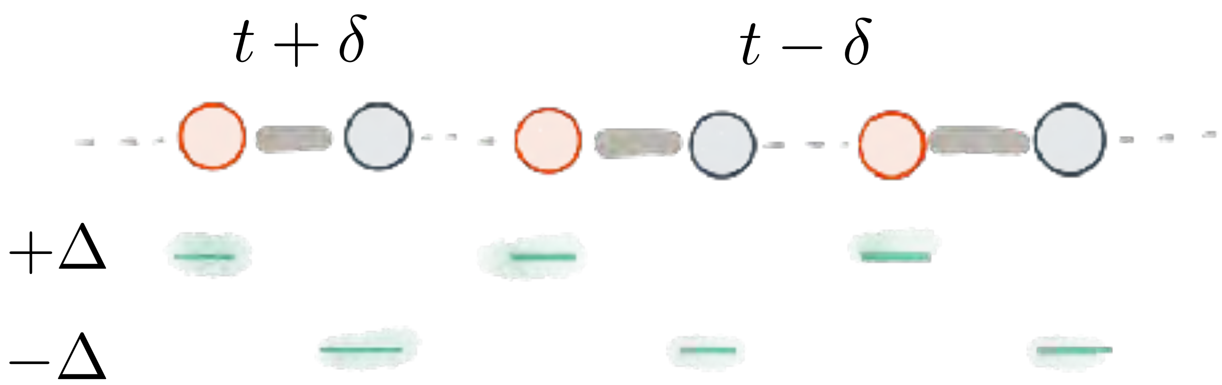

Maximum polarization $\Delta = \delta$

1D model with large polarization (ferroelectric)

Rice-Mele model

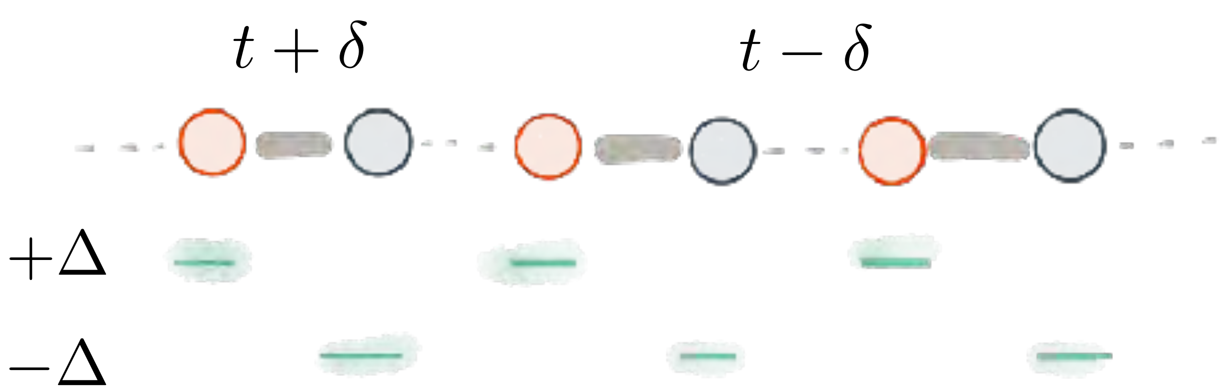

Maximum polarization $\Delta = \delta$

Coupled chains

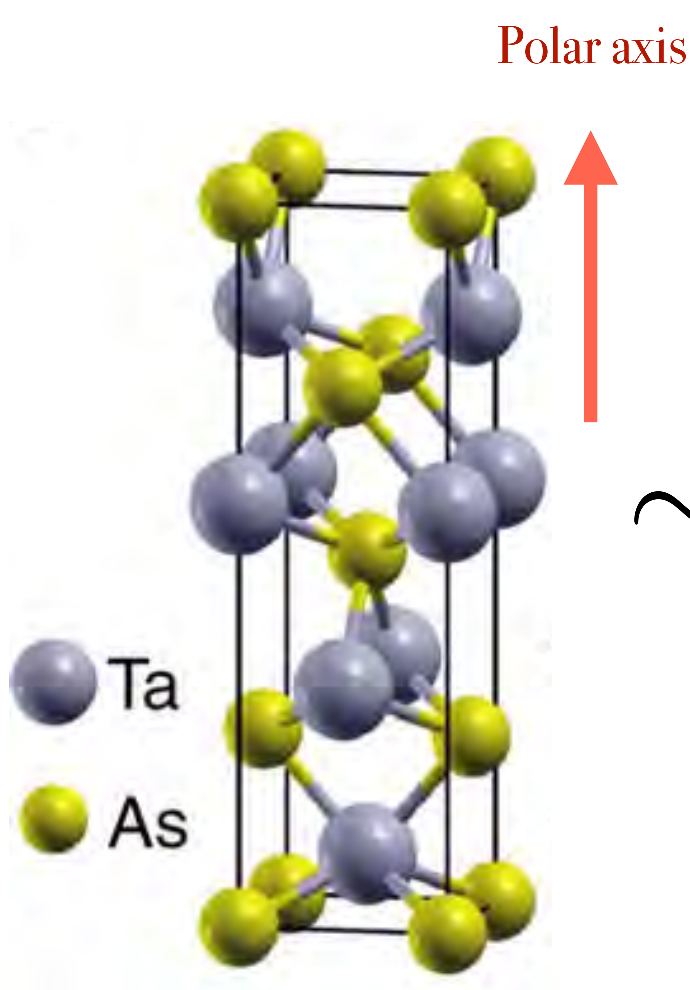

$\sim$

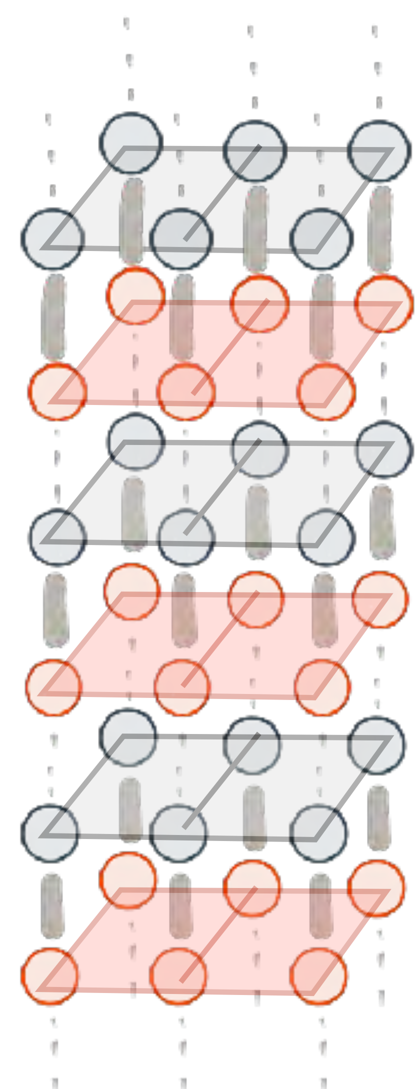

Coupled Rice Mele model

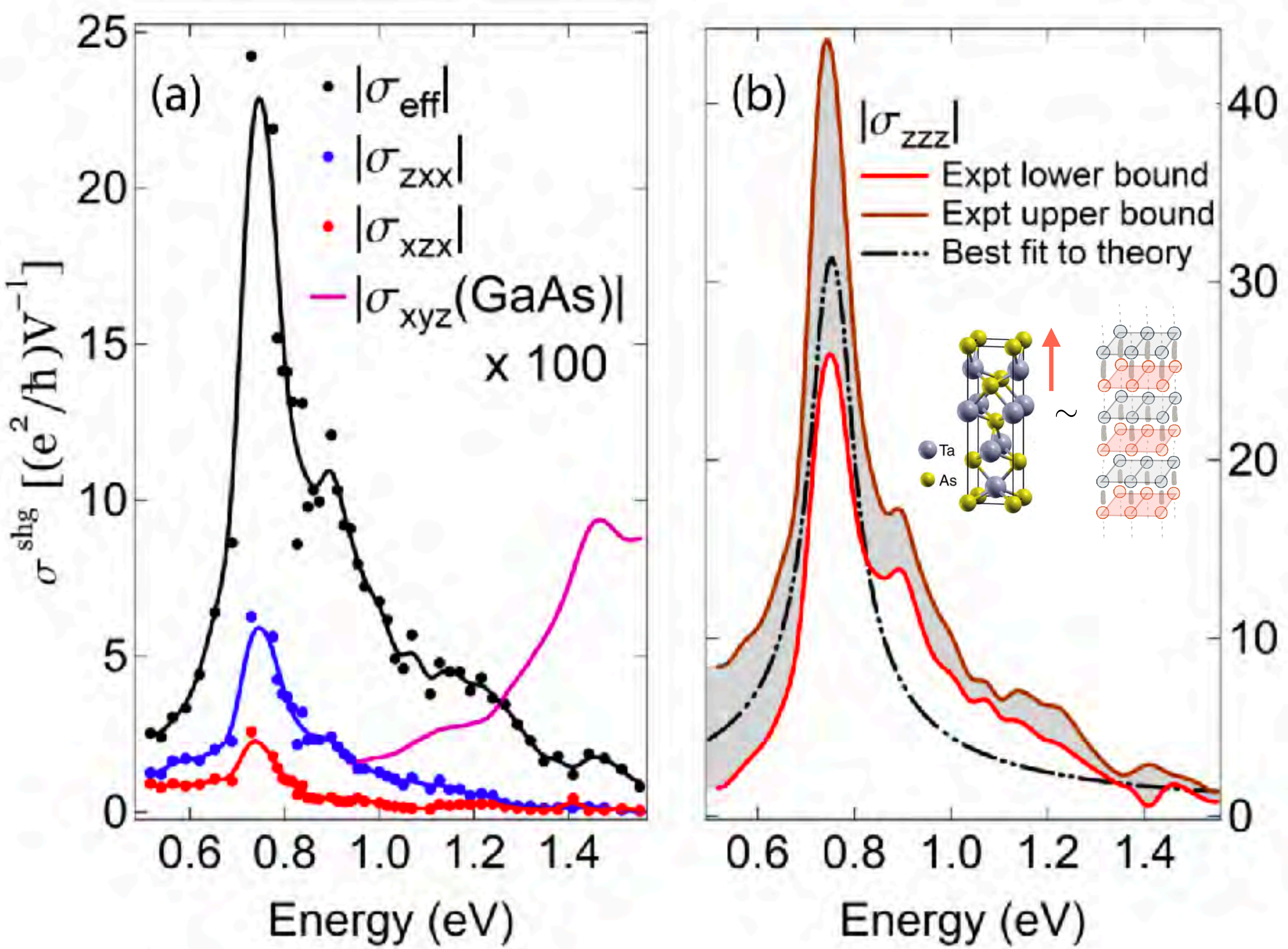

How large can this get?

$$\Sigma \equiv \int d\omega Re\{\sigma^{(2)}(2\omega;\omega,\omega)\}$$

Coupled RM bound

$$\Sigma = \frac{\pi e^3}{64\hbar^2}\frac{a^2}{bc}F(t/\Delta,\delta/\Delta)$$

F max at 0.23

TaAs

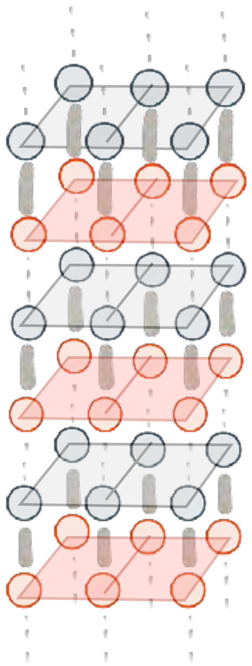

$$\frac{a^2}{bc} \sim 20$$

TaAs saturates RM bound

2 band models

$$\Sigma = \frac{\pi e^3}{2\hbar^2}C_3$$

“Skewness” of the polarization distribution

see also: Tan and Rappe, arXiv (2017)

A new sum-rule

C_1 is the polarization $P = C_1$

Vanderbilt, King-Smith, Resta

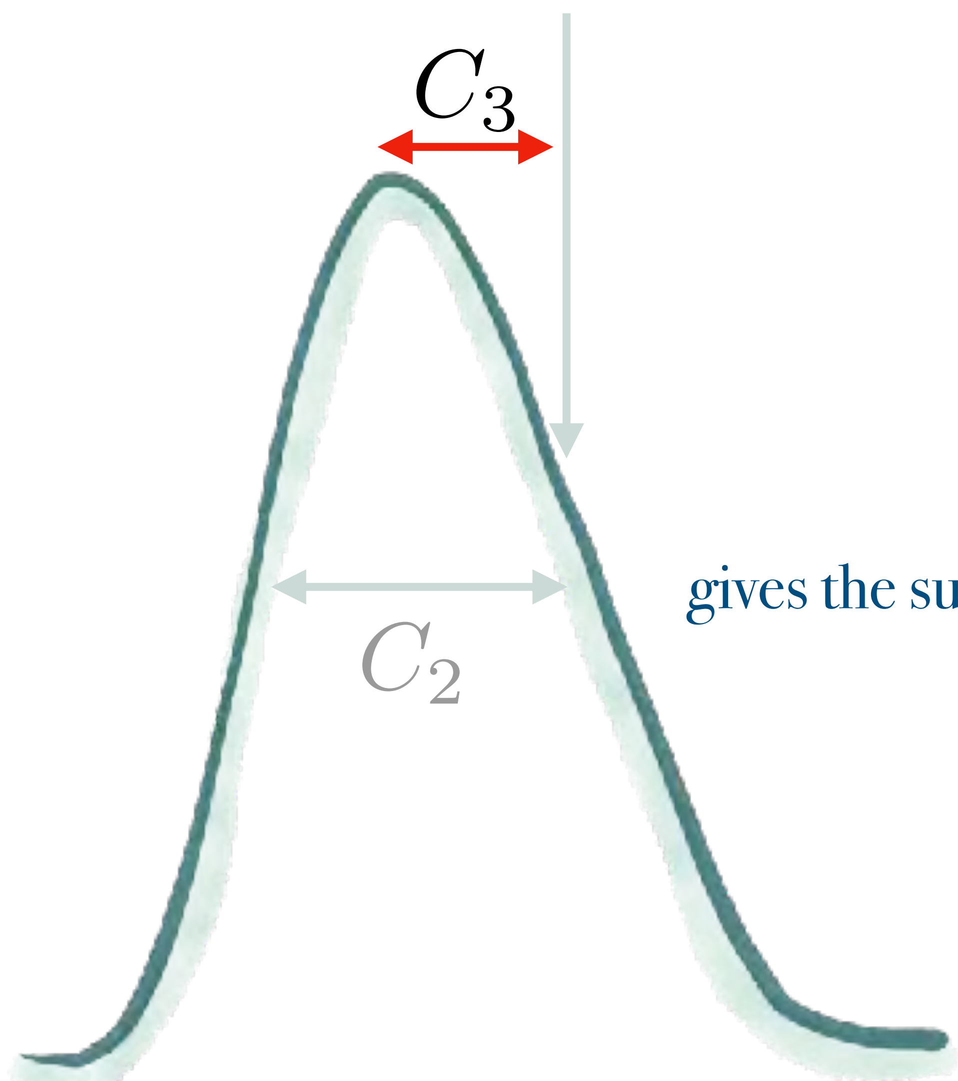

Wannier function in a Polar crystal

C_2 gives the sum rule on linear response

$$\int d\omega \mathrm{Re}[\sigma^{(1)}(\omega)] = \frac{\pi e^2}{\hbar} C_2$$

Souza, Wilkens and Martin

New result:

C_3 gives sum rule for shift current and SHG

$$\int d\omega Re\{\sigma^{(2)}(2\omega;\omega,\omega)\} = \frac{\pi e^3}{2\hbar^2} C_3$$

(enhanced with longer range hoppings)

How large can this get?

$$\Sigma \equiv \int d\omega Re\{\sigma^{(2)}(2\omega;\omega,\omega)\}$$

Coupled RM bound

$$\Sigma = \frac{\pi e^3}{64\hbar^2}\frac{a^2}{bc}F(t/\Delta,\delta/\Delta)$$

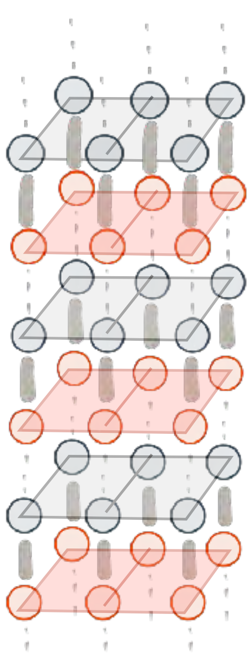

F max at 0.23

$$\frac{a^2}{bc} \sim 20$$

2 band models:

$$\Sigma = \frac{\pi e^3}{2\hbar^2}C_3$$

"Skewness" of the polarization distribution

General bound?

?

see also: Tan and Rappe, arXiv (2017)

All chiral metals have large and quantized injection currents

TaAs: largest and anisotropic SHG

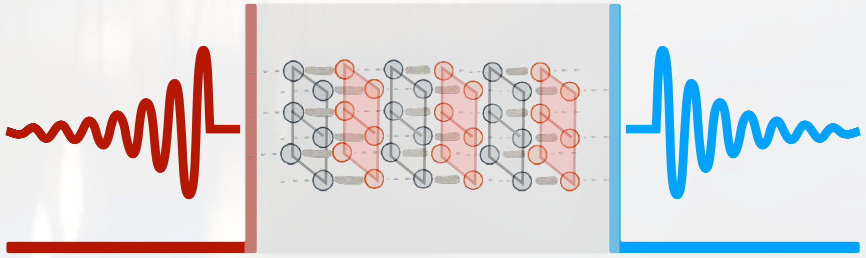

Polarization skewness = upper bound for SHG

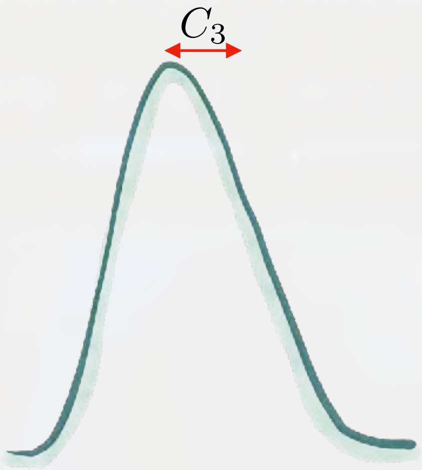

The importance of real space embedding